Transcriptional and Translational Regulation of the Ectoenzyme CD39 and its Role in *In Vivo* Thromboregulation

by

Amy E. Baek

A dissertation submitted in partial fulfillment
Of the requirements for the degree of
Doctor of Philosophy
(Molecular and Integrative Physiology)
in the University of Michigan
2014

Doctoral Committee:

Professor David J. Pinsky, Chair
Professor Philip C. Andrews
Professor Christin Carter-Su
Professor Richard Mortensen

Acknowledgments

In the years that have led me to write this thesis, I have come to know and to rely on so many people. Now, in this opportunity to say my thanks, words seem so wholly inadequate.

My wonderful mentor, Dr. Pinsky, who has helped me to become a better scientist, has always been able to shine a helpful light whenever I needed guidance. I could not have made it this far without his extraordinary patience and his scientific insight.

The Pinsky lab, the Lama lab, and the Day lab were all together when I first joined. To all of you: I will never forget the camaraderie and the lovely atmosphere of scientific enthusiasm you provided. I learned everything I could from you and I thank you all for being patient enough to teach me. I would like to thank Dr. Hui Liao especially, who, over my education in this lab, has been in invaluable source for knowledge, guidance, and more guidance. And Dana, you made everything ten times more fun and I'm so happy you came back to us!

I would also like to specially thank Linda Badri, who was the best teacher and who has become one of my dearest friends, whose support and kindness I value deeply.

My dear friends Sonu and Tom who went through graduate school with me, who have both inspired me, and who have both supported me through all these years: you are the best.

Gaurav, you've helped me so much in so many ways, that I hardly know where to begin. The hard parts were bearable, thanks to you. Thank you for encouraging me, and always believing in me. I love you so much.

Last but not least, Mom, and Dad: Thank you for raising me, for telling me that I can do whatever I want to in life, and for sacrificing so much for me. I love you both very much.

Table of Contents

List of Figures

Figures

LIST OF ABBREVIATIONS

ADP: adenosine diphosphate
AMP: adenosine monophosphate
ATP: adenosine triphosphate
cAMP: cyclic adenosine monophosphate
CAV1: caveolin 1
CD39/NTPDase1: ectonucleoside triphosphate diphosphohydrolase
CD73: ecto-5′-nucleotidase
cGMP: cyclic guanosine monophosphate
Cil: cilostazol
CREB: cAMP response element binding protein
CYP: cytochrome p450 enzymes
DAMP: damage-associated molecular pattern molecules
DVT: deep vein thrombosis
HUVEC: human umbilical vein endothelial cells
IL-1β: interleukin-1 β
Mil: milrinone
MRI: magnetic resonance imaging
NALP3: NACHT, LRR and PYD-containing protein 3
PBS: phosphate buffered saline
PDEIII/PDE3: phosphodiesterase III
PKA: protein kinase A
PLC: phospholipase C
TNF-α: tumor necrosis factor α
TEM: transmission electron microscopy
TG: transgenic
WT: wild type

Abstract

Transcriptional and Translational Regulation of the Ectoenzyme CD39 and its Role in *In Vivo* Thromboregulation

by

Amy E. Baek

Chair: David J. Pinsky

Extracellular purinergic signaling through ATP and ADP has been shown to be a potent trigger for inflammation and thrombosis. Modulating the purinergic signaling pathway is the plasmalemmal ectonucleotidase, CD39/NTPDase1 (ectonucleoside triphosphate diphosphohydrolase). CD39 is expressed by a number of cell types including endothelial cells, B and T lymphocytes, and monocytes and macrophages. It hydrolyzes the terminal phosphate of ATP and ADP in an enzymatic cascade that generates AMP.

Under pathological conditions such as atherosclerosis, deep vein thrombosis and ischemia of various organs, the coexisting pathways of inflammation and thrombosis contribute to disease progression. As such, those enzymes and key steps in the various signaling pathways involved in inflammation and those involved in coagulation are targets for future therapies. CD39 is one such enzyme, which can modulate purinergic signaling pathways to limit thrombosis and inflammation.

Interest in CD39 and its function has grown since its discovery, and much has been learned about its protective role against thrombosis, its sequence and structure, its activity under targeted mutations, and its role in inflammatory and thrombotic disease models. There remain, however, many gaps in our basic knowledge about CD39. To address these gaps and to contribute in a meaningful way to the body of work surrounding CD39, three projects were designed, focused on regulation of CD39 on both the transcriptional and translational levels as well as its *in vivo* actions.

The work presented here investigates the possibility of pharmacologically regulating expression and activity as well as the microenvironment in which it resides. Furthermore, these experiments address the issue of how this regulation might modulate the capacity of CD39 to function, and the protective effects of this in an integrated biological system.

Chapter I: A Brief Background on CD39

The overarching aim of this thesis is to identify regulatory transcriptional and posttranslational mechanisms governing the enzyme ectonucleoside triphosphate diphosphohydrolase (CD39), and to identify their relevance *in vivo*.

An Introduction to ATP and Purinergic Signaling

Adenosine triphosphate, or ATP, was discovered in 1929, far before the discovery of CD39 and its ATP/ADPase activity, and before the concept that purine compounds can act as extracellular signaling molecules. It was first isolated from muscle tissue by Karl Lohmann (1), and then in 1941, intracellular ATP was found to be the main energy transfer molecule of cellular metabolism by Fritz Albert Lipmann (2). The earliest evidence for the physiologic effects of adenine-based compounds in the extracellular milieu came later that same year, when the effects of adenosine and adenylic acid (adenosine monophosphate, AMP) were tested upon mammalian hearts (3). By 1945, apyrases, enzymes that break down ATP and ADP but are resistant to inhibition by other ATP-ase inhibitors, were isolated from potatoes (4).

Evidence that extracellular nucleotides could act as signaling entities, however, came much later in 1970, when Burnstock et al. demonstrated that ATP was likely

acting as a neurotransmitter in the gut (5). Receptors for adenosine and ATP were identified soon thereafter, and named P1 and P2 respectively (6). P1 receptors are G protein-coupled receptors and are divided into 4 receptor subtypes: A_1, A_{2A}, A_{2B}, and A_3. The P2 family was further categorized as P2X and P2Y based on receptor morphology. The P2X receptor family includes 7 members, $P2X_1$ through $P2X_7$. These are purine-gated ion channels permeable to small monovalent cations such as sodium and potassium, with some permeable to calcium (7). These receptors form channels as either homomeric or heteromeric multimers. The P2Y receptor family is composed of G protein-coupled receptors (8). These receptors have the classical GPCR structure of 7 transmembrane domains, and signal predominately through the second messenger cyclic adenosine monophosphate (cAMP) or through phospholipase C (PLC).

Initially, the purinergic hypothesis of signaling (9, 10) was controversial and the hypothesis that ATP could have a significant role apart from that of an energy transfer molecule was not readily accepted. Since that time, however, research into purinergic signaling gained momentum, and it became well-established that ATP is an important co-transmitter at neuronal synapses (10).

Extracellular ATP and ADP

In the following years, interest in purinergic signaling grew beyond the limits of the nervous system, and signaling studies on P2 receptor-mediated pathways have

demonstrated a wide range of effects controlled by P2 receptors, including platelet aggregation, leukocyte activation, cytotoxicity, and apoptosis (11-14).

Signaling by extracellular nucleotides such as ATP at low concentrations serves as an indicator of normal function to normal cells through the binding of P2X and P2Y receptors. Conversely, there exist endogenous danger signals termed damage-associated molecular pattern molecules (DAMPs) that indicate that cellular damage has occurred, and are in place to initiate an immune response. These molecules are largely intracellular components, and examples of DAMPs include extracellular DNA, RNA, and ATP. The large concentration gradient that exists between the intracellular and extracellular compartments for ATP, favors a release of ATP in those circumstances where the cell plasma membrane is perturbed, either by shear forces, injury, or death (15). In the case of cellular damage leading to ATP release, $P2X_7$ receptors, which are expressed on granulocytes, monocytes, macrophages, and B- lymphocytes (16), and which are attuned to high concentrations of ATP, are activated. The binding of these receptors triggers signaling that induces the release of pro-inflammatory cytokines such as IL-1β. Here, binding of ATP to its receptor opens the $P2X_7$ ion channel and allows efflux of potassium ions, which triggers the NALP3 inflammasome, the recruitment of caspase-1, and the cleavage of pro-IL-1β into mature IL-1β. Binding of $P2X_7$ can also lead to cell death (17, 18).

Extracellular ADP is also a potent signaling molecule that acts on $P2Y_{12}$ receptors on the surface of platelets to activate them and thus induce platelet aggregation (19). Further release of ADP from dense granules of platelets also induces aggregation. Several antagonists for $P2Y_{12}$ receptors have been developed to block this pathway, such as clopidogrel and prasugrel, in the treatment of acute coronary syndromes, and the prevention of further ischemic events (20). These drugs belong to the thienopyridine class of anti-platelet drugs, and both are irreversible $P2Y_{12}$ receptor antagonists, and remain bound to their targets for the life of the platelet. While they are effective in their intended use, there are several drawbacks to each, due to their mechanism of action. As irreversible antagonists that permanently disable platelet function, there is an inherent bleeding risk associated with the use of these agents. Additionally, polymorphisms in cytochrome p450 (CYP) enzymes that are required for metabolism of clopidogrel into its active form, result in variable responses to the drug. Due to these drawbacks, the search for better anti-platelet treatments continues, and it is in this context that we frame our discussion on CD39, an enzyme that phosphohydrolyzes both pro-inflammatory extracellular ATP and pro-thrombotic ADP, while still preserving platelet function.

The First Detection of CD39

In 1982, an important integral membrane protein and the focal point of this work, CD39, was first detected in a slurry of Epstein-Barr virus-stimulated B-cells, and initially thought to be a receptor for homotypic B cell adhesion (21). The primary role of

CD39 was determined in 1996 when work by Wang et al. first established that CD39 had apyrase activity, or the enzymatic function of phosphohydrolyzing the terminal phosphate of ATP and adenosine diphosphate (ADP) to yield AMP and phosphate (22, 23).

CD39 is a 54 kDa integral membrane protein with two transmembrane domains that anchor a large extracellular domain, and is a homomeric tetramer (24). The human CD39 contains 6 sites of glycosylation and a palmitoylated N-terminus that preferentially targets CD39 to cholesterol-rich subcellular domains called caveolae (25). CD39 protein is modified with N-linked glycans in the endoplasmic reticulum, which ensure correct folding of the protein, and are necessary for surface localization and maximal apyrase function (26).

Caveolae, a subset of lipid rafts, are omega (Ω)-shaped structures enriched in caveolin proteins, and are thought to be "signaling platforms" that coordinate cell signaling (27). Within these domains, CD39 is co-expressed with ecto-5′-nucleotidase (CD73), a glycosyl phosphatidylinositol (GPI)-anchored cell surface enzyme that phosphohydrolyzes AMP to generate adenosine (28). Adenosine can bind P1 adenosine receptors, which are expressed on leukocytes, lymphocytes and platelets, to suppress the release of pro-inflammatory cytokines, inhibit platelet aggregation, and act as a vasodilator. Adenosine binding to the P1 receptor subtype A_{2A}, for example, can suppress the release of cytokines such as tumor necrosis factor alpha (TNF-α),

interferon gamma (IFNγ), and IL-12 (29). Ligand binding to A_{2A} and A_{2B} subtypes inhibits platelet aggregation by elevation of intracellular cAMP caused by activation of adenylate cyclase (30). Ligand binding to A_{2A} receptors can also stimulate vasodilation through the activation of adenylate cyclase (31). Therefore, the signaling cascade that depletes extracellular ATP and ADP is completed with the formation of adenosine, which stimulates pathways that limit inflammation.

With its ability to locally control extracellular levels of ATP and ADP and thus purinergic signaling, CD39 is at a critical juncture, able to modulate the activation of multiple signaling pathways.

Relevance of CD39 in Disease

Across middle to high-income countries, including the United States, ischemic heart disease and stroke are the top causes of death, and account for one in four deaths worldwide in 2010 (32). Ischemic heart disease and stroke are driven or exacerbated by two physiological responses: thrombosis and inflammation (33, 34).

In the context of atherosclerosis, a disease characterized by the accumulation of cholesterol-laden plaques along arterial vessels, an ever-increasing literature supports it being a disease of inflammation. Circulating low density lipoprotein (LDL) activates macrophages and the endothelium, thus stimulating the expression of cell-surface adhesion molecules such P-selectin, vascular cell adhesion molecule 1 (VCAM)-1,

intercellular adhesion molecule 1 (ICAM-1), platelet endothelial cell adhesion molecule 1 (PECAM-1), and junctional adhesion molecules (JAMs) (35). Activated endothelial cells release P-selectin that is stored within Weibel-Palade bodies. These selectins bind P-selectin glycoprotein ligand-1 (PSGL-1), which is expressed on leukocytes and lymphocytes. The binding of selectin to its ligand allows for rolling adhesion of monocytes along the endothelium. Further interactions with adhesion molecules strengthen adhesion to tether monocytes to the endothelium. Binding to JAMs facilitates leukocyte transmigration across the endothelial layer into the subendothelial space (36-39). Here, these monocytes mature into foam cells, which absorb and store excess cholesterol, and over time become the core of the developing atherosclerotic lesion. As the severity of the plaque grows, so too does the likelihood that the plaque will rupture, thereby releasing the contents of the plaque, which can trigger a thrombogenic response. Platelets are activated, leading to platelet granular secretion. The contents of platelet granules include many pro-inflammatory and platelet activating factors. Dense granules release ATP and ADP, and alpha granules release coagulation factors such as factor V, and cell adhesion- and coagulation-promoting proteins such as von Willebrand factor, fibrinogen, P-selectin, and platelet factor 4 (40, 41).

Thrombi released from these events can then travel to other areas through the vasculature and cause further injury, including cerebral ischemia, as they are able to

impede blood flow supplying the brain. Cerebral ischemic events can be initiated in other ways as well, including plaques within cerebral vasculature. Such ischemic events can then trigger pro-inflammatory signaling, beginning with the release of pro-inflammatory cytokines from resident microglia and cerebral endothelium. These signals include IL1-β and TNF-α (42-44), which recruit macrophages and neutrophils, which then release even more cytokines. Further injury comes in the form of permeable endothelial barriers, which leads to greater fluid accumulation in injured areas as well as the extravasation of leukocytes into the subendothelial space and migration into tissue parenchyma.

Inflammation contributes to thrombotic events occurring in the venous system as well. Deep vein thrombosis (DVT) occurs in deep veins found within groups of muscles, and most often in lower extremities. Venous thrombi occur in vein valve-pockets, where the core of the main erythrocyte mass is covered in layers of platelets, leukocytes, and fibrin (45). Originally, the cause of DVT was thought to center on three factors in Virchow's triad: stasis, endothelial injury, and hypercoagulability. However, newer research supports the contribution of inflammation to DVT. These data show that cell adhesion molecules and selectins that allow transmigration of leukocytes as described above are also involved in the development of venous thromboembolism (VTE) (46).

The processes of inflammation and coagulation are necessary functions. The recruitment of leukocytes/lymphocytes such as dendritic cells, macrophages, and T-cells, for example, are necessary to detect and kill infected cells. Intact hemostatic function is also necessary in order to repair damaged blood vessels. Under pathological conditions such as those described previously, however, the dual pathways of inflammation and thrombosis have been demonstrated to contribute to disease progression. As such, those enzymes and key steps in the various signaling pathways involved in inflammation and those involved in coagulation have been targeted as part of efforts to limit inflammation or thrombosis, respectively. CD39 is one such enzyme, which can modulate purinergic signaling pathways to limit thrombosis and inflammation.

Why is there a need for further research on CD39 and purinergic signaling, given that there are antiplatelet therapies available? One limitation to these therapies is that there are known resistances to antiplatelet drugs such as clopidogrel, which irreversibly inhibits ADP-activated $P2Y_{12}$ receptors. Resistance is due to natural polymorphisms in the population in genes that encode cytochrome P450 (CYP) eyzymes (47), which are necessary to convert the pro-drug into its active form. Both the pharmacokinetics and the pharmacodynamics of clopidogrel are affected in patients carrying reduced-function *CYP2C19* alleles (48, 49). Other limitations include risk of uncontrolled bleeding and delays due to the time required to metabolize the drug. Most importantly, while

antiplatelet drugs such as clopidogrel and prasugrel (another $P2Y_{12}$ antagonist) do prevent platelet aggregation, they do so at the expense of normal hemostatic function. In contrast to thienopyridine-class antiplatelet drugs, whose irreversible binding of $P2Y_{12}$ receptors renders platelets permanently inactive, the mechanism of CD39's enzymatic depletion of ADP is able to limit platelet aggregation while preserving normal platelet function.

Interest in CD39 and its function has grown since its cloning, and much has been learned about its protective role against thrombosis, sequence and structure, activity under targeted mutations, and role in inflammatory and immune disease models (50-52). There remain, however, many gaps in our basic knowledge about CD39. For example, apart from a publication from this lab in 2010, nothing was known about the transcriptional regulation of CD39, and apart from a publication from this lab in 2013, there is next to nothing known about the turnover of CD39 and mechanisms of CD39 degradation. To address these gaps and to contribute in a meaningful way to the body of work surrounding CD39, three projects were designed. The overarching aim of this thesis is to identify regulatory transcriptional and posttranslational mechanisms governing CD39, and to identify their relevance *in vivo*.

My early project began by observing CD39 responses to HMG-CoA reductase inhibitors (statins). This class of drugs remains in use by a significant portion of the

aging population, not in the United States alone, but all over the world. They are used to limit cholesterol biosynthesis, and their main mechanism of action is inhibiting HMG-CoA reductase, the enzyme which controls the rate-limiting step of cholesterol synthesis in the mevalonate pathway. Here, 3-hydroxy-3methylglutaryl-CoA (HMG-CoA) is reduced to mevalonic acid and CoA by HMG-CoA reductase, ultimately leading to the downstream synthesis of cholesterol. Statin drugs inhibit mevalonic acid synthesis by binding the active site of HMG-CoA reductase, thereby inhibiting the remainder of the mevalonate pathway.

While statins as a class of drugs has been shown to be an effective means of lowering serum cholesterol, the pleiotropic actions of these drugs are also well-documented (53, 54). For example, in the presence of statins, downstream reactions from the mevalonate pathway that generate isoprenoid intermediates such as geranylgeranyl pyrophosphate (GGPP) and farnesylpyrophosphate (FPP) (55) are disrupted. These lipid intermediates serve as covalently bonded posttranslational modifiers of members of the Ras superfamily of small GTPases, which includes Ras, Rho, and Rab families of proteins. Ras family members act as molecular switches that modulate an array of cellular functions, from vesicle formation and cytoskeletal rearrangement to nuclear transport (56, 57).

Researchers have shown that CD39 is among the proteins affected by statins (58). CD39 levels are very potently upregulated by statin drug treatment. This result led to an early project, which probed the effects of statin treatment on expression, activity, and intracellular trafficking of CD39.

A second project focused on transcriptional mechanisms of CD39 regulation was also initiated based on findings from our work describing the role of cAMP in modulating CD39 (59). Although several potential regulatory sites were found in the CD39 promoter region, only one of these, a cAMP-response element (Cre)-like motif located 210 base pairs upstream of the transcriptional start site, was proximal enough to be a potential regulator of CD39. It was found that CD39 expression in macrophages is transcriptionally driven by cAMP signaling, through the activation of cAMP-dependent protein kinase (PKA), leading ultimately to the binding of cAMP response element binding protein (CREB) to the Cre-like sequence.

Based on this work, we hypothesized that cAMP-modulating drugs might be able to modulate CD39 expression levels. This raises the possibility of repurposing currently used drugs to modulate endogenous levels of CD39. Phosphodiesterases (PDE) are enzymes that hydrolyze phosphodiester bonds that are found in the cyclic nucleotides cAMP and cGMP. As cAMP and cGMP are both ubiquitous second messengers that mediate pathways involved in inflammation, oxidative stress, cell

proliferation, vasodilation, and platelet activation, PDEs play an important regulatory role in intracellular signaling and continue to be investigated as therapeutic targets. Different phosphodiesterase family members have varying affinities for bonds present in cAMP versus cGMP. The PDE superfamily contains 11 different families of PDEs (PDE 1-11), each of which contain multiple splice variants. Of these, PDE families 1-4, 7,8,10, and 11 can hydrolyze cAMP (60, 61). Two drugs that inhibit the enzyme phosphodiesterase III (PDEIII), cilostazol and milrinone, were chosen to test the hypothesis that cAMP modulating drugs might be able to modulate CD39 expression levels. Each has been approved for humans, with cilostazol used in the treatment of intermittent claudication caused by peripheral artery disease and milrinone in the treatment of heart failure.

The results of this project were surprising in that CD39 was found to be differently regulated by PDE3 inhibition in endothelial cells versus macrophages. In macrophages, regulation is at the level of transcription, but in endothelial cells, this was not the case, as there were no differences in mRNA levels between cells treated with cAMP or cilostazol. The difference in responses between macrophages and endothelial cells prompted investigation into the mechanism through which endothelial CD39 protein might accumulate in response to elevated cAMP levels. Results from this investigation provide novel insights into CD39 posttranslational regulation. Together, the conclusions of this study indicate that CD39 protein can be elevated using existing

pharmaceutical agents that have already been approved for clinical use. There is, therefore, potential for repurposing of this PDE3 inhibitor that was developed to treat claudication, in the manipulation of CD39 for medical benefit.

The third and final project describes the protective effects of CD39 overexpression in a transgenic mouse model of cerebral ischemia. A transgenic mouse was developed as a tool to study *in vivo* responses to globally over-expressed CD39 as well as tissue-specifically expressed CD39. Both types of transgenic mice had lower cerebral infarct volumes, and both exhibited fewer neurological deficits compared to wild-type mice. Globally transgenic mice also had fewer infiltrating macrophages and neutrophils, showed less tissue damage when brains were visualized after TTC staining, and had lower levels of pro-inflammatory cytokines localized to ischemic hemispheres. These results indicate that CD39 has a protective role against cerebral ischemia, and that elevated expression of CD39, even in mice that already express endogenous CD39, confers additional protection against tissue damage.

REFERENCES

1. Lohmann, K. 1929. Uber die pyrophosphatfraktion im muskel. *Naturwissenschaften* 17:624-625.
2. Lipmann, K. 1941. Metabolic generation and utilization of phosphate bond energy. *Adv. Enzymol.* 1:99-162.
3. Drury, A.N., and Szent-Gyorgyi, A. 1929. The physiological activity of adenine compounds with especial reference to their action upon the mammalian heart. *J Physiol* 68:213-237.

4. Meyerhof, O. 1945. The origin of the reaction of Harden and Young in cell-free alcoholic fermentation. *J. Biol. Chem.* 157:105-119.
5. Burnstock, G., Campbell, G., Satchell, D., and Smythe, A. 1970. Evidence that adenosine triphosphate or a related nucleotide is the transmitter substance released by non-adrenergic inhibitory nerves in the gut. *Br J Pharmacol* 40:668-688.
6. Burnstock, G. 1978. A basis for distinguising two types of purinergic receptor. In *Cell membrane receptors for drugs and hormones: A multidisciplinary approach.* New York: Raven Press.
7. North, R.A. 2002. Molecular physiology of P2X receptors. *Physiol Rev* 82:1013-1067.
8. Abbracchio, M.P., Burnstock, G., Boeynaems, J.M., Barnard, E.A., Boyer, J.L., Kennedy, C., Knight, G.E., Fumagalli, M., Gachet, C., Jacobson, K.A., et al. 2006. International Union of Pharmacology LVIII: update on the P2Y G protein-coupled nucleotide receptors: from molecular mechanisms and pathophysiology to therapy. *Pharmacol Rev* 58:281-341.
9. Burnstock, G. 1972. Purinergic nerves. *Pharmacol Rev* 24:509-581.
10. Burnstock, G. 1976. Do some nerve cells release more than one transmitter? *Neuroscience* 1:239-248.
11. Dubyak, G.R., and el-Moatassim, C. 1993. Signal transduction via P2-purinergic receptors for extracellular ATP and other nucleotides. *Am J Physiol* 265:C577-606.
12. Fabre, J.E., Nguyen, M., Latour, A., Keifer, J.A., Audoly, L.P., Coffman, T.M., and Koller, B.H. 1999. Decreased platelet aggregation, increased bleeding time and resistance to thromboembolism in P2Y1-deficient mice. *Nat Med* 5:1199-1202.
13. Di Virgilio, F., Sanz, J.M., Chiozzi, P., and Falzoni, S. 1999. The P2Z/P2X7 receptor of microglial cells: a novel immunomodulatory receptor. *Prog Brain Res* 120:355-368.
14. Di Virgilio, F., Chiozzi, P., Falzoni, S., Ferrari, D., Sanz, J.M., Venketaraman, V., and Baricordi, O.R. 1998. Cytolytic P2X purinoceptors. *Cell Death Differ* 5:191-199.
15. Fitz, J.G. 2007. Regulation of cellular ATP release. *Trans Am Clin Climatol Assoc* 118:199-208.
16. Collo, G., Neidhart, S., Kawashima, E., Kosco-Vilbois, M., North, R.A., and Buell, G. 1997. Tissue distribution of the P2X7 receptor. *Neuropharmacology* 36:1277-1283.
17. Kim, M., Jiang, L.H., Wilson, H.L., North, R.A., and Surprenant, A. 2001. Proteomic and functional evidence for a P2X7 receptor signalling complex. *EMBO J* 20:6347-6358.
18. Di Virgilio, F. 2007. Liaisons dangereuses: P2X(7) and the inflammasome. *Trends Pharmacol Sci* 28:465-472.

19. Dorsam, R.T., and Kunapuli, S.P. 2004. Central role of the P2Y12 receptor in platelet activation. *J Clin Invest* 113:340-345.
20. Wiviott, S.D., Braunwald, E., McCabe, C.H., Montalescot, G., Ruzyllo, W., Gottlieb, S., Neumann, F.J., Ardissino, D., De Servi, S., Murphy, S.A., et al. 2007. Prasugrel versus clopidogrel in patients with acute coronary syndromes. *N Engl J Med* 357:2001-2015.
21. Rowe, M., Hildreth, J.E., Rickinson, A.B., and Epstein, M.A. 1982. Monoclonal antibodies to Epstein-Barr virus-induced, transformation-associated cell surface antigens: binding patterns and effect upon virus-specific T-cell cytotoxicity. *Int J Cancer* 29:373-381.
22. Wang, T.F., and Guidotti, G. 1996. CD39 is an ecto-(Ca2+,Mg2+)-apyrase. *J Biol Chem* 271:9898-9901.
23. Handa, M., and Guidotti, G. 1996. Purification and cloning of a soluble ATP-diphosphohydrolase (apyrase) from potato tubers (Solanum tuberosum). *Biochem Biophys Res Commun* 218:916-923.
24. Wang, T.F., Ou, Y., and Guidotti, G. 1998. The transmembrane domains of ectoapyrase (CD39) affect its enzymatic activity and quaternary structure. *J Biol Chem* 273:24814-24821.
25. Koziak, K., Kaczmarek, E., Kittel, A., Sevigny, J., Blusztajn, J.K., Schulte Am Esch, J., 2nd, Imai, M., Guckelberger, O., Goepfert, C., Qawi, I., et al. 2000. Palmitoylation targets CD39/endothelial ATP diphosphohydrolase to caveolae. *J Biol Chem* 275:2057-2062.
26. Zhong, X., Kriz, R., Kumar, R., and Guidotti, G. 2005. Distinctive roles of endoplasmic reticulum and golgi glycosylation in functional surface expression of mammalian E-NTPDase1, CD39. *Biochim Biophys Acta* 1723:143-150.
27. Schwencke, C., Braun-Dullaeus, R.C., Wunderlich, C., and Strasser, R.H. 2006. Caveolae and caveolin in transmembrane signaling: Implications for human disease. *Cardiovasc Res* 70:42-49.
28. Resta, R., and Thompson, L.F. 1997. T cell signalling through CD73. *Cell Signal* 9:131-139.
29. Abbracchio, M.P., and Ceruti, S. 2007. P1 receptors and cytokine secretion. *Purinergic Signal* 3:13-25.
30. Johnston-Cox, H.A., and Ravid, K. 2011. Adenosine and blood platelets. *Purinergic Signal* 7:357-365.
31. Sato, A., Terata, K., Miura, H., Toyama, K., Loberiza, F.R., Jr., Hatoum, O.A., Saito, T., Sakuma, I., and Gutterman, D.D. 2005. Mechanism of vasodilation to adenosine in coronary arterioles from patients with heart disease. *Am J Physiol Heart Circ Physiol* 288:H1633-1640.
32. Lozano, R., Naghavi, M., Foreman, K., Lim, S., Shibuya, K., Aboyans, V., Abraham, J., Adair, T., Aggarwal, R., Ahn, S.Y., et al. 2012. Global and regional

mortality from 235 causes of death for 20 age groups in 1990 and 2010: a systematic analysis for the Global Burden of Disease Study 2010. *Lancet* 380:2095-2128.
33. Libby, P. 2002. Inflammation in atherosclerosis. *Nature* 420:868-874.
34. Jonasson, L., Holm, J., Skalli, O., Bondjers, G., and Hansson, G.K. 1986. Regional accumulations of T cells, macrophages, and smooth muscle cells in the human atherosclerotic plaque. *Arteriosclerosis* 6:131-138.
35. Galkina, E., and Ley, K. 2007. Vascular adhesion molecules in atherosclerosis. *Arterioscler Thromb Vasc Biol* 27:2292-2301.
36. Galkina, E., and Ley, K. 2009. Immune and inflammatory mechanisms of atherosclerosis (*). *Annu Rev Immunol* 27:165-197.
37. Berliner, J.A., Navab, M., Fogelman, A.M., Frank, J.S., Demer, L.L., Edwards, P.A., Watson, A.D., and Lusis, A.J. 1995. Atherosclerosis: basic mechanisms. Oxidation, inflammation, and genetics. *Circulation* 91:2488-2496.
38. Ross, R. 1999. Atherosclerosis--an inflammatory disease. *N Engl J Med* 340:115-126.
39. Libby, P. 2006. Inflammation and cardiovascular disease mechanisms. *Am J Clin Nutr* 83:456S-460S.
40. Harrison, P., and Cramer, E.M. 1993. Platelet alpha-granules. *Blood Rev* 7:52-62.
41. Youssefian, T., Masse, J.M., Rendu, F., Guichard, J., and Cramer, E.M. 1997. Platelet and megakaryocyte dense granules contain glycoproteins Ib and IIb-IIIa. *Blood* 89:4047-4057.
42. Schielke, G.P., Yang, G.Y., Shivers, B.D., and Betz, A.L. 1998. Reduced ischemic brain injury in interleukin-1 beta converting enzyme-deficient mice. *J Cereb Blood Flow Metab* 18:180-185.
43. Doyle, K.P., Simon, R.P., and Stenzel-Poore, M.P. 2008. Mechanisms of ischemic brain damage. *Neuropharmacology* 55:310-318.
44. Liu, T., McDonnell, P.C., Young, P.R., White, R.F., Siren, A.L., Hallenbeck, J.M., Barone, F.C., and Feurestein, G.Z. 1993. Interleukin-1 beta mRNA expression in ischemic rat cortex. *Stroke* 24:1746-1750; discussion 1750-1741.
45. Saha, P., Humphries, J., Modarai, B., Mattock, K., Waltham, M., Evans, C.E., Ahmad, A., Patel, A.S., Premaratne, S., Lyons, O.T., et al. 2011. Leukocytes and the natural history of deep vein thrombosis: current concepts and future directions. *Arterioscler Thromb Vasc Biol* 31:506-512.
46. Wakefield, T.W., Myers, D.D., and Henke, P.K. 2008. Mechanisms of venous thrombosis and resolution. *Arterioscler Thromb Vasc Biol* 28:387-391.
47. Cattaneo, M. 2010. New P2Y(12) inhibitors. *Circulation* 121:171-179.
48. Hulot, J.S., Bura, A., Villard, E., Azizi, M., Remones, V., Goyenvalle, C., Aiach, M., Lechat, P., and Gaussem, P. 2006. Cytochrome P450 2C19 loss-of-function

polymorphism is a major determinant of clopidogrel responsiveness in healthy subjects. *Blood* 108:2244-2247.

49. Mega, J.L., Close, S.L., Wiviott, S.D., Shen, L., Hockett, R.D., Brandt, J.T., Walker, J.R., Antman, E.M., Macias, W.L., Braunwald, E., et al. 2009. Cytochrome P450 genetic polymorphisms and the response to prasugrel: relationship to pharmacokinetic, pharmacodynamic, and clinical outcomes. *Circulation* 119:2553-2560.
50. Marcus, A.J., Broekman, M.J., Drosopoulos, J.H., Islam, N., Alyonycheva, T.N., Safier, L.B., Hajjar, K.A., Posnett, D.N., Schoenborn, M.A., Schooley, K.A., et al. 1997. The endothelial cell ecto-ADPase responsible for inhibition of platelet function is CD39. *J Clin Invest* 99:1351-1360.
51. Gayle, R.B., 3rd, Maliszewski, C.R., Gimpel, S.D., Schoenborn, M.A., Caspary, R.G., Richards, C., Brasel, K., Price, V., Drosopoulos, J.H., Islam, N., et al. 1998. Inhibition of platelet function by recombinant soluble ecto-ADPase/CD39. *J Clin Invest* 101:1851-1859.
52. Kaczmarek, E., Koziak, K., Sevigny, J., Siegel, J.B., Anrather, J., Beaudoin, A.R., Bach, F.H., and Robson, S.C. 1996. Identification and characterization of CD39/vascular ATP diphosphohydrolase. *J Biol Chem* 271:33116-33122.
53. Liao, J.K., and Laufs, U. 2005. Pleiotropic effects of statins. *Annu Rev Pharmacol Toxicol* 45:89-118.
54. Laufs, U., and Liao, J.K. 1998. Post-transcriptional regulation of endothelial nitric oxide synthase mRNA stability by Rho GTPase. *J Biol Chem* 273:24266-24271.
55. Goldstein, J.L., and Brown, M.S. 1990. Regulation of the mevalonate pathway. *Nature* 343:425-430.
56. Wennerberg, K., Rossman, K.L., and Der, C.J. 2005. The Ras superfamily at a glance. *J Cell Sci* 118:843-846.
57. Zhang, F.L., and Casey, P.J. 1996. Protein prenylation: molecular mechanisms and functional consequences. *Annu Rev Biochem* 65:241-269.
58. Kaneider, N.C., Egger, P., Dunzendorfer, S., Noris, P., Balduini, C.L., Gritti, D., Ricevuti, G., and Wiedermann, C.J. 2002. Reversal of thrombin-induced deactivation of CD39/ATPDase in endothelial cells by HMG-CoA reductase inhibition: effects on Rho-GTPase and adenosine nucleotide metabolism. *Arterioscler Thromb Vasc Biol* 22:894-900.
59. Liao, H., Hyman, M.C., Baek, A.E., Fukase, K., and Pinsky, D.J. 2010. cAMP/CREB-mediated transcriptional regulation of ectonucleoside triphosphate diphosphohydrolase 1 (CD39) expression. *J Biol Chem* 285:14791-14805.
60. Lugnier, C. 2006. Cyclic nucleotide phosphodiesterase (PDE) superfamily: a new target for the development of specific therapeutic agents. *Pharmacol Ther* 109:366-398.

61. Omori, K., and Kotera, J. 2007. Overview of PDEs and their regulation. *Circ Res* 100:309-327.

Chapter II: Transcriptional and Posttranslational Regulation of CD39

Abstract

CD39, an enzyme expressed on the plasma membrane of endothelial cells and leukocytes, phosphohydrolyzes ATP and ADP to generate AMP. CD39 is thus able to limit local levels of extracellular ATP and ADP, which are potent promoters of inflammation and platelet aggregation. This action has implications for a number of disease states, including atherosclerosis. HMG-CoA reductase inhibitors (statins) protect against atherosclerosis by inhibiting cholesterol synthesis, but they also limit inflammation and thrombosis, the mechanistic basis of which are not fully understood. We hypothesized that if CD39 expression were regulated by statins, it may underlie some of these pleiotropic protective mechanisms of statins.

CD39 is known to be targeted to caveolae, invaginated, cholesterol-rich plasma membrane domains linked to many cellular processes, including endocytosis, transcytosis, and various signaling pathways. The formation of caveolae depends on the presence of caveolin proteins, which associate with each other and with cholesterol. When treated with the statin fluvastatin (10 mM, 24 hrs), compared to control DMSO treatment, human umbilical vein endothelial cells (HUVECs) exhibit a significant

decrease in caveolin-1 (67%, $p<0.05$, n=4). HUVECS treated with fluvastatin exhibit significant increases in CD39 mRNA (13-fold, $p<0.01$ n=7), protein (8.1-fold over DMSO treatment, $p<0.01$, n=4) and activity (2.1-fold). CD39 mRNA and protein levels increase dose-dependently in response to fluvastatin treatment (0.1, 1, 10, 25μM). An siRNA construct was highly effective in silencing Cav-1 mRNA (85% reduction in Cav-1 mRNA and protein), and CD39 mRNA and protein levels were unaffected by Cav1 mRNA levels. Silencing Cav1 mRNA also did not prevent fluvastatin from increasing CD39 mRNA and protein (12- and 12-fold respectively). These data indicate that Cav1 levels do not modulate CD39 mRNA or protein. However, the question of whether the statin-driven disruption of caveolae imposes post-translational, localization, or functional changes of CD39 remains to be ascertained, but has potential implications for vascular diseases such as atherosclerosis.

Introduction

ATP is a biologically critical molecule that has distinct functions depending on where it is found. When compartmentalized within the intracellular environment, it is used as an energy source, but when released in the extracellular milieu, it signals injury and promotes platelet activation, platelet aggregation and inflammation (1-3). As discussed in Chapter I, CD39 is a nucleotidase expressed on the plasma membrane of endothelial cells and leukocytes, and it terminally phosphohydrolyzes ATP to generate

ADP and AMP (2, 4-12). This ecto-enzyme is co-expressed in plasmalemmal microdomains called caveolae with CD73 (13), another ectonucleotidase that hydrolyzes AMP to adenosine. Through this cascade mechanism, CD39 is able to locally dissipate extracellular ATP and ADP and simultaneously increase levels of AMP available for conversion to adenosine, thereby inhibiting platelet aggregation and the release of pro-inflammatory signals (2, 3, 12, 14-17). This potent endogenous molecule can, therefore, serve a protective role in a number of various disease states driven by thrombosis and inflammation, including stroke and atherosclerosis.

Atherosclerosis is a cardiovascular disease wherein blood vessels narrow as a result of cholesterol-rich plaque deposition, with both coagulation and inflammation contributing to its progression (1, 3, 18, 19). It is one of the leading causes of death in the US, and of the population between the ages of 40 and 75 who have or are at risk for cardiovascular disease, the majority of patients are prescribed HMG-CoA reductase inhibitors (statins) (20), a class of drugs that limit cholesterol synthesis. Numerous studies over recent years, however, have shown that statins are beneficial independent of their known property to inhibit the rate-limiting step in cholesterol synthesis (21-25). For example, they protect against inflammation and platelet aggregation (4, 23), help preserve endothelial function (26-28), promote neovascularization of ischemic tissue (29), and inhibit plaque rupture (30). The question of how statins exert these many pleiotropic effects remains largely unanswered, and the importance of investigating

these independent mechanisms is growing, not only due to interest from a basic scientific point of view, but also to the increasing prevalence of statin use at the population level, and the large population burden of atherosclerotic disease. The study of the myriad downstream effects of statins is not only informative about how statins work, but also about how these statin-driven mechanisms can best be utilized in the search for novel therapeutic strategies. Therefore, this project aims to establish whether statins can act independently of their lipid-lowering effects, through CD39 regulation, to deliver pleiotropic benefits. While there are several ways through which statins might modulate CD39, this project focuses on the question of how CD39 changes after statins suppress the formation of the CD39 microenvironment, the caveola.

Caveolae are part of many cellular processes, including endocytosis, transcytosis, cholesterol transport, and numerous signaling pathways (31-42), and caveolae in endothelial cells have been shown to contribute to the progression of atherosclerosis. Previous studies have demonstrated that CD39 is targeted by way of palmitoylation to caveolae (6), where the co-localization of CD39 and CD73 allows the coordinated breakdown of ATP down to adenosine. The concerted action of this enzyme pair restores vascular homeostasis, by dissipating ATP and ADP (pro-inflammatory and pro-coagulant signals) as well as by increasing the anti-inflammatory and the endothelial-protective signal of adenosine (2, 3, 12, 15). The formation of caveolae requires the presence of caveolin proteins, which associate with each other and with

cholesterol to form endocytic vesicles that bud into the cell surface, resulting in the invagination of the plasmalemma. Proteins that are targeted to caveolae are already present in these endocytic vesicles (pro-caveolae), and their targeting to caveolae is often determined by post-translational modifications (e.g. palmitoylation). In endothelial cells, the predominant caveolin proteins are caveolin-1 and -2, with caveolin-1 determining whether caveolae will form and with caveolin-2 serving a relatively minor role in determining caveolar morphology. When treated with statins, caveolin-1 expression in endothelial cells has been shown to decrease (42). Our data show that CD39 mRNA, protein, and activity all increase with statin treatment, and others have shown that CD39 remains inactive until it has reached the plasma membrane (7). These data suggest that CD39 is capable of residing on the plasma membrane, independent of caveolae, and that normal trafficking of CD39 may be altered in the presence of statins.

To date, the specific role of the caveolar microenvironment in determining CD39 activity, and the physiological relevance of statin-mediated disruption of caveolae for CD39 function and events downstream thereof are unknown. In endeavoring to answer these questions, the intent of this project is to further our knowledge about the enzyme CD39, which plays a demonstrably critical role in inhibiting inflammation and coagulation. The research presented below addresses the possibility of pharmacologically regulating CD39 and the microenvironment in which it resides.

Furthermore, these experiments address the issue of how the presence of statins and regulation of the CD39 microenvironment might modulate the capacity of CD39 to function, and the beneficial effects of this in an integrated biological system, with implications for the disease states of atherosclerosis and deep vein thrombosis (DVT) in particular.

Methods

Human umbilical vein endothelial cell (HUVEC) isolation

Fresh umbilical cords were rinsed in an isotonic buffer composed of sterile ddH_2O, glucose, NaCl, KCl, and HEPES. The ends were trimmed and a sterile 10 mL syringe was inserted into umbilical cord veins and held in place with sterilized surgical sutures. Veins were washed three times with 5 mL of buffer each time, and then injected with collagenase III, and the open end held shut with sterilized hemostatic clamps. Cords were left to digest at 37 °C for 15 minutes. Collagenase from veins was collected, diluted with more isotonic buffer, and centrifuged for 4 minutes at 4 °C and 190 x g. The resulting pellets were gently resuspended in complete growth media composed of M199 media (Invitrogen), 20% FBS (Sigma), and supplemented with 1% penicillin/streptomycin, $NaHCO_3$, L-glutamine and ECGS. Cells were then plated onto 35 mm gelatin-coated dishes and used through the fourth passage.

Statin treatment

The statins fluvastatin, mevastatin, lovastatin, simvastatin and pravastatin were used. Stock solutions were made in DMSO and added to cells at a final concentration of 10 μM in serum-free growth medium. Controls were treated with equal corresponding volumes of DMSO. Pravastatin was also used as a control, as the highly hydrophilic nature of pravastatin prevents its uptake by cells, and can thus serve as a control treatment (26, 43). HUVECs were treated with a varying range of statin doses over a range of treatment durations. Five different statins were tested individually in order to assess the capability of statins in general to induce *CD39* expression.

RNA isolation and quantification

HUVECs were washed twice with ice-cold PBS (Gibco) and reagents from a Qiagen RNeasy kit were used to complete RNA isolation. Purified RNA was measured immediately using a spectrometer and then diluted to a concentration of 1 μg/10 μL of water. A cDNA synthesis kit (Applied Biosystems) was used to make cDNA, which was then used in further analyses via qRT-PCR. Specific primers for human *CD39* and *CAV1* were used (Applied Biosystems). All samples were normalized by expression relative to human β_2-microglobulin.

Thin Layer Chromatography

HUVECs were treated with either fluvastatin or DMSO in preparation for thin-layer chromatography (TLC), to measure differences in ATP phosphohydrolysis as a measurement of CD39 activity (44). Cells were incubated with [8-^{14}C]ATP in the presence of the following inhibitors: ouabain to inhibit the Na^+/K^+-ATPase, α,β-methylene adenosine 5′-diphophate (APCP) to inhibit the conversion of AMP to adenosine by CD73, and AKI to inhibit the conversion of ADP into ATP and AMP by adenylate kinase. These inhibitors are necessary to isolate the phosphohydrolysis of ATP by CD39. Control cells received an equal volume of media. The reaction mixture was stopped with 8 M formic acid and spotted onto silica gel TLC plates, where nucleotides were separated. The enzymatic activity of CD39 was assessed by densitometrically measuring the relative levels of [8-^{14}C]ATP, [8-^{14}C]ADP, and [8-^{14}C]AMP. Enzymatic activity increased with fluvastatin treatment relative to control treatment. This measurement was normalized by total cell number, and future experiments will be normalized by CD39 protein concentration.

Immunostaining

HUVECs were grown in Labtek chamber slides (Thermo Scientific) coated with 2% gelatin. Cells were treated with either fluvastatin of DMSO before being washed twice in wash buffer composed of 1% BSA (Sigma), and 0.02 M glycine (Sigma) in PBS. Slides were fixed in ice-cold methanol for 10 minutes, and then endogenous peroxidase

activity quenched with 0.3% H_2O_2 for 30 minutes. Slides were then washed and blocked for 1 hr at RT (Vectorlabs), and then incubated with primary antibodies for CD39 (AbCam) overnight at 4 °C in a humid chamber. Slides were then washed and incubated with biotinylated secondary anti-mouse antibodies for 30 minutes. ABC reagent, a preformed avidin-biotin peroxidase complex, (Vectorlabs) was then added for 30 minutes at room temperature. A tetramethylrhodamine-labeled tyramide (Perkin-Elmer) was added for 4 minutes at room temperature, and then slides were washed again. In dual stained slides, the procedure was repeated for a second set of antibodies for CAV1 detection (AbCam) with fluorescein (Perkin-Elmer). In the final set of washes, 1 μg/mL of DAPI was added as a counter stain. Slides were mounted with Prolong Gold Antifade Reagent (Invitrogen), and slides were allowed to cure in the dark at room temperature for 24 hours. Slides were then sealed with nail polish and immediately imaged on an Eclipse TE2000-E microscope (Nikon Instruments) using MetaMorph software (Molecular Devices). Slides were then stored at -20 °C.

Confocal imaging

HUVECs were fluorescently labeled with antibodies as described above and visualized using a 100x oil objective on an Olympus IX-71 inverted confocal microscope. Each image shown is from one slice of a z-series. After DMSO treatment, cells express basal levels of CD39 and CAV1 localized to the plasma membrane. After fluvastatin

treatment, CD39 staining shows brighter staining, and CAV1 staining shows a more diffuse intracellular pattern of distribution (**Figure 2.3**).

Membrane protein preparation

Cells were washed twice with ice-cold PBS (Gibco) and scraped off the plate with a rubber policeman. Ice-cold hypotonic lysis buffer was added containing 50 mM sucrose, 10 mM Hepes pH 7.4, and one tablet of a complete protease inhibitor tablet (Roche). Cells were then transferred to a Dounce homogenizer (Kontes Glass) and homogenized with 25 strokes of a tight pestle. 264 μL of a second buffer containing 65% sucrose in 10 mM Hepes was added to 2 mL of the homogenate and then centrifuged twice for 20 minutes at 2,000 x g at 4 °C in order to separate nuclei, mitochondria and cellular debris. Membranes were purified from the supernatant by centrifuging again for 30 minutes at 100,000 x g at 4 °C. The final pellet was washed in hypotonic lysis buffer and then resuspended in the second buffer. Membranes were frozen at -80 °C.

Western blot

After protein was harvested and measured using a Bio-Rad protein assay, equal amounts of protein were mixed with LDS loading buffer (Invitrogen) and boiled for 3 minutes at 100 °C. Proteins were then loaded onto 10% Bis-Tris or 4-12% Bis-Tris polyacrylamide gels. Gels were then transferred onto PVDF membranes, blocked for 1

hr with 5% NFDM/0.05% TBS-T, and then incubated with primary antibody against CD39 (AbCam) overnight at 4 °C. Membranes were then washed 3x in TBS-T and then incubated with a peroxidase labeled anti-mouse secondary antibody (Sigma). Membranes were washed again 3x and then autoradiographed using the enhanced chemiluminescence detection system (Amersham).

Electron Microscopy with cerium chloride staining to observe ATPase activity

HUVECs were treated with either fluvastatin or DMSO. Following 24 hours of treatment, cells were washed with an ice-cold solution of 0.05 M Na-cacodylate buffer, pH 7.2. Cells were then fixed for 10 minutes with 2% paraformaldehyde, 0.5% glutaraldehyde, 0.25 mM sucrose, 2 mM $MgCl_2$ in the same 0.05 M Na-cacodylate buffer. Cells were then incubated for 20 minutes at 37 °C in reaction buffer containing 0.01 M Tris-maleate buffer, 2 mM ATP, 2 mM $MgCl_2$, 20 mM KCl, 100 mM ouabain, and 2 mM $CeCl_3$. Cells were then embedded in a thin layer of histopaque, and rinsed in Tris-maleate buffer and cacodylate buffer before post-fixation with 1% OsO_4. Cells were dehydrated in ethanol, exposed to propylene oxide, and a jeweler's saw was used to cut the fixed tissue from the plastic dish on which the cells were grown. Cells were then embedded in Epon. Blocks were then cut into 40 nm sections using a Reichert Ultracut-E (Leica Microsystems Inc.) and imaged with a Philips CM-100 transmission electron microscope.

Transgenic mouse generation

Human CD39 cDNA was inserted into the following vector, pcCALL2: CMV/Chicken β-actin promoter/enhancer, followed by a floxed stop signal encoded by three consecutive poly A sequences, followed by multiple cut sites for the gene insertion, along with a Neo cassette for selection (45). Five transgenic founder mice were born, and were bred to establish the transgenic colony. Transgenic progeny were crossed with tissue-specific Cre mice to generate mice that overexpress human CD39 in specific tissues. The availability of species-specific antibodies for CD39 will make it possible to differentiate endogenous mouse CD39 from CD39 produced from the transgene.

Flow Cytometry

Lungs from mice were rinsed briefly in PBS, and minced thoroughly. Minced tissue was then transferred to into 2% collagenase A in PBS for 40 minutes at 37 °C and then pushed through an 18 G syringe. The resulting homogenate was then pushed through a 50 μM filter and washed in FACS buffer containing 5% FBS and 0.1% NaN_3 in PBS. Red cells were lysed using ACK (ammonium-chloride-potassium) lysis buffer (Invitrogen), and then cells were pelleted in FACS tubes for 4 minutes at 190 x g, resuspended in 100 μL of FACS buffer, and blocked with Fc block (BD Pharmingen) for

30 minutes at 4°C. Cells were then stained with PE –labeled primary mouse antibody against CD39 for 30 minutes at 4 °C. Cells were washed 3x in FACS buffer, and immediately analyzed on a BD FACSCalibur unit.

Statistics

Data was analyzed by one-way ANOVA and statistical significance will be determined by $p<0.05$. Prism software will be used for analyses. All experiments contain an n=6.

Results

CD39 mRNA levels increased in a dose-dependent manner following statin administration (1 to 50 μM, data not shown), and a dose of 10 μM was chosen for use in all subsequent experiments. This dose was chosen because it was the lowest dose at which maximum induction of CD39 was observed. A time point of 24 hours was standardized for all experiments based on the expression of CD39 mRNA after statin treatment, which was the highest at 24 hours (**Figure 2.1A**). Parameters were narrowed to include one statin and pravastatin (control) instead of the original set of five statins, due to the similar responses observed after treatment (data not shown). Fluvastatin was selected out of these. Pravastatin, a relatively hydrophilic statin, served as a control as its hydrophilic nature prevents its uptake into cells. Silencing *CAV1* expression (80%

decrease) using a siRNA against *CAV1* did not change the ability of fluvastatin to increase *CD39* expression (**Figures 2.1B** and **2.1C**).

Figure 2.1: *CD39* mRNA increases after statin treatment but *CAV1* mRNA is not affected. A) HUVECs were treated with 10 μM fluvastatin for the indicated times and CD39 mRNA was measured. B) HUVECs were treated with DMSO, fluvastatin, control siRNA, siRNA against Cav1, or both fluvastatin and Cav1 siRNA. Cav1 mRNA was measured. C) HUVECs were treated as in panel B, and CD39 mRNA was measured.

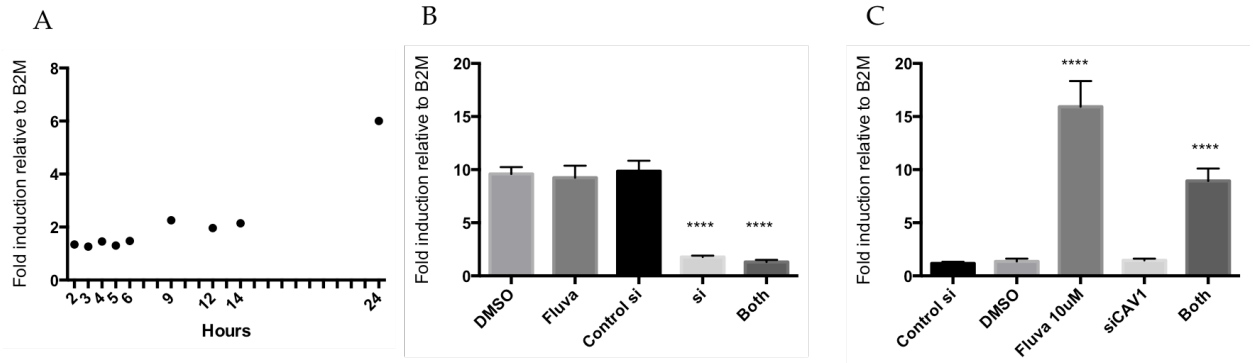

Cell membrane proteins of a parallel set of HUVECs were harvested for protein analysis by Western blot. CD39 protein increased in a dose-dependent manner following statin treatment, whereas pravastatin did not induce CD39 protein expression, confirming its use as a vehicle control (**Figure 2.2A**). In contrast, CAV1 protein decreased following statin treatment as expected, as depletion of cholesterol has been shown to disrupt the formation of caveolae by downregulating Cav1 expression (**Figure 2.2B**). Samples from cell in which CAV1 mRNA was silenced using a siRNA also show that CAV1 protein is

diminished, while CD39 protein is elevated, after statin (fluvastatin, 10 μM) treatment (**Figure 2.2C** and **2.2D**).

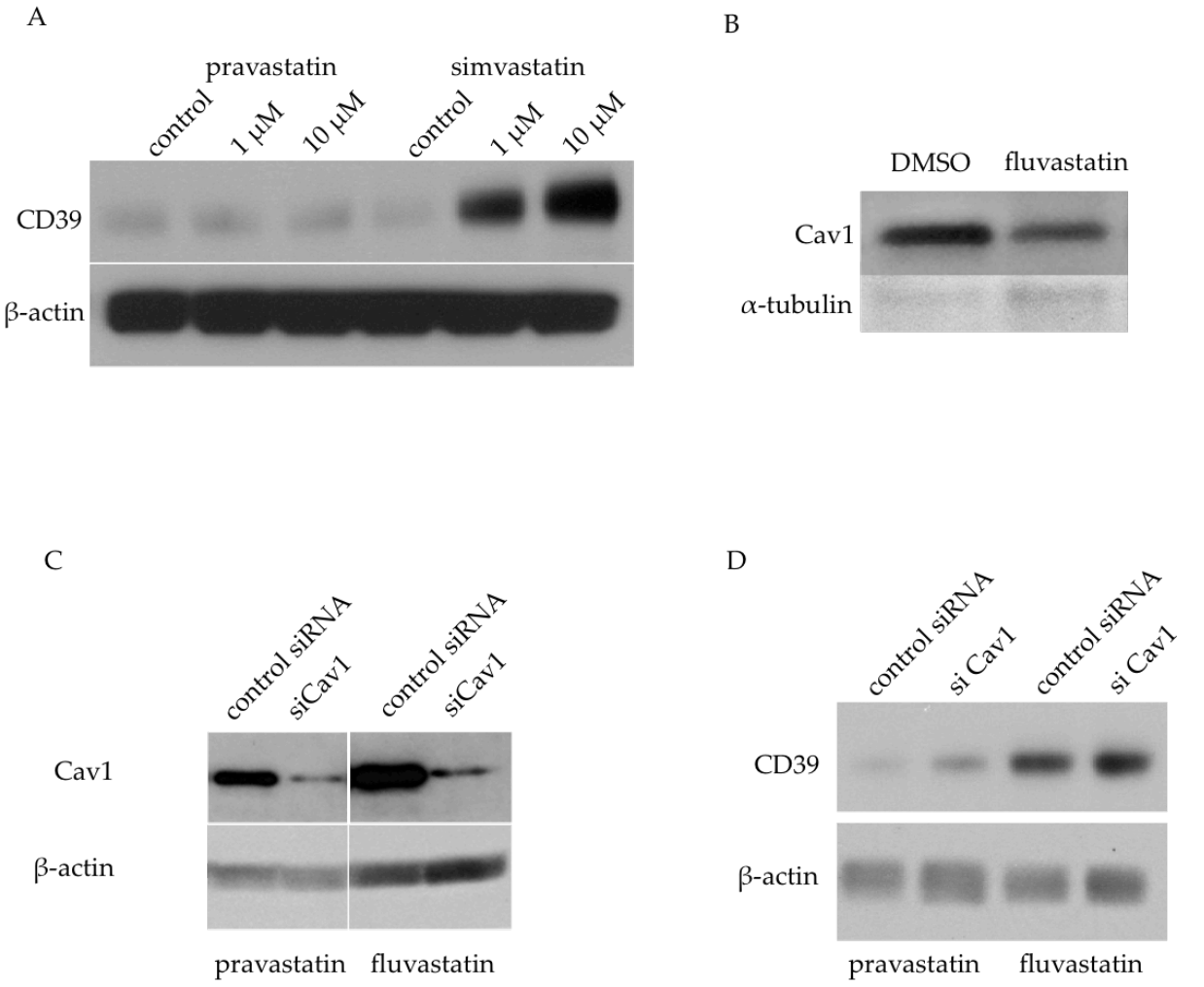

Figure 2.2: CD39 protein increases after statin treatment, whereas CAV1 protein decreases. A) HUVECs were treated with either pravastatin as a control or fluvastatin for 24 hours, and CD39 protein measured by Western blot. B) HUVECs were treated with either DMSO or 10 μM fluvastatin for 24 hours and Cav1 protein was measured by Western blot. C) HUVECs were either transfected with control siRNA or siRNA against Cav1, and treated with pravastatin as control or fluvastatin for 24 hours. D) HUVECs were treated with control siRNA or siRNA against Cav1, and treated with pravastatin as control or fluvastatin for 24 hours.

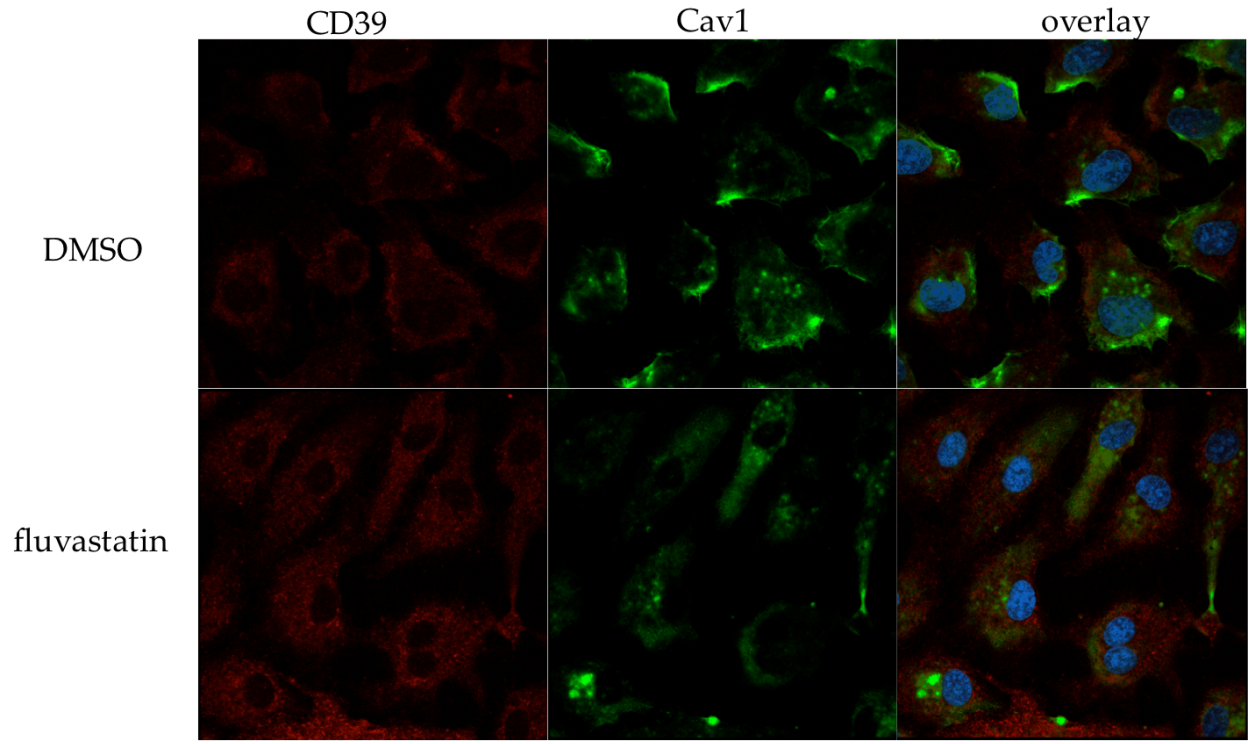

Figure 2.3: HUVECs were treated with fluvastatin or DMSO and then Cav1 (green) and CD39 (red) were detected immunofluorescently. DAPI was used as a counter stain. Images are shown at 20x magnification using a confocal microscope. Each panel show one slice of a z-stack image of 1 micron depth.

Then, cells treated with statins or control DMSO were visualized using confocal microscopy, in order to visualize the localization of CD39 and CAV1 (**Figure 2.3**). CD39 expression is elevated in the presence of statins, and the expression patterns of both CAV1 and CD39 become more diffuse and less localized to the plasma membrane after statin treatment.

Next, activity of CD39 was measured in the presence and absence of statins, in order to determine whether statin-induced CD39 is functional. CD39 activity was measured using thin layer chromatography and radio-labeled ATP (**Figure 2.4A**).

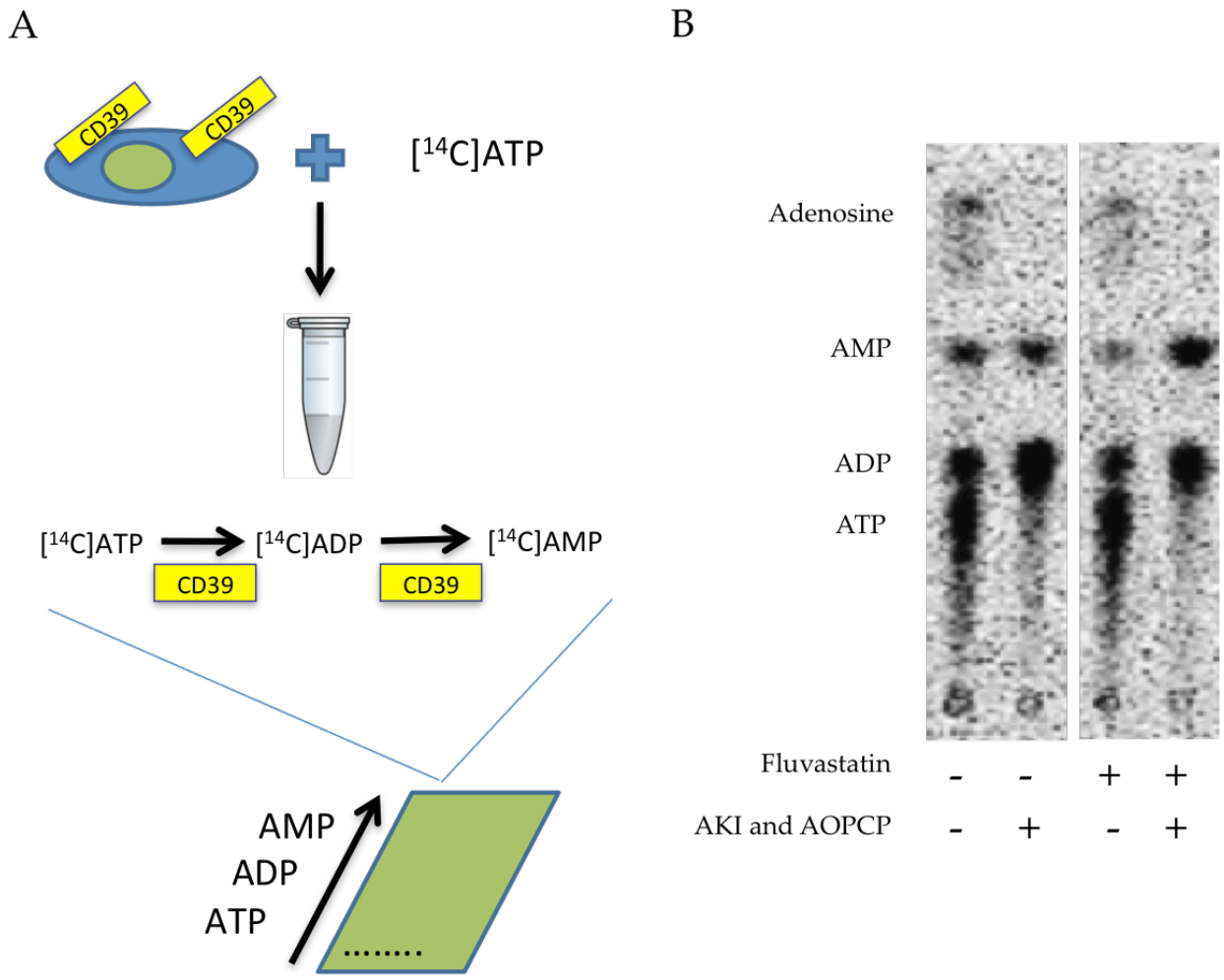

Figure 2.4: CD39 enzymatic activity increases after statin treatment. A) A schematic of the thin layer chromatography assay used to measure CD39 activity. B) HUVECs were treated with either fluvastatin or DMSO, and then apyrase activity was measured by TLC. Adenylate kinase inhibitor (AKI) and APCP were added in order to prevent interconversion of adenine nucleotides and inhibit CD73 activity, respectively.

The conversion of labeled ATP to AMP was greater in samples containing fluvastatin treated HUVECs (34% versus 16%). Ouabain and inhibitors for adenylate kinase and CD73 were included in order to inhibit the activity of Na^+/K^+ pumps, to

prevent back conversion of ADP to AMP and ATP, to prevent the degradation of AMP to adenosine, respectively (**Figure 2.4B**).

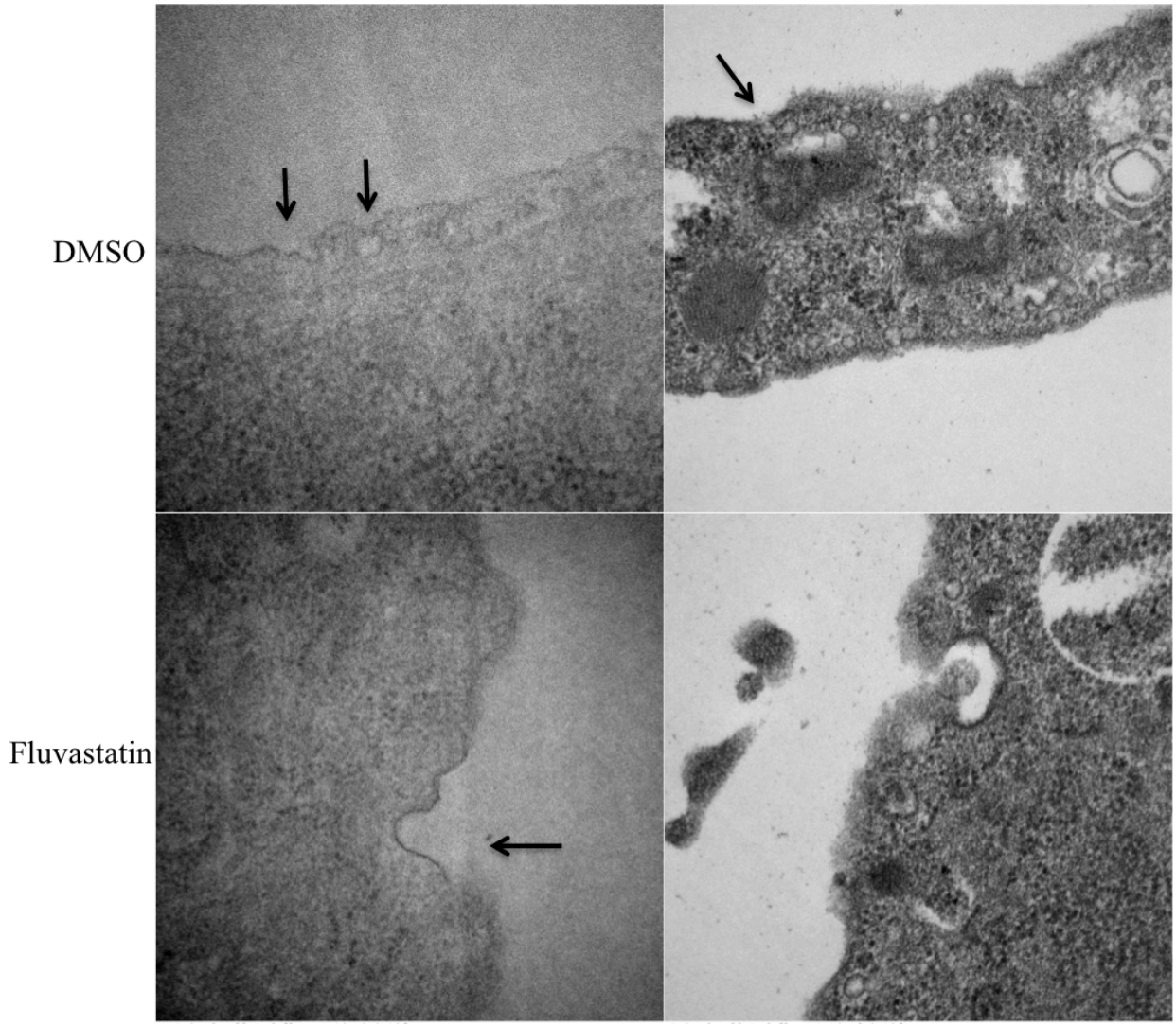

Figure 2.5: Statin treatment disrupts caveolae in endothelial cells. HUVECs were treated with either DMSO or fluvastatin and then electron micrographs were taken along the plasmalemma. Electron micrographs to the left are 92,000x magnified and the micrographs to the right are 64,000 x magnified.

HUVECs were then treated with fluvastatin (10μM) or DMSO and imaged via transmission electron microscopy (TEM) (**Figure 2.5**). The images show that the presence of fluvastatin disrupts the formation of caveolae, and that whatever invaginations are visible are morphologically different from DMSO treated samples, both in terms of size and shape. The presence of fluvastatin alters caveola shape so that rather than retaining their classical Ω shape, they appear larger and less invaginated.

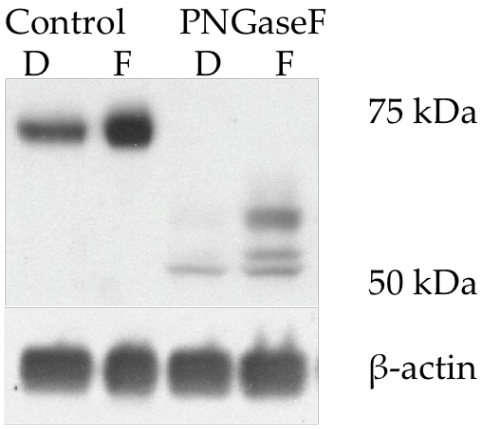

Figure 2.6: CD39 protein is modified after statin treatment. HUVECs were treated with either DMSO (D) or fluvastatin (F) for 24 hours. After protein was harvested, samples were treated with PNGaseF to eliminate N-glycosylation. Samples were then analyzed by Western blot.

CD39 is a heavily glycosylated protein, and the addition of N-linked glycans to CD39 is necessary proper localization of CD39 (7). In order to test whether the presence of statins also changed the posttranslational state of CD39, we removed all N-linked glycans from CD39. Membrane preparations of HUVECs treated with either DMSO or fluvastatin (10μM) were harvested for protein analysis by Western blot (10% Bis-Tris

gel). Samples were incubated with PNGase F in order to deglycosylate CD39 (**Figure 2.6**). PNGase F removes all N-glycosylations. CD39 protein samples were cleaved by PNGase F, and digestion reveals three distinct bands of CD39 in statin treated samples. In contrast, only the lower band is present in DMSO-treated samples.

In order to investigate the action of statins on CD39 and caveolae in a biological system, a transgenic mouse was designed using the following cloning and breeding scheme (**Figure 2.7**). Human CD39 will be expressed in mice after the engineered stop signal that interrupts transcriptional activity is excised. This excision is accomplished by the co-expression of Cre recombinase, which excises all DNA found between flanking LoxP sites.

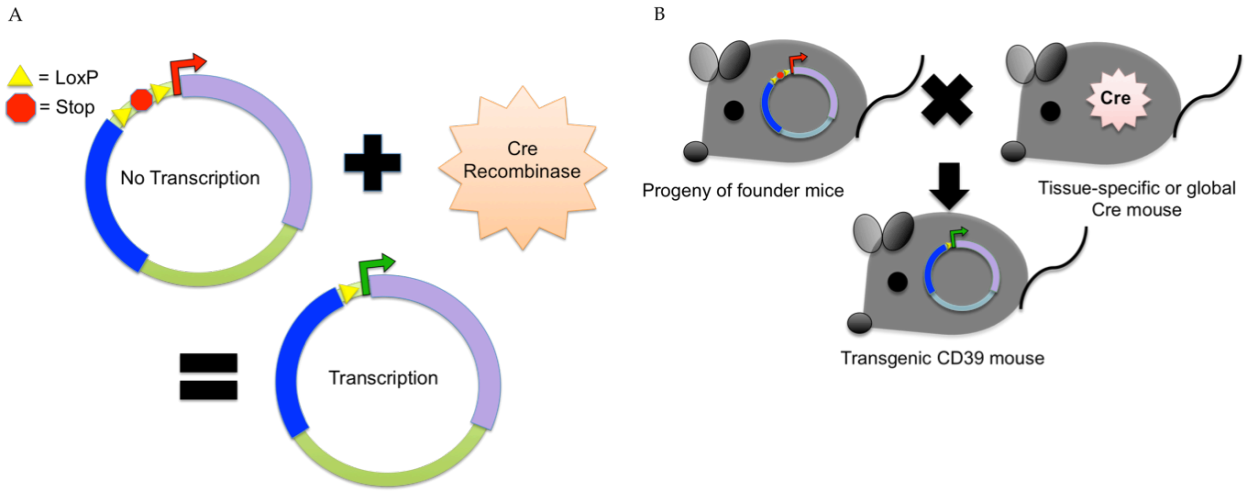

Figure 2.7: Schematic representation of transgenic mouse design and generation. A) A construct containing a chicken β-actin promter/CMV enhancer promoter (blue) followed by a floxed stop signal was obtained and the sequence for full length CD39 was inserted. In the presence of cre recombinase, the stop signal, composed of a polyA sequence, is excised, and transcription is enabled. B) Expressed in mice, those that carry the stop sequence do not express human CD39. Once bred with mice expressing cre recombinase, offspring that carry the recombined gene will express human CD39.

Figure 2.8A shows a positive-control standard using known concentrations of the CD39-pCALL2 plasmid in mouse tail DNA. The result of a genotyping PCR follows. DNA samples from 17 mice were analyzed, and the five visible bands indicate founder mice, which carry hCD39 (**Figure 2.8B**).

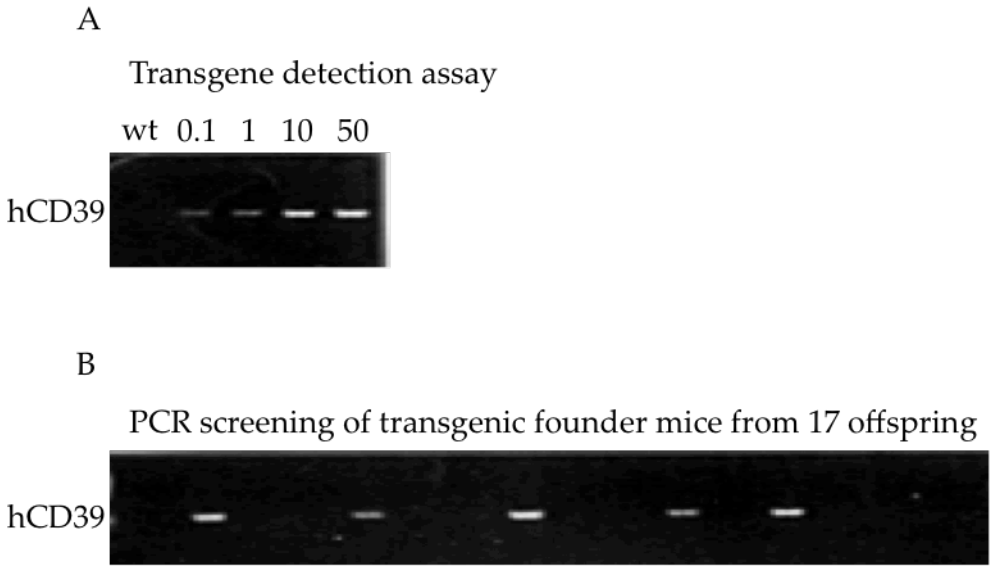

Figure 2.8: An assay to detect human CD39 in transgenic mice was developed. A) Five mouse DNA samples were probed with specific primers for human CD39 via PCR, and then separated by gel electrophoresis. All lanes contained normal wild type C57bl/6 mouse genomic DNA, and lanes 2-5 were loaded with the indicated copy number (calculated based on DNA concentration) of the human transgene. B) The human CD39 transgene was microinjected into C57Bl/6 eggs and transferred to female mice. DNA was taken from mouse tails of the first litter born from these mice, and probed with specific primers for human CD39 in order to identify transgenic founders. Out of 17 mice, 5 mice expressed the transgene.

Flow cytometric quantification and comparison of CD39 expression levels was conducted on lung tissue. Lungs were harvested from mice and then minced. Cells were dissociated by incubating the minced tissue in collagenase A, and then passing the

digested tissue through a 50 μm mesh filter. Analysis shows that transgenic progeny of global-Cre mice (EIIA) have approximately 5-fold higher expression compared to non-transgenic litter mates (5.02% of total compared to 24.43% for 50,000 events) (**Figure 2.9**).

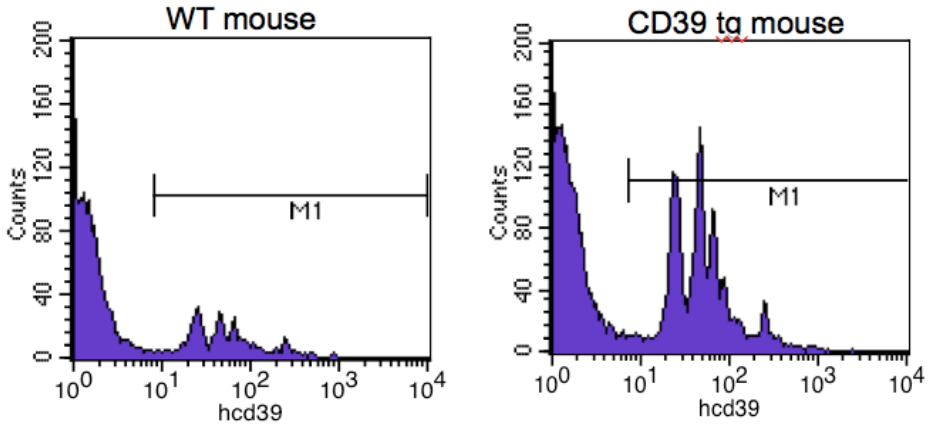

Figure 2.9: Transgenic mice express more CD39. Transgenic mice expressing the human transgene were bred with mice expressing cre recombinase driven by the global EIIA promoter. Lungs from transgenic offspring of these mice expressing the recombined (active) transgene and wild type mice were harvested and analyzed by flow cytometry. Cells were labeled with a human CD39 antibody. Unlabeled cells are shown between 10^0 and 10^1, and positively labeled cells are shown between 10^1 and 10^4.

Discussion

This project set out to determine whether the increase of CD39 activity observed after statin treatment is mediated by regulation of CD39 post-translational modifications, by changes in topographic CD39 localization, or by both of these mechanisms in concert. Previous studies have described the preferential expression of CD39 in cholesterol-rich domains called caveolae (6). Caveolae measure between 60 and

80 nm in diameter, and can be imaged using electron microscopy (41). Functions attributed to caveolae include signal transduction, endocytosis, suppression of eNOS, and cholesterol regulation. Endothelial caveolae contain caveolin-1 (CAV1) proteins, which are associated with cholesterol, and which are required to form their Ω-shaped structures (46). Due to their requirement for caveolin-1 and cholesterol, they are readily distinguished from lipid rafts by caveolin-1 protein expression, and demonstrably disrupted by several methods of cholesterol depletion and small interfering RNAs (siRNA) against CAV1. Some studies indicate that the structure of caveolae may be disrupted in the presence of statins (47, 48), as inferred by measurements of CAV1 protein, and observed in electron micrographs of smooth muscle cells (which also form caveolae, but with CAV3 instead of CAV1). Electron micrographs of CD39 enzymatic activity showed highly concentrated, punctate areas of activity on the surface of cells expressing either full-length CD39 or C-terminus truncated mutant CD39 (6). On the other hand, the N-terminus truncated mutant-CD39 expressing cells showed no activity. CD39 is palmitoylated at the N-terminus, and it has been demonstrated that this specific fatty-acid modification targets CD39 to caveolae. Since our data show that CD39 remains active after statin treatment, and we know that CD39 activity is kept suppressed until it reaches the plasma membrane, it follows that CD39 must either localize elsewhere following statin treatment, perhaps in other cholesterol-rich lipid rafts, due to the fact that CD39 is targeted to caveolae in basal states and that caveolae

are reportedly sensitive to fluctuations in cholesterol availability (9). If CD39 membrane localization is indeed altered by statin treatment, then it leads to the question of whether statins specifically affect CD39 function. Indeed, the activity of the vasculoprotective endothelial nitric oxide synthase (eNOS), another protein localized to caveolae, is suppressed by interactions with caveolin proteins (42). eNOS activity is also increased by the presence of statins, which deplete caveolin-1 protein. Our initial results suggest that such a mechanism may be possible in the case of CD39 as well, since the presence of statins appears to change the posttranslational state of CD39 (**Figure 2.5**). Therefore, we hypothesized that statin mediated disruption of caveolae, will result in altered CD39 membrane localization and an increase in CD39 activity that is driven by differential post-translational modifications of CD39.

In Vivo investigation of CD39 and caveolae

The second major aim of this project was to determine whether statin-driven changes in CD39 expression, localization, and activity are physiologically relevant to the anti-inflammatory and anti-thrombotic effects of CD39 *in vivo*. For this purpose, a transgenic CD39 mouse was generated and characterized with the aim of testing CD39 trafficking in mice, in comparison to caveolin-1 knockout mice.

Overall significance

CD39 is an important vascular enzyme, which, based on its potential as a target for therapeutic innovation alone, merits further study. It tips the balance of the scale against inflammation and against thrombosis, and yet there are many questions pertaining to the fundamental aspects of this enzyme's form, function, and regulation that have not been answered in the literature. Added to this, is the ever-increasing proportion of the population that is currently using statin drugs. By 2002, 87% of all lipid-lowering medications used were statins (49), and in between 2005 and 2008, 25% of adults over 45 years of age used statins (50). That these drugs have other effects is not necessarily surprising, but the idea that one of these effects is the positive regulation of an independently potent and protective enzyme certainly is. The purpose of this project was not simply to further our knowledge about the enzyme CD39, but to understand the dynamic adaptations of CD39 in response to its changing environment. In continuing this work in the future, many questions come to mind that should be addressed. To this end, a research plan has been developed that is focused on the posttranslational regulation of CD39 in the context of its microenvironment, and will be discussed in Chapter V.

REFERENCES

1. Gawaz, M., Langer, H., and May, A. E. (2005) Platelets in inflammation and atherogenesis. *The Journal of clinical investigation* **115**, 3378-3384
2. Dwyer, K. M., Robson, S. C., Nandurkar, H. H., Campbell, D. J., Gock, H., Murray-Segal, L. J., Fisicaro, N., Mysore, T. B., Kaczmarek, E., Cowan, P. J., and d'Apice, A. J. (2004) Thromboregulatory manifestations in human CD39 transgenic mice and the implications for thrombotic disease and transplantation. *The Journal of clinical investigation* **113**, 1440-1446
3. Di Virgilio, F., and Solini, A. (2002) P2 receptors: new potential players in atherosclerosis. *British journal of pharmacology* **135**, 831-842
4. Hyman, M. C., Petrovic-Djergovic, D., Visovatti, S. H., Liao, H., Yanamadala, S., Bouis, D., Su, E. J., Lawrence, D. A., Broekman, M. J., Marcus, A. J., and Pinsky, D. J. (2009) Self-regulation of inflammatory cell trafficking in mice by the leukocyte surface apyrase CD39. *The Journal of clinical investigation* **119**, 1136-1149
5. Kaneider, N. C., Egger, P., Dunzendorfer, S., Noris, P., Balduini, C. L., Gritti, D., Ricevuti, G., and Wiedermann, C. J. (2002) Reversal of thrombin-induced deactivation of CD39/ATPDase in endothelial cells by HMG-CoA reductase inhibition: effects on Rho-GTPase and adenosine nucleotide metabolism. *Arteriosclerosis, thrombosis, and vascular biology* **22**, 894-900
6. Koziak, K., Kaczmarek, E., Kittel, A., Sevigny, J., Blusztajn, J. K., Schulte Am Esch, J., 2nd, Imai, M., Guckelberger, O., Goepfert, C., Qawi, I., and Robson, S. C. (2000) Palmitoylation targets CD39/endothelial ATP diphosphohydrolase to caveolae. *The Journal of biological chemistry* **275**, 2057-2062
7. Zhong, X., Malhotra, R., Woodruff, R., and Guidotti, G. (2001) Mammalian plasma membrane ecto-nucleoside triphosphate diphosphohydrolase 1, CD39, is not active intracellularly. The N-glycosylation state of CD39 correlates with surface activity and localization. *The Journal of biological chemistry* **276**, 41518-41525
8. Zhong, X., Kriz, R., Kumar, R., and Guidotti, G. (2005) Distinctive roles of endoplasmic reticulum and golgi glycosylation in functional surface expression of mammalian E-NTPDase1, CD39. *Biochimica et biophysica acta* **1723**, 143-150
9. Papanikolaou, A., Papafotika, A., Murphy, C., Papamarcaki, T., Tsolas, O., Drab, M., Kurzchalia, T. V., Kasper, M., and Christoforidis, S. (2005) Cholesterol-dependent lipid assemblies regulate the activity of the ecto-nucleotidase CD39. *The Journal of biological chemistry* **280**, 26406-26414

10. Eltzschig, H. K., Kohler, D., Eckle, T., Kong, T., Robson, S. C., and Colgan, S. P. (2009) Central role of Sp1-regulated CD39 in hypoxia/ischemia protection. *Blood* **113**, 224-232
11. Liao, H., Hyman, M. C., Baek, A. E., Fukase, K., and Pinsky, D. J. (2010) cAMP/CREB-mediated transcriptional regulation of ectonucleoside triphosphate diphosphohydrolase 1 (CD39) expression. *The Journal of biological chemistry* **285**, 14791-14805
12. Robson, S. C., Kaczmarek, E., Siegel, J. B., Candinas, D., Koziak, K., Millan, M., Hancock, W. W., and Bach, F. H. (1997) Loss of ATP diphosphohydrolase activity with endothelial cell activation. *The Journal of experimental medicine* **185**, 153-163
13. Kittel, A., Kiss, A. L., Mullner, N., Matko, I., and Sperlagh, B. (2005) Expression of NTPDase1 and caveolins in human cardiovascular disease. *Histochemistry and cell biology* **124**, 51-59
14. Enjyoji, K., Sevigny, J., Lin, Y., Frenette, P. S., Christie, P. D., Esch, J. S., 2nd, Imai, M., Edelberg, J. M., Rayburn, H., Lech, M., Beeler, D. L., Csizmadia, E., Wagner, D. D., Robson, S. C., and Rosenberg, R. D. (1999) Targeted disruption of cd39/ATP diphosphohydrolase results in disordered hemostasis and thromboregulation. *Nature medicine* **5**, 1010-1017
15. Hasko, G., Linden, J., Cronstein, B., and Pacher, P. (2008) Adenosine receptors: therapeutic aspects for inflammatory and immune diseases. *Nature reviews. Drug discovery* **7**, 759-770
16. Robson, S. C., Wu, Y., Sun, X., Knosalla, C., Dwyer, K., and Enjyoji, K. (2005) Ectonucleotidases of CD39 family modulate vascular inflammation and thrombosis in transplantation. *Seminars in thrombosis and hemostasis* **31**, 217-233
17. Qawi, I., and Robson, S. C. (2000) New developments in anti-platelet therapies: potential use of CD39/vascular ATP diphosphohydrolase in thrombotic disorders. *Current drug targets* **1**, 285-296
18. Mehra, V. C., Ramgolam, V. S., and Bender, J. R. (2005) Cytokines and cardiovascular disease. *Journal of leukocyte biology* **78**, 805-818
19. Lusis, A. J. (2000) Atherosclerosis. *Nature* **407**, 233-241
20. Pencina, M. J., Navar-Boggan, A. M., D'Agostino, R. B., Sr., Williams, K., Neely, B., Sniderman, A. D., and Peterson, E. D. (2014) Application of new cholesterol guidelines to a population-based sample. *The New England journal of medicine* **370**, 1422-1431
21. Jain, M. K., and Ridker, P. M. (2005) Anti-inflammatory effects of statins: clinical evidence and basic mechanisms. *Nature reviews. Drug discovery* **4**, 977-987
22. Landmesser, U., Bahlmann, F., Mueller, M., Spiekermann, S., Kirchhoff, N., Schulz, S., Manes, C., Fischer, D., de Groot, K., Fliser, D., Fauler, G., Marz, W., and Drexler, H. (2005) Simvastatin versus ezetimibe: pleiotropic and lipid-lowering effects on endothelial function in humans. *Circulation* **111**, 2356-2363

23. Dichtl, W., Dulak, J., Frick, M., Alber, H. F., Schwarzacher, S. P., Ares, M. P., Nilsson, J., Pachinger, O., and Weidinger, F. (2003) HMG-CoA reductase inhibitors regulate inflammatory transcription factors in human endothelial and vascular smooth muscle cells. *Arteriosclerosis, thrombosis, and vascular biology* **23**, 58-63
24. Vaughan, C. J., Gotto, A. M., Jr., and Basson, C. T. (2000) The evolving role of statins in the management of atherosclerosis. *Journal of the American College of Cardiology* **35**, 1-10
25. Sowers, J. R. (2003) Effects of statins on the vasculature: Implications for aggressive lipid management in the cardiovascular metabolic syndrome. *The American journal of cardiology* **91**, 14B-22B
26. Sen-Banerjee, S., Mir, S., Lin, Z., Hamik, A., Atkins, G. B., Das, H., Banerjee, P., Kumar, A., and Jain, M. K. (2005) Kruppel-like factor 2 as a novel mediator of statin effects in endothelial cells. *Circulation* **112**, 720-726
27. Lin, Z., Kumar, A., SenBanerjee, S., Staniszewski, K., Parmar, K., Vaughan, D. E., Gimbrone, M. A., Jr., Balasubramanian, V., Garcia-Cardena, G., and Jain, M. K. (2005) Kruppel-like factor 2 (KLF2) regulates endothelial thrombotic function. *Circulation research* **96**, e48-57
28. SenBanerjee, S., Lin, Z., Atkins, G. B., Greif, D. M., Rao, R. M., Kumar, A., Feinberg, M. W., Chen, Z., Simon, D. I., Luscinskas, F. W., Michel, T. M., Gimbrone, M. A., Jr., Garcia-Cardena, G., and Jain, M. K. (2004) KLF2 Is a novel transcriptional regulator of endothelial proinflammatory activation. *The Journal of experimental medicine* **199**, 1305-1315
29. Vasa, M., Fichtlscherer, S., Adler, K., Aicher, A., Martin, H., Zeiher, A. M., and Dimmeler, S. (2001) Increase in circulating endothelial progenitor cells by statin therapy in patients with stable coronary artery disease. *Circulation* **103**, 2885-2890
30. Koh, K. K. (2000) Effects of statins on vascular wall: vasomotor function, inflammation, and plaque stability. *Cardiovascular research* **47**, 648-657
31. Bist, A., Fielding, P. E., and Fielding, C. J. (1997) Two sterol regulatory element-like sequences mediate up-regulation of caveolin gene transcription in response to low density lipoprotein free cholesterol. *Proceedings of the National Academy of Sciences of the United States of America* **94**, 10693-10698
32. Frank, P. G., and Lisanti, M. P. (2004) Caveolin-1 and caveolae in atherosclerosis: differential roles in fatty streak formation and neointimal hyperplasia. *Current opinion in lipidology* **15**, 523-529
33. Frank, P. G., Lee, H., Park, D. S., Tandon, N. N., Scherer, P. E., and Lisanti, M. P. (2004) Genetic ablation of caveolin-1 confers protection against atherosclerosis. *Arteriosclerosis, thrombosis, and vascular biology* **24**, 98-105
34. Park, D. S., Cohen, A. W., Frank, P. G., Razani, B., Lee, H., Williams, T. M., Chandra, M., Shirani, J., De Souza, A. P., Tang, B., Jelicks, L. A., Factor, S. M.,

Weiss, L. M., Tanowitz, H. B., and Lisanti, M. P. (2003) Caveolin-1 null (-/-) mice show dramatic reductions in life span. *Biochemistry* **42**, 15124-15131
35. Liu, P., Rudick, M., and Anderson, R. G. (2002) Multiple functions of caveolin-1. *The Journal of biological chemistry* **277**, 41295-41298
36. Plenz, G. A., Hofnagel, O., and Robenek, H. (2004) Differential modulation of caveolin-1 expression in cells of the vasculature by statins. *Circulation* **109**, e7-8; author reply e7-8
37. Minshall, R. D., Sessa, W. C., Stan, R. V., Anderson, R. G., and Malik, A. B. (2003) Caveolin regulation of endothelial function. *American journal of physiology. Lung cellular and molecular physiology* **285**, L1179-1183
38. Bauer, P. M., Yu, J., Chen, Y., Hickey, R., Bernatchez, P. N., Looft-Wilson, R., Huang, Y., Giordano, F., Stan, R. V., and Sessa, W. C. (2005) Endothelial-specific expression of caveolin-1 impairs microvascular permeability and angiogenesis. *Proceedings of the National Academy of Sciences of the United States of America* **102**, 204-209
39. Schlegel, A., Pestell, R. G., and Lisanti, M. P. (2000) Caveolins in cholesterol trafficking and signal transduction: implications for human disease. *Frontiers in bioscience : a journal and virtual library* **5**, D929-937
40. Stan, R. V. (2002) Structure and function of endothelial caveolae. *Microscopy research and technique* **57**, 350-364
41. Parton, R. G., and Simons, K. (2007) The multiple faces of caveolae. *Nature reviews. Molecular cell biology* **8**, 185-194
42. Feron, O., Dessy, C., Desager, J. P., and Balligand, J. L. (2001) Hydroxy-methylglutaryl-coenzyme A reductase inhibition promotes endothelial nitric oxide synthase activation through a decrease in caveolin abundance. *Circulation* **103**, 113-118
43. Hamelin, B. A., and Turgeon, J. (1998) Hydrophilicity/lipophilicity: relevance for the pharmacology and clinical effects of HMG-CoA reductase inhibitors. *Trends in pharmacological sciences* **19**, 26-37
44. Marcus, A. J., Safier, L. B., Hajjar, K. A., Ullman, H. L., Islam, N., Broekman, M. J., and Eiroa, A. M. (1991) Inhibition of platelet function by an aspirin-insensitive endothelial cell ADPase. Thromboregulation by endothelial cells. *The Journal of clinical investigation* **88**, 1690-1696
45. Roh, M., Kim, J., Song, C., Wills, M., and Abdulkadir, S. A. (2006) Transgenic mice for Cre-inducible overexpression of the oncogenes c-MYC and Pim-1 in multiple tissues. *Genesis* **44**, 447-453
46. Parton, R. G., Hanzal-Bayer, M., and Hancock, J. F. (2006) Biogenesis of caveolae: a structural model for caveolin-induced domain formation. *Journal of cell science* **119**, 787-796

47. Patel, H. H., Zhang, S., Murray, F., Suda, R. Y., Head, B. P., Yokoyama, U., Swaney, J. S., Niesman, I. R., Schermuly, R. T., Pullamsetti, S. S., Thistlethwaite, P. A., Miyanohara, A., Farquhar, M. G., Yuan, J. X., and Insel, P. A. (2007) Increased smooth muscle cell expression of caveolin-1 and caveolae contribute to the pathophysiology of idiopathic pulmonary arterial hypertension. *FASEB journal : official publication of the Federation of American Societies for Experimental Biology* **21**, 2970-2979
48. Pugh, S. D., MacDougall, D. A., Agarwal, S. R., Harvey, R. D., Porter, K. E., and Calaghan, S. (2014) Caveolin contributes to the modulation of basal and beta-adrenoceptor stimulated function of the adult rat ventricular myocyte by simvastatin: a novel pleiotropic effect. *PloS one* **9**, e106905
49. Ma, J., Sehgal, N. L., Ayanian, J. Z., and Stafford, R. S. (2005) National trends in statin use by coronary heart disease risk category. *PLoS medicine* **2**, e123
50. (2011) In *Health, United States, 2010: With Special Feature on Death and Dying*, Hyattsville (MD)

Chapter III: PDEIII-Mediated Inhibition of CD39 Expression

The first half of this research was originally published in The Journal of Biological Chemistry. Hui Liao, Matthew C. Hyman, Amy E. Baek, Keigo Fukase and David J. Pinsky. J. Biol. Chem. 2010; 285: 14791-14805. © the American Society for Biochemistry and Molecular Biology.

The second half of this research was originally published in The FASEB Journal. Amy E. Baek, Yogendra Kanthi, Nadia R. Sutton, Hui Liao, and David J. Pinsky. FASEB J. 2013; 27(11): 4419-4428.

Abstract

The ectoenzyme CD39 suppresses thrombosis and inflammation by suppressing ATP and ADP to AMP. However, mechanisms of CD39 transcriptional and post-translational regulation are not well known. Here we show that CD39 is transcriptionally up-regulated by cAMP and CD39 expression and activity can be modulated by inhibition of phosphodiesterase 3 (PDE3). RAW macrophages and human umbilical vein endothelial cells (HUVECs) were treated with the PDE3 inhibitors cilostazol and milrinone, then analyzed using qRT-PCR, immunoprecipitation/Western blot, immunofluorescent staining, radio-thin-layer chromatography, a malachite green assay, and ELISA. HUVECs expressed elevated CD39 protein (2-fold [$P<0.05$] for cilostazol and 2.5-fold [$P<0.01$] for milrinone), while macrophage CD39 mRNA and protein were both elevated after PDE3 inhibition.

HUVEC ATPase activity increased by 25% with cilostazol and milrinone treatment (P<0.05 and P<0.01, respectively), as did ADPase activity (47% and 61%,P<0.001). There was also a dose-dependent elevation of soluble CD39 after treatment with 8-Br-cAMP, with maximal elevation of 60% more CD39 present compared to controls (1 mM, P<0.001). Protein harvested after 8-Br-cAMP treatment showed that ubiquitination of CD39 was decreased by 43% compared to controls. A DMSO or PBS vehicle control was included for each experiment based on solubility of cilostazol, milrinone, and 8-Br-cAMP. These results indicate that PDE3 inhibition regulates endothelial CD39 at a post-translational level.

Introduction

The processes of thrombosis and inflammation contribute significantly to the severity and progression of numerous disease states, including stroke, deep vein thrombosis (DVT), and atherosclerosis (1, 2). Extracellular purinergic signaling through ATP and ADP has been shown to be a potent trigger for inflammatory cell recruitment and thrombosis. Modulating this pathway is the plasmalemmal ectonucleotidase, CD39/NTPDase1 (ectonucleoside triphosphate diphosphohydrolase). CD39 is expressed by a number of cell types including endothelial cells, B and T lymphocytes, and monocytes and macrophages, and hydrolyzes the terminal phosphate of ATP and ADP in an enzymatic cascade that generates AMP (3-5). By depleting the potent pro-thrombotic and pro-inflammatory signals of ADP and ATP, CD39 preserves

homeostasis in the vascular environment. A growing body of literature describes the involvement of CD39 and its apyrase activity in limiting thrombosis and inflammation (6) yet relatively little is known about the regulation of CD39, at either a transcriptional or translational level.

A Potential Site of Transcriptional Regulation of CD39

In silico analysis of the CD39 promoter region showed only one potential transcription factor binding site proximal enough to the CD39 transcriptional start site to be likely to regulate CD39 expression. This was a cAMP responsive element (CRE)-like sequence, and such sequences are recognized by cAMP response element binding protein (CREB) in pathways stimulated by cAMP. cAMP acts largely through protein kinase A (PKA), which is located in the cytoplasm as an inactive heterotetramer of regulatory and catalytic subunits. cAMP liberates the catalytic subunits, which allows their translocation into the nucleus. The catalytic subunit then phosphorylates a serine residue (Ser^{133}) of CREB. CREB dimers then bind to CRE sequences (TGACGTCA) in the promoter of various genes. The phosphorylated serine of CREB can then act as a scaffold for the transcriptional co-activator CREB-binding protein and p300. This complex then recruits RNA polymerase II to stimulate transcription (7-11). Activating transcription factor (ATF) and CREB are both members of the large basic leucine zipper

(bZIP) family of transcription factors. Members of the ATF/CREB subfamily can interact to form homo- or heteromultimers to bind CRE sequences of target genes.

The role of cAMP in modulating vascular tone has been well established. In cardiac myocytes, increased cAMP leads to increased contractility and tachycardia. In vascular smooth muscle, cAMP acts as a vasodilator, by activating cAMP-dependent protein kinase (PKA), which then phosphorylates myosin light chain kinase and reduces its phosphorylation of myosin light chain, thereby inhibiting contractile function of the actin/myosin complex (12-14). cAMP also has a known important role in the endothelium, where it preserves endothelial monolayer barrier function (15).

This study tests the effect of cAMP in macrophages on CD39 expression and the importance of this CRE site to the regulation of functional CD39. In this work, we demonstrate that CD39 RNA and functional protein are upregulated potently by cAMP in murine macrophages through the phosphorylation of CREB and ATF2 and their subsequent binding to the CRE site on the CD39 promoter (16).

Investigation of cAMP effects in endothelial cells and macrophages via modulation of cAMP

To further investigate the effect of cAMP in endothelial cells on CD39 expression, a pharmacologic approach was employed to modulate intracellular levels of cAMP. In order to more fully understand how CD39 is regulated in cells of the vascular wall, we explored the effects of cAMP on CD39 in human endothelium and macrophages. Our

objective was to investigate additional facets underlying control of leukocyte-endothelial interaction in thrombosis and inflammation.

Cilostazol has been administered as a safe and effective drug for the treatment of claudication in peripheral arterial disease; it inhibits phosphodiesterase 3 (PDE3), an enzyme that depletes intracellular cAMP by hydrolyzing its 3'-cyclic phosphate bond by competitively binding to the cAMP-specific binding site of the PDE3 (17, 18). Milrinone is used clinically in patients with heart failure to improve contractility. Milrinone was chosen as an independent tool to confirm the effect of PDE3 inhibition on the expression of CD39 (19). The cell membrane-permeable cAMP analogue, 8-Bromo-cAMP was also used to increase intracellular cAMP. Here, we show that increased intracellular cAMP (through the specific inhibition of PDE3) leads to the upregulation of functional CD39 protein in human endothelial cells as well as in murine macrophages. Most significantly, we found that macrophages and endothelial cells regulate CD39 through separate pathways, with the former utilizing transcriptional upregulation and the latter utilizing post-translational regulation (20).

Methods

Cell culture- All chemical reagents were obtained from Invitrogen (Grand Island, NY, USA) unless specified. Human umbilical vein endothelial cells (HUVEC) were isolated from human umbilical cords based on previously described methods (21).

Fresh cords were washed. The umbilical vein was attached to a 10 mL syringe, and flushed with isotonic saline buffer. The cord was incubated with 2% collagenase 3 (Worthington Biochemical Corp., Lakewood, NJ, USA) in HBSS buffered with HEPES at 37°C. Veins were then flushed with isotonic buffer, and the flow through was centrifuged at 4°C, 190 x g, 7 minutes. Pellets were plated onto 35 mm plates coated with 0.2% gelatin. Cells were not used beyond passage 4. EBM-2 media and EGM-2 growth supplement bullet kits (Lonza, Allendale, NJ, USA) were reconstituted according to manufacturer instructions. RAW cells (a transformed murine macrophage cell line) were obtained from ATCC (Manassas, VA, USA), and cultured in RPMI 1640 medium supplemented with penicillin (50 units/mL), streptomycin (5 μg/mL), and 10% fetal bovine serum (Invitrogen). Cells were treated with 8-Br-cAMP (Sigma, St. Louis, MO, USA), PDE3 inhibitors (cilostazol (Sigma), milrinone (Sigma)), or DMSO (Fisher, Pittsburgh, PA, USA) control for indicated times in serum- and supplement-free EBM-2 media or serum-free RPMI 1640 media.

Murine Peritoneal Macrophage Isolation—Peritoneal macrophages were isolated as described previously (21). In brief, 10-week-old male C57Bl6/J mice were injected intraperi- toneally with 3.0 ml of a 5% thioglycollate solution (BD Bio- sciences). Four days later, macrophages were isolated by peri- toneal lavage and placed in ice-cold phosphate-buffered saline. The cells were plated in 6-well plates at a concentration of 1 x 10^6 cells/well for total RNA isolation or 150-mm dishes for membrane protein

extraction.

Quantitative Reverse Transcription-PCR (qRT-PCR)- qRT-PCR was used to quantify RNA levels. HUVEC were plated onto 0.2% gelatin coated 6-well plates (Falcon). When cells were confluent, they were serum-starved in EBM-2 and then treated with a range of doses of cilostazol (30-100 μM) or DMSO (1 μL/mL) (22, 23). After treatment, cells were washed twice in PBS, and then total RNA was isolated using RNAeasy kits (Qiagen, Valencia, CA, USA). cDNA was made using cDNA synthesis kits (Applied Biosystems, Grand Island, NY, USA). Real time qPCR was carried out using the 7000 detection system (Applied Biosystems) with 2x universal mastermix and primers for human CD39 and human β_2 microglobulin (Applied Biosystems). All data were normalized to β_2 microglobulin.

Platelet-rich Plasma Isolation and Platelet Aggregometry— Mouse blood was drawn from the inferior vena cava using a 20-gauge needle containing 3.2% sodium citrate. One volume of HT Buffer (137 mM NaCl, 2.68 mM KCl, 12 mM NaHCO3, 0.36 mM NaH_2PO4, 10 mM HEPES, 0.2% bovine serum albumin) was added and spun at 50 x *g* for 10 min at room temperature. The citrated blood was brought back to the original volume with HT Buffer and spun at 50 x *g* for 10 min at room temperature. Platelet-rich plasma was collected. Platelet-rich plasma aggregometry was then performed using a Chrono-log 560CA with the Aggro/Link 810. 1 x 10^8 platelets in 500 μL of HT buffer were mixed with 20 μg of membrane protein of either 250 μM 8-Br-cAMP-treated or

non-treated peritoneal macrophages before stimulation with 1 μM ADP (Chrono-log).

Isolation of a Mouse Cd39 Genomic Clone- A 4555-bp fragment containing 4474 bp of the 5′-flanking (-4474) region and 81 bp of the untranslated first exon (+81) of mouse *Cd39* was isolated from RAW cell total genomic DNA using PCR. The primers (5′-CACTTACTCGGGCATGCTGTTGAAC-3′ and 5′CCCCCTGAAGGGTTTGGATCAAATCAGTTCTGG- 3′) were designed by analysis of the sequence of the mouse Cd39 gene, 5′ flank (GenBankTM accession number NM_ 009848). The 4555-bp insert was subcloned into pCR-XL- TOPO vector (Invitrogen) using the TOPO XL PCR cloning kit (Invitrogen) and sequenced to confirm identity.

Construction of Mouse Cd39 Promoter-Luciferase Reporter Plasmids and Site-directed Mutagenesis- PCR was used to amplify mouse *CD39* promoter-luciferase reporter constructs representing 5′-deleted CD39 upstream sequences, and these PCR products were subcloned into the pGL3-basic vector (Promega) using a T4 ligase and Quick Ligasing buffer (Promega). In these PCRs, the CD39 genomic clone (described above) was used as a template. The 5′-deletion constructs of the CD39 promoter represent the spans -250 to +32 (pCD39/250) and -52 to +32 (pCD39/52). The *Cd39* promoter -220 to -189 fragment (containing a CRE element) was cloned into pCD39/52 to make the deletion construct pCD39/ΔCRE. For mutants, oligonucleotides used for priming were synthesized based on 5′-flanking region sequence of the mouse *Cd39* gene. The site-

directed mutants of the pCD39/CREmut constructs were generated using QuikChange site-directed mutagenesis kits (Stratagene). In these PCRs, the 5′-deletion construct, pCD39/250, was used as a template. Two mutated priming oligonucleotides representing overlapping sense and antisense sequences of the mutant site were used to amplify the entire pGL3 plasmid and insert. The mutated primers are shown as follows (target regions are indicated by underlines and alterations are indicated by boldface type): 5′-GAGTTTTGAACACATACTAC**CA**CAAGCCTAGAAAAAAG-3′ and 5′-CTTTTTTCTAGGCTTG**TG**GTAGTATGTGTTCAAAACTC-3′. Forward and reverse DNA sequencing of inserts confirmed the sequences of all constructs employed for transfection assays.

Construction of Mouse Creb1, Atf2, and Dominant Negative Creb Overexpression Plasmids- The cDNA clones of mouse Creb1 and Atf2 were ordered from ATCC. Creb1 expression plasmid (pCREB1) and Atf2 expression plasmid (pATF2) were constructed by first using PCR to amplify the open reading frame of the Creb1 and Atf2 cDNAs. The open reading frames of Creb1 and Atf2 cDNA were each cloned into pcDNA3.1 (Invitrogen) expression vectors. The primers used for PCR to amplify the open reading frame of the Creb1 and Atf2 cDNAs are as follows: Creb1, 5′-GGAGAAGCTTGTACCACCGGTAACTAAATGACC-3′ and 5′-CACTCGAGAACTTAAATCCCAAATTAATCTG-3′; Atf2, 5′-AACAGGTACCTGTGGAATATGAGTGATG-3′ and 5′-

GCACTCGAGGTTTTAATCAACTTCCTGAGG-3′.

The site-directed mutants of the dominant negative Creb overexpression plasmid (pCREB/Ser^{133}Mut) constructs were generated using QuikChange site-directed mutagenesis kits (Stratagene). In these PCR reactions, pCREB1 was used as a template.

The mutated priming oligonucleotides represented overlapping sense and antisense sequences of the mutant site that amplified the entire pGL3 plasmid and insert. The mutated primers are shown as follows (target regions are indicated by underlines, and alterations are indicated by boldface type): 5′-CCTTTCAAGGAGGCCT**G**CCTACAGGAAAATTTTG-3′ and 5′-CAAAATTTTCCTGTAGGCAGGCCTCCTTGAAAGG-3′.

Transient Transfections—RAW cells were co-transfected using SuperFect transfection reagent (Qiagen). The day before transfection, RAW cells were plated on 12-well plates (Costar) with 1 x 10^5 cells/well and grown in RPMI 1640 (Invitrogen) containing 10% fetal calf serum (Invitrogen). Cultures were incubated at 37 °C in a humidified atmosphere containing 5% CO2 until they reached 50 – 80% confluence. The cells were co-transfected using 0.75 μg of *Cd39* promoter-pGL3 reporter plasmid and 0.75 μg of control plasmid, pCMV/β-galactosid- ase, which served as an internal control to normalize transfection efficiency, as well as 7.5 μL of SuperFect transfection reagent in 75 μL of serum-free RPMI 1640 medium. This was followed by incubation at room

temperature for 10 min, after which the complexes were mixed with 0.4 ml of RPMI 1640 medium with 10% FBS. After incubating at 37 °C and 5% CO2 for 3 h, the cells were washed 3 times with HBSS (Invitrogen) and then incubated with RPMI with 10% FBS. After 24 – 48 h of incubation, the cell medium was changed to RPMI 1640, and then the cells were treated with 250 μM of 8-Br-cAMP or RPMI 1640 only (control) for 5 h. Luciferase reporter assays were performed using a luciferase reporter assay system (Promega). Transfected cells were washed two times with cold phosphate- buffered saline and then harvested, lysed, and assayed for luciferase activity by a VICTOR LIGHT luminometer (PerkinElmer Life Sciences). β-Galactosidase enzyme activity was measured using a β-galactosidase enzyme assay system (Promega). Fifty μLof the sample was mixed with 50 μL of 2x buffer containing 200 mM sodium phosphate, pH 7.3, 2 mM $MgCl_2$, 100 mM β-mercaptoethanol, and 1.33 mg/ml o-nitrophenyl-β-galactopyranoside in a 96-well plate. After incubating for 30 min at 37 °C, the absorbances of the samples were read at 420 nm in a VersaMax tunable microplate reader (Molecular Devices). For the overexpression experiments, RAW cells were co-transfected with pCREB1, pATF2, or empty vector (pcDNA3.1) with pCD39/250 and pCMV/β-galactosidase vector. The method of transfection and reporter assay used are described above.

Chromatin Immunoprecipitation (ChIP) Assay- The ChIP assay was performed using an EZ ChIPTM chromatin immunoprecipitation kit (Upstate Biotechnology). RAW cells were

cross-linked at 37 °C for 10 min in 1% formaldehyde. Cells were then sonicated in lysis buffer (1% SDS, 10 mM EDTA, 50 mM Tris, pH 8.0, 1 mM phenylmethylsulfonyl fluoride, 1 μg/ml aprotinin, 1 μg/ml leupeptin) 12 times at 4 °C using 15 sonicating pulses at 30% output. The supernatant was divided into three tubes for subsequent immunoprecipitation. Samples were precleared in immunoprecipitation buffer (0.01% SDS, 1.1% Triton, 1.2 mM EDTA, 16.7 mM Tris, pH 8.1, 167 mM NaCl, 1 mM phenylmethylsulfonyl fluoride, 1 μg/ml aprotinin, 1 μg/ml leupeptin) and added to protein A-Sepharose beads. The mixture was placed on a rotator for 1 h at 4 °C, after which beads were spun out and discarded (this step was to clear the mixture of excess IgG). To the supernatant, 5 μg of anti-phosphorylated CREB1 (Ser^{133}), phosphorylated ATF2 (Thr^{71}) antibody (Santa Cruz), or rabbit IgG were then added, and the mixture was placed on a rotator for 16 h at 4 °C. Immunoprecipitates were recovered by adding protein A-Sepharose beads, which were washed for 5 min with low salt immune complex wash buffer (0.1% SDS, 1% Triton, 2 mM EDTA, 20 mM Tris, pH 8.1, and 150 mM NaCl) and then for 5 min with high salt immune complex wash buffer (0.1% SDS, 1% Triton, 2 mM EDTA, 20 mM Tris, pH 8.1, and 500 mM NaCl), 5 min with LiCl immune complex wash buffer (0.25 M LiCl, 1% Nonidet P-40, 1% sodium deoxycholate, 1 mM EDTA, and 10 mM Tris, pH 8.1) and twice for 3 min with TE buffer (10 mM Tris, pH 8.0, and 1 mM EDTA, pH 8.0). Immune complexes were eluted during rotation with 1% SDS and 0.1 M NaHCO3 for a total of 30 min at room temperature.

Immunoprecipitates and inputs were reverse cross-linked with 200 mM NaCl at 65 °C for 16 h. Samples were then incubated 1 h at 45 °C with 10 mM EDTA, 40 mM Tris, pH 6.5, and 40 μg/ml proteinase K. DNA was extracted by the Qiaquick PCR purification kit (Qiagen). The input DNA and ChIP DNA were amplified by qRT-PCR. Primers used for PCR correspond to the mouse Cd39 region (-239 to -172; 5′-primer, 5′-GGGAAG GAGAGAGTGAGTTTTGAA-3′; 3′-primer, 5′-CACCGGGTTGTAATTTCTTTTTTC-3′; probe, ACATACTACGTCAAGCCT-3′). Ct values of ChIP DNA were normalized to the Ct values of input DNA.

Whole-Cell Protein Isolation- Following treatment with PDE3 inhibitors or DMSO as a negative control, cells were washed twice with PBS (Invitrogen), scraped with a rubber policeman, and suspended in ice-cold RIPA buffer supplemented with a tablet of a cOmplete mini protease inhibitor tablet (Roche, Branchburg, NJ, USA). Cells were homogenized by 10 strokes through a sterile 30 gauge 1 mL insulin syringe. Lysed cells were centrifuged for 10 minutes at 13,000 x g at 4°C and the resulting supernatants were transferred to new tubes. The samples were flash frozen in aliquots and stored at -80°C. Concentrations were determined via a colorimetric protein assay (Bio-Rad, Hercules, CA, USA).

Enzyme-linked immunosorbent assay (ELISA)- HUVEC were plated on 24-well plates (Corning, Tewksbury, MA, USA) coated with 0.2% gelatin and grown until confluent. Cells were serum-starved for 6 hours before serum-free treatment with 100,

250, 500, and 1000 μM 8-Br-cAMP for 8 hours. Media was transferred into microcentrifuge tubes (Eppendorf, Hauppauge, NJ, USA), and samples centrifuged (500 x g, 5 minutes, 4°C). 100 μL of cell-free supernatants were then loaded onto 96-well plates (Nunc-Nalgene, Lafayette, CO, USA) that had been coated overnight at 4°C with a rat anti-CD39 antibodies (5ug/mL, R&D MAB4398), and then blocked for 1 hour at room temperature with 4% BSA (Sigma) in PBS. Standard lanes were included in each assay plate, with recombinant human CD39 (R&D, Minneapolis, MN, USA) in PBS. Wells were then washed three times with 0.05% Tween-20 in PBS, and then probed with a sheep anti-CD39 antibody (5 μg/mL, 2 hours, room temperature, R&D AF4398). Wells were washed three times again before probing with anti-sheep biotinylated antibody for 1 hour at room temperature. This was followed by three more washes, and then avidin conjugated to alkaline phosphatase (1:800, 1 hour, room temperature, Sigma) was added. Wells were then washed three times, and 5 mg of p-Nitrophenyl Phosphate, Disodium Salt (PNPP) in 5 mL of diethanolamine buffer (Thermo Scientific, Pierce, Rockford, IL, USA). Color was allowed to develop for up to 30 minutes, stopped with 2 N NaOH, and then absorption measured at 405 nm by a SpectraMax M5 microplate reader.

LDH assay - Using a colorimetric LDH assay (Pierce Biotechnology, Rockford, IL, USA), 15,000 cells were plated in triplicate in a 96-well format, and allowed to adhere overnight before treatment with either vehicle control (Medium 199 (GIBCO, Grand

Island, NY, USA)), or 8-Bromo-cAMP for 8 hours. LDH was then measured according to manufacturer instructions. Briefly, cells were incubated in a reaction mixture containing lactate, tetrazolium salt (2-(4-iodophenyl)-3-(4-nitrophenyl)-5-phenyl-2H-tetrazolium) and diaphorase, and a red formazan product was allowed to develop. Absorption was then measured at 490 and 680 nm using a SpectraMax M5 microplate reader.

Immunoprecipitation- HUVEC were plated on 24-well plates (Corning) coated with 0.2% gelatin and grown until confluent. Cells were serum-starved for 6 hours before serum-free treatment with 250 μM 8-Br-cAMP for 18 hours.

Cell supernatants were collected on ice and incubated with gentle rocking overnight with protein-G agarose beads (Roche), and then incubated with anti-human CD39 antibody (Abcam, Cambridge, MA, USA) coated beads at 4°C. Beads were washed and purified CD39 protein was eluted and quantified via standard Western blotting techniques.

cAMP measurement: Competitive Enzyme Immunoassay- HUVEC were treated with cilostazol (100 μM) or an equivalent volume of DMSO, washed twice in PBS to wash away traces of DMSO, and then intracellular cAMP levels were measured according to manufacturer instructions of the competitive enzyme immunoassay kit (Cayman, Ann Arbor, MI, USA).

Immunofluorescence - HUVEC were plated on 4-well plastic chamber slides (LabTek), with 0.2% gelatin coating. After cells had adhered and grown to 40%

confluence, cells were treated in serum-free conditions with the following: Lonza EBM-2 basal medium with DMSO as vehicle control, cilostazol (50, 100, 400 μM), or milrinone (100, 200, 400 μM). Cells were then fixed for 15 minutes with ice cold methanol, and then incubated overnight with a mouse anti-CD39 antibody (1:100) at 4°C followed by biotinylated horse anti-mouse IgG (1:100, Vector Laboratories, Burlingame, CA, USA) for 1 hour at room temperature. An avidin-biotin-peroxidase complex was formed for 30 minutes at room temperature and then added to samples. Finally, a tetramethylrhodamine labeled tyramide was added (Perkin Elmer, Waltham, MA, USA). Nuclei were stained with DAPI. Slides were mounted with Prolong Gold (Invitrogen) and cured for 24 hours. Slides were then imaged using a Nikon Eclipse TE2000-E microscope.

Radio-Thin Layer Chromatographic (TLC) Analysis of CD39 activities- TLC was used to assess CD39 enzymatic function. Total protein of HUVEC was mixed with 1.0 mM [8-^{14}C]ATP (MP Biomedicals, Santa Ana, CA, USA) and 286 μM AOPCP (Sigma) in Medium 199 (Gibco), and incubated at 37°C for 30 minutes. Reactions were stopped using 8M formic acid and the reaction mixture was then spotted onto silica gel TLC plates (Fluka, Invitrogen). A ladder of [8-^{14}C]ATP, [8-^{14}C]ADP, and [8-^{14}C]AMP (MP Biomedicals) was used. Nucleotides were separated by thin layer chromatography with isobutyl alcohol, isoamyl alcohol, 2-ethoxyethanol, ammonia, and water (9:6:18:9:15) (5). Separation was allowed to occur for 5 hours before plates were dried, exposed to a

phosphorimaging screen (Eastman Kodak Co., Rochester, NY, USA), and then analyzed using a Typhoon Trio+ Variable Mode Imager (GE Healthcare, Livonia, MI, USA).

Western Blotting Assay- Total protein was quantified and added to 4x sample buffer (Invitrogen), boiled for 3 minutes at 100°C, separated by 10% SDS-PAGE, and electrophoretically transferred onto PVDF membranes (Invitrogen). Membranes were probed with mouse monocolonal IgG_1 anti-CD39 antibodies (Abcam) and HRP-conjugated anti-mouse antibodies (Sigma), and then autoradiographed using enhanced chemiluminescence (ECL detection system, Amersham Biosciences, Piscataway, NJ, USA).

Statistics- Statistical analysis was performed using analysis of variance to detect differences between groups. Groups were analyzed with a one-way ANOVA, and further post-hoc analysis using the student Newman-Keuls method was applied (Prism®). Differences were considered significant if p was <0.05.

Results

Peritoneal macrophages were treated with 8-Br-cAMP, and total RNA and membrane protein were isolated. From these samples, CD39 mRNA levels were measured using qRT-PCR. The data showed that in cAMP-treated cells, CD39 mRNA increased by 2-fold, relative to non-cAMP-treated controls ($p < 0.01$, **Figure 3.1A**). We then measured CD39 protein expression on the cell membrane by Western blot. cAMP increased CD39 protein expression by 2.87-fold compared with the non-treated control ($p < 0.01$). The functional enzymatic activity of CD39 on peritoneal macrophages was measured using a TLC assay and a platelet aggregation assay. The result showed that the conversion of ATP to AMP was increased by 2.5-fold and that platelet aggregation was reduced by 46% in 8-Br-cAMP-treated macrophages compared with non-treated controls (**Figure 3.1, C and D**).

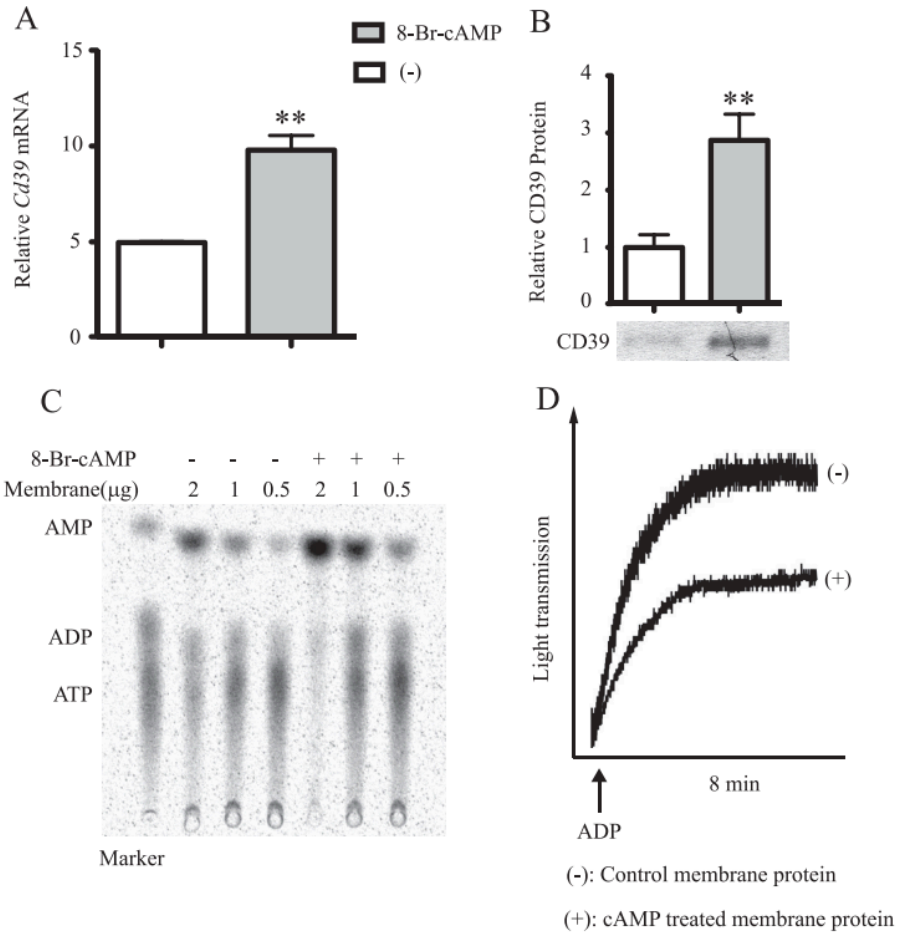

Figure 3.1: Effect of cAMP on CD39 expression in primary macrophage cultures. 10-week-old male C57Bl6/J mice were injected intraperitoneally with 3.0 ml of a 5% thioglycollate solution. Four days later, macrophages were isolated by peritoneal lavage, red blood cells were lysed, and remaining cells were plated. After 24 h, the recovered cells were pretreated with 20 M H89, 50 M LY294002, or DSMO (vehicle) for 20 min. To this medium, 250 M 8-Br-cAMP was added, after which the cells were allowed to incubate for 2 h. A) Total RNA was then isolated from the plated murine peritoneal macrophages, and qRT-PCR was used to assay levels of CD39 mRNA. Isolated peritoneal macrophages were treated with 250 8-Br-cAMP for 16 h before membrane protein was extracted. B) CD39 protein expression was measured by Western blot, and C) CD39 enzymatic activity was tested using a TLC assay and D) a platelet aggregation assay. **, $p < 0.01$ compared with non-treated controls. ###, $p<0.001$ compared with the 8-Br-cAMP-treated group.

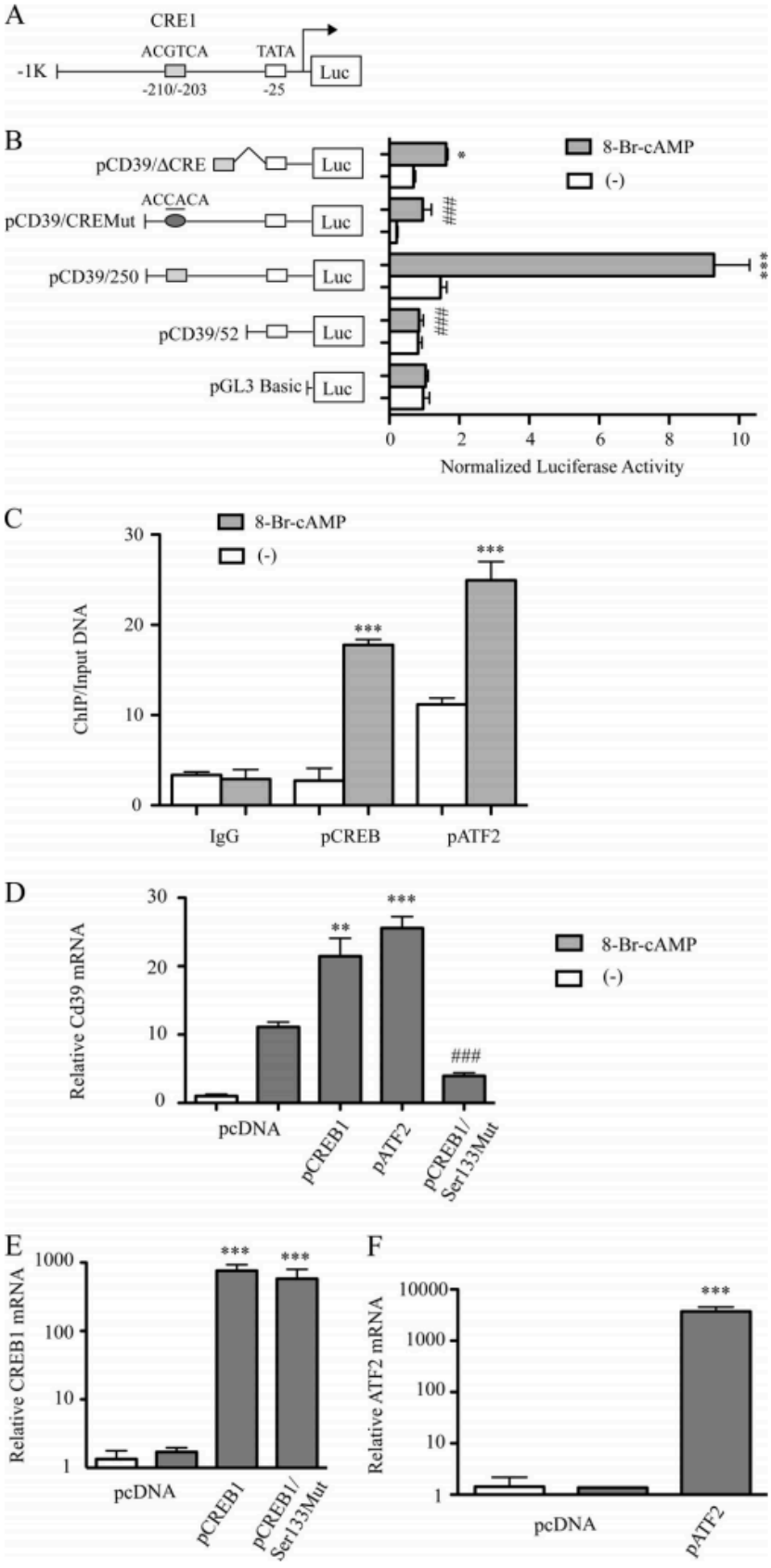
A
CRE1
ACGTCA
TATA
-1K
-210/-203
-25
Luc
B
pCD39/ΔCRE
ACCACA
pCD39/CREMut
pCD39/250
pCD39/52
pGL3 Basic
8-Br-cAMP
(-)
Normalized Luciferase Activity
C
ChIP/Input DNA
IgG
pCREB
pATF2
D
Relative Cd39 mRNA
pcDNA
pCREB1
pATF2
pCREB1/ Ser133Mut
E
Relative CREB1 mRNA
F
Relative ATF2 mRNA

Figure 3.2: cAMP-induced CD39 expression results from transcriptional activation at CRE-like sites; deletional analysis of the *Cd39* promoter. A) Schematic of the 5′-flanking region of the mouse *Cd39* gene with its CRE-like binding sites. Transient co-transfection of RAW cells was performed using either pCD39/250, pCD39/52, or pCD39/D206; pCD39/CRE1mut; and pCMV/β-galactosidase. B) Cultures were transfected with each of the indicated constructs using the SuperFect procedure, and then cells were treated with 250 μM 8-Br-cAMP. Luciferase activities were then determined. Relative firefly luciferase activity is normalized to control pCMV/β-galactosidase activity (***, p <0.001 compared with non-treated controls; ###, p < 0.001 compared with pCD39/250-transfected and cAMP-treated groups). C) ChIP of CREB1 or ATF2 interaction with CD39 promoter in RAW cells. RAW cells were treated with 250 μM 8-Br-cAMP for 30 min. qRT-PCR products targeting -239 to -172 of the CD39 promoter are shown. *Ct* values of ChIP DNA were normalized to the *Ct* values of the input DNA. ***, $p< 0.001$ compared with non-treated control. (D and F) Effect of CREB1 or AFT2 overexpression on Cd39 mRNA expression. RAW cells were transfected either with a pCREB1 overexpression construct, a pATF2 overexpression construct, a dominant negative "phosphorylation-resistant" CREB1 overexpression construct (pCREB/Ser^{133}Mut), or vector alone. After 48 h, transfected cells were treated with 250 μM 8-Br-cAMP for 5 h, total RNA was extracted for reverse transcription, and quantitative PCR was done to evaluate Cd39 (D), Creb1 (E), or Atf2 (F) mRNA levels. *, p< 0.05; **, p <0.01; ***, p< 0.001 compared with non-treated controls. ###, p < 0.001 compared with pCREB1-transfected and 8-Br-cAMP-treated groups.

CD39 promoter analysis

The CD39 promoter sequence was cloned 1000 bp upstream of transcriptional start site (**Figure 3.2A**). Transcriptional activity at the promoter region was measured using a firefly luciferase reporter gene and by truncating and mutating the promoter region in order to identify promoter elements that regulate CD39. Promoter-luciferase reporter constructs were transfected into RAW 264.7 cells to measure transcriptional response in the presence or absence of 8-Br-cAMP. Luciferase activity was increased in RAW cells treated with cAMP and transfected with pCD39/250 (5.94-fold, p<0.0001)

compared to untreated controls (**Figure 3.2B**). Truncations closer to the transcriptional start site (at -52 bp) resulted in a complete loss of reporter activity, indicating that cAMP regulates CD39 transcription through a segment of DNA located between -250 and -52 bp away from the transcriptional start site. Analysis of the region showed that one transcription factor binding site, a CRE, was located in the -210/-203 region of the CD39 promoter. This site was designated CRE1. CRE1 (pCD39/ΔCRE) was fused to a short promoter segment at -52 bp. Treatment with 8-Br-cAMP increased luciferase activity compared to untreated cells. This site was then mutated, and this construct showed an 86.6% decrease in transcriptional activity relative to wild type constructs. This suggests that CRE binding to the CD39 promoter is important for CD39 transcriptional activation by cAMP.

ChIP assays were performed to demonstrate that CREB and ATF2 can bind the CD39 promoter. After treatment with 8-Br-cAMP, cross-linked RAW cell lysates were immunoprecipitated with anti-phosphorylated CREB1 or anti-phosphorylated ATF2 antibodies. qRT-PCR was used to amplify fragment of the promoter from -239 to -172. These ChIP data show that binding of phosphorylated CREB and phosphorylated ATF2 to the mouse CD39 promoter was increased 6.48- and 2.3-fold, respectively, in 8-Br-cAMP-treated cells compared to untreated control cells (**Figure 3.2C**).

RAW cells were then transfected with a pCREB1 overexpression construct or one

in which Ser^{133} in CREB was mutated to Ala^{133} in order to make a CREB overexpression construct that is resistant to phosphorylation. This construct was transfected into RAW cells and RAW cells were treated with 8-Br-cAMP. Total RNA was harvested and qRT-PCR performed to evaluate CD39 mRNA (**Figure 3.2D**), CREB1 mRNA (**Figure 3.2E**), and ATF2 mRNA (**Figure 3.2F**). CD39 levels were increased by cAMP treatment in empty-vector transfected samples, and in those transfected with non-mutated pCREB1 and pATF2 constructs. The mutated pCREB construct, however, resulted in an 82% decrease in mRNA levels. When all these data are considered together, they show that cAMP stimulates CREB and that Ser^{133} is a critical residue that must be phosphorylated in order to drive CD39 transcription.

cAMP increases CD39 in the extracellular milieu- To analyze the potential role of cAMP in regulating human endothelial CD39, we began by measuring CD39 in HUVEC supernatants as a function of cAMP levels (**Figure 3.3A**).

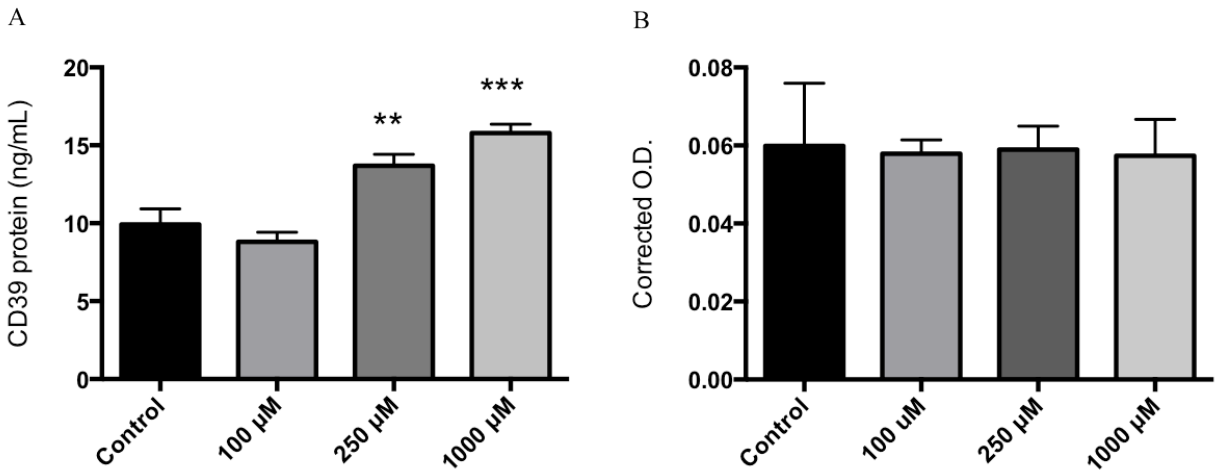

Figure 3.3. A) CD39 protein levels measured by ELISA after cAMP treatment: Supernatants of HUVEC treated with either PBS (control) or 8-Br-cAMP were measured for CD39 via ELISA. Treatment with this cell permeable analogue of cAMP increases extracellular CD39. $p<0.001$ between 1 mM vs. control and $p<0.05$ between 250 µM and control. B) LDH levels were measured in HUVEC treated with either vehicle control or 8-Br-cAMP. cAMP treatment did not change levels of LDH release.

The cell-permeant cAMP analogue 8-Bromo-cAMP was used to achieve a gradation in cAMP levels. ELISA data showed that CD39 protein increased with the addition of cAMP, in what appeared to be a cAMP dose-dependent manner. These supernatant samples were measuring CD39 as released into the surrounding medium, thus indicating that intracellular cAMP levels regulate CD39 levels. This suggested that either more CD39 was being made or released, or less was being eliminated. LDH levels were also measured (**Figure 3.3B**), in order to confirm that CD39 elevation after cAMP treatment was not a result of cytotoxicity. Results showed LDH levels in cAMP-treated samples were the same across all conditions as LDH levels in control samples.

PDE3 inhibition increases CD39 transcription- Having determined that extracellular CD39 elevated in response to cAMP, we subsequently sought to establish whether modulating intracellular cAMP would alter membrane CD39 expression. Cilostazol was a primary candidate to modulate cAMP because of its specific PDE3 inhibitory activity (18) and for its safety profile in humans. Treatment of RAW murine macrophages with cilostazol resulted in increased CD39 mRNA as well as protein as measured by qRT-PCR and Western blot, respectively (**Figures 3.4-3.5**).

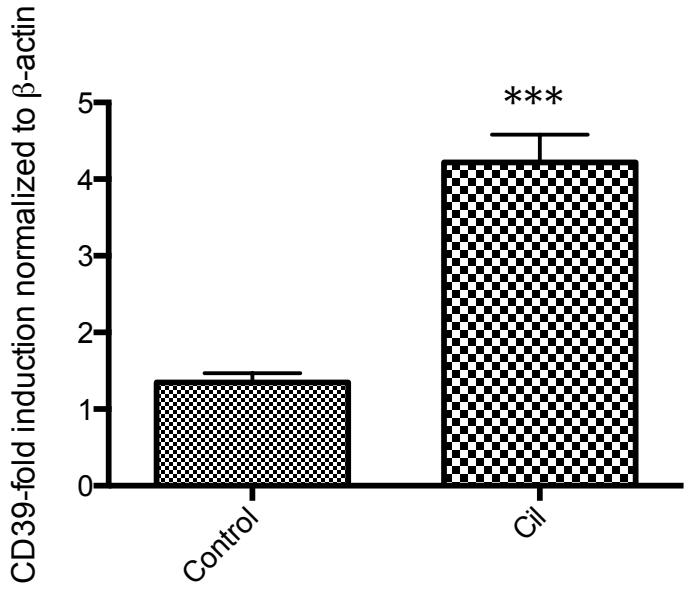

Figure 3.4. Effect of PDE3 inhibition on CD39 mRNA: Raw macrophages were treated with 30 μM cilostazol for 18 hours and then harvested for measurement of total mRNA by qRT-PCR. $p < 0.001$ compared to control, n=4.

To confirm this finding as a PDE3 class effect, RAW cells were also treated with milrinone and CD39 protein was measured. These results were consistent with previous work, which showed that murine peritoneal macrophage CD39 is strongly upregulated

by treatment with 8-Bromo-cAMP (16) and that a defined transcriptional pathway exists for such regulation.

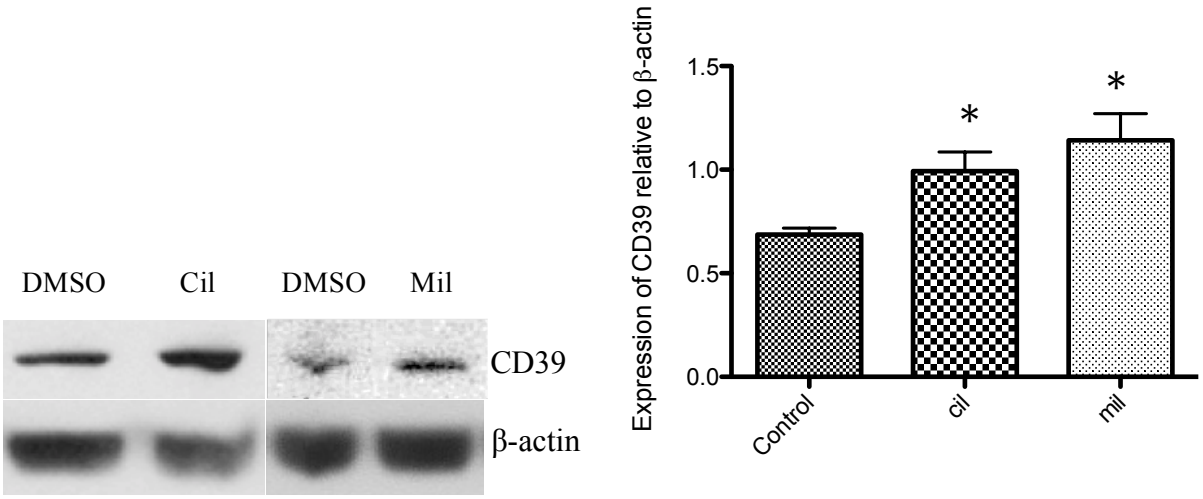

Figure 3.5. Effect of PDE3 inhibition on CD39 protein: Raw macrophages were treated with DMSO (control), 30 μM cilostazol, or 50 μM milrinone for 21 hours, harvested for total protein, and analyzed by Western blot. Raw macrophages treated with cilostazol expressed 44% more CD39 compared to DMSO treated controls ($p<0.05$, n=3). Macrophages treated with milrinone had a 74% increase in CD39 compared to DMSO ($p<0.05$, n=3).

PDE3 inhibition increases CD39 protein expression- In human endothelial cells, there is no prior work establishing a link between cAMP and CD39. Given the significant role of endothelial cells in the maintenance of vascular homeostasis, human endothelial cells (HUVEC) were used to investigate whether endothelium stimulated by cAMP can result in the upregulation of CD39. To confirm that intracellular cAMP levels were indeed elevated after the indicated treatment times using PDE3 inhibitors in HUVEC, endogenous cAMP levels were measured with or without cilostazol (**Figure 3.6**).

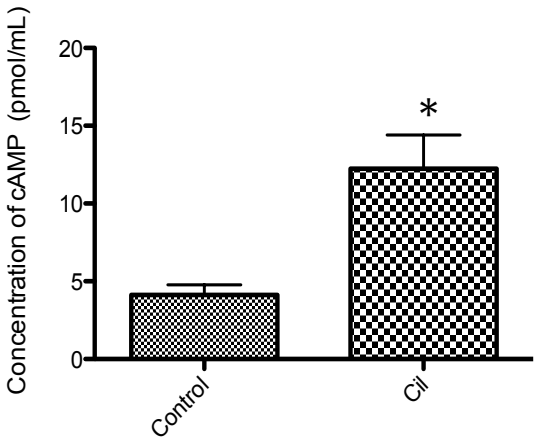

Figure 3.6. Quantification of intracellular cAMP level: HUVEC treated with 100 μM cilostazol show 2.97-fold increase in cAMP levels ($p<0.05$, $n=7$). Analysis of intracellular cAMP performed via competitive binding assay.

Results demonstrated that cAMP levels were significantly elevated with cilostazol treatments. Surprisingly, endothelial cells exhibited markedly different responses to cAMP elevation, compared with macrophages subjected to PDE3 inhibition. While CD39 protein levels measured by Western blot elevated after treatment (**Figure 3.7**), there was no change in mRNA levels for CD39 (**Figure 3.8**), indicating that the increase in CD39 protein was not at the transcriptional level. Further evidence for the effect of PDE3 inhibition on CD39 protein is shown in **Figure 3.9**. HUVEC were treated with a range of doses of either cilostazol or milrinone and compared to control wells treated with DMSO as a vehicle control.

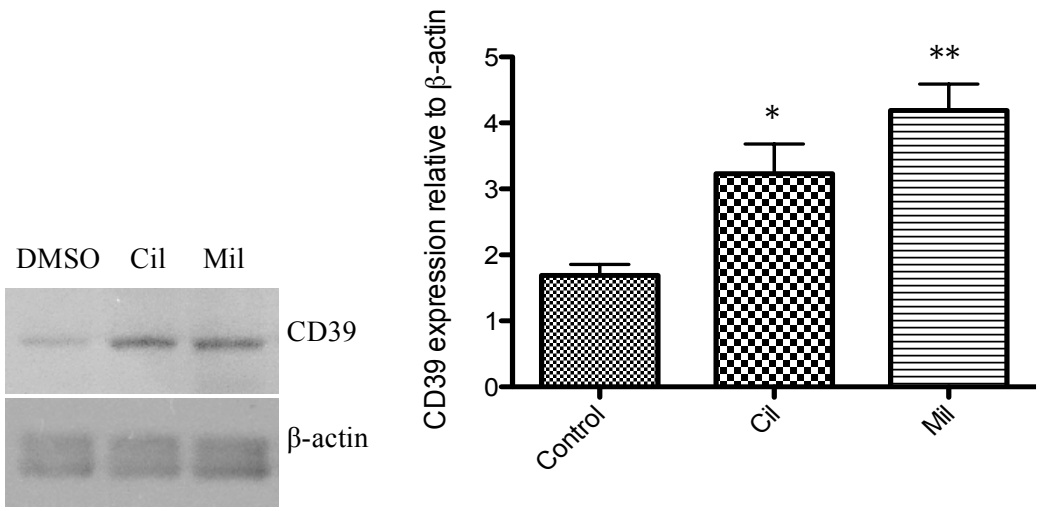

Figure 3.7. CD39 protein expression by Western blot: CD39 expression in HUVEC increased after 18 hours of treatment with 50 μM of cilostazol or 200 μM of milrinone (2-fold and 2.5 –fold respectively) compared to DMSO control ($p<0.05$ and $p<0.01$, n=3).

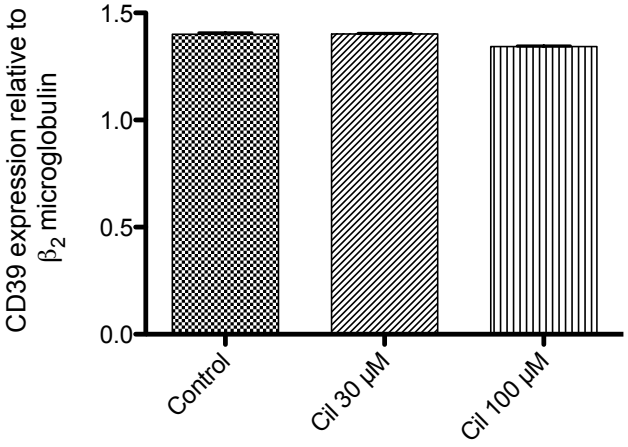

Figure 3.8. CD39 mRNA levels by qRT-PCR: HUVEC treated with 30 or 100 μM cilostazol showed no difference in CD39 mRNA expression compared to control (n=3).

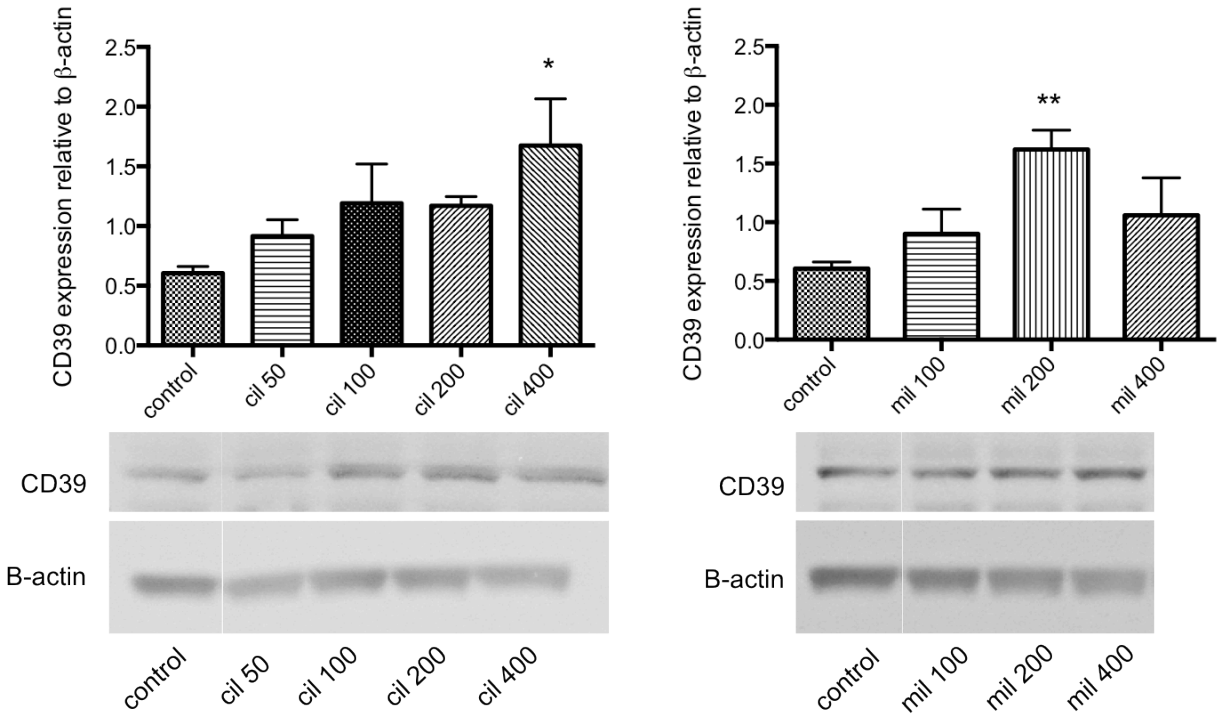

Figure 3.9. Effect of PDE3 inhibition on CD39 is dose-dependent: HUVEC were treated with varying concentrations of cilostazol (50-400 μM) or milrinone (100-400 μM). After 18 hours of treatment, cells were washed, and collected for analysis via Western blot. The results show that CD39 increases in a dose dependent manner (n=3, $p<0.05$ for cilostazol for control v. 400 μM and $p<0.01$ for milrinone control v. 200 μM)

Results from Western blots of whole cell lysates indicate a marked rise in CD39 protein levels as a function of cilostazol or milrinone dose. CD39 elevation peaks between 200 and 400 μM. Higher doses of milrinone were used in order to account for the relatively short half-life of milrinone compared to cilostazol, which has been cited as approximately 2.3 hours and 11 hours respectively (24, 25).

Immunofluorescent imaging of HUVEC treated with milrinone or cilostazol and then surface stained for CD39 with tetramethylrhodamine (**Figures 3.10 and 3.11**) further confirmed that CD39 protein is elevated after treatment.

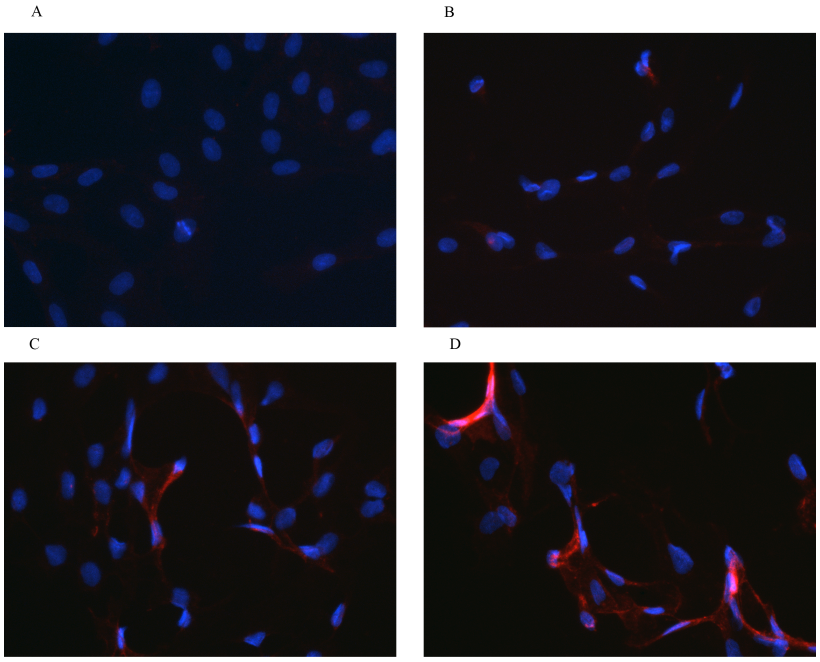

Figure 3.10. Effect of PDE3 inhibition on CD39 protein visualized by immunofluorescence microscopy: HUVEC were treated for 18 hours with control DMSO or milrinone (100-400 μM). Cells were then fixed in methanol and labeled CD39 with tetramethylrhodamine and nuclei with DAPI before imaging using a 20x objective. (a) DMSO (control); (b) 100 μM milrinone; (c) 200 μM milrinone; (d) 400 μM milrinone.

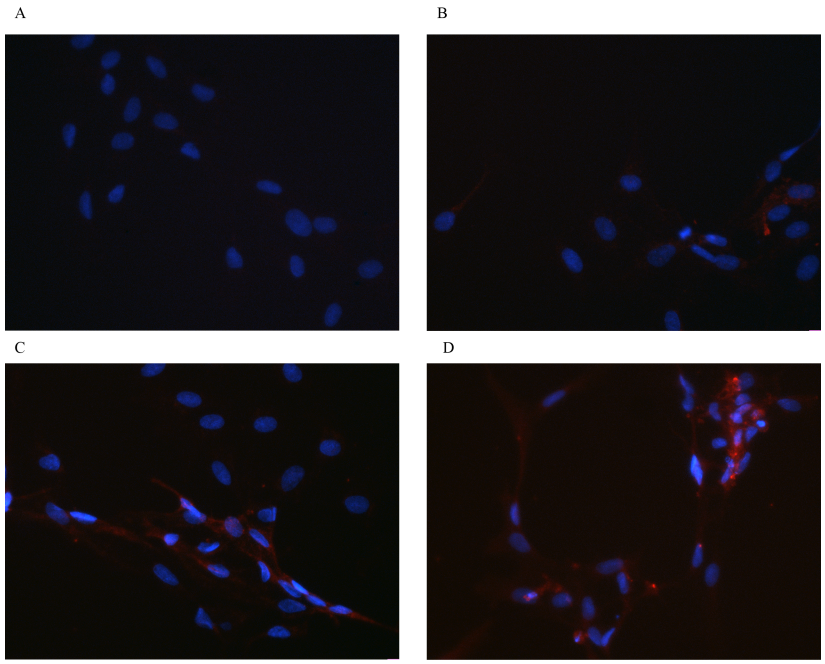

Figure 3.11. Effect of PDE3 inhibition on CD39 protein visualized by immunofluorescence microscopy: HUVEC were treated for 18 hours with control DMSO or cilostazol (50-400 μM). Cells were then fixed in methanol and labeled CD39 with tetramethylrhodamine and nuclei with DAPI before imaging using a 20x objective. (a) DMSO (control); (b) 50 μM cilostazol; (c) 100 μM cilostazol; (d) 400 μM cilostazol.

This also demonstrated that CD39 expression is increased after PDE3 inhibition on the plasma membrane, where it has been shown to be active (26).

Since CD39 mRNA was not affected by treatment, we considered the possibility that regulation of CD39 in HUVEC may occur via posttranslational modifications, possibly involving changes in the intracellular trafficking or release of CD39. Posttranslational control was supported by an immunoprecipitation assay probing for ubiquitinated CD39 (**Figure 3.12**).

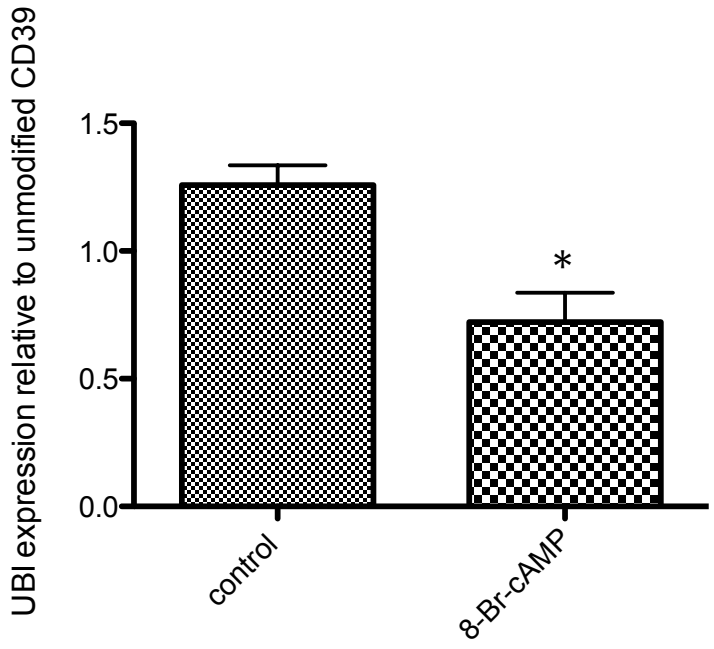

Figure 3.12. Effect of PDE3 inhibition on ubiquitination of CD39: HUVEC were treated for 18 hours with 8-Br-cAMP or control PBS. Cells were then washed in PBS, harvested, and incubated with beads coated with anti-human CD39 antibody. Beads were then washed and the protein eluted and analyzed via Western blot. Membranes were first probed with anti-ubiquitin antibody, then stripped and reprobed with anti-human CD39 antibody ($n=3$, $p<0.05$). Treatment with 8-Br-cAMP resulted in 43% less ubiquitin bound to CD39.

Here, HUVEC were treated with either control DMSO or 8-Br-cAMP, followed by precipitation with beads coated with anti-human CD39 antibody. Using Western blot, samples were sequentially evaluated for ubiquitin and CD39 expression. The ratio

of ubiquitin expression to CD39 expression was diminished after treatment with 8-Br-cAMP (by 43%, n=3, $p<0.05$). The data indicated that cAMP is likely raising CD39 levels by preventing CD39 ubiquitination in HUVEC.

Effect of PDE3 inhibition on CD39 activity- To assess whether increases in CD39 protein, as measured by Western blots of cell lysates, resulted in changes in ATPase and ADPase activity, an activity assay measuring the breakdown of radioactively labeled ATP was performed. Nucleotides were separated by thin layer chromatography (TLC) (**Figure 3.13**). Signal density indicates the relative levels of nucleotides present in samples at the time of measurement and thus serves as a measure of CD39 activity. Peaks 1, 2 and 3 correspond to ADP measured in HUVEC samples treated with DMSO (control), cilostazol, or milrinone, respectively.

Both cilostazol and milrinone increased CD39 activity significantly compared with control DMSO-treated HUVEC. As a confirmatory test of relative differences in CD39 activity after PDE3 inhibitor treatment, a malachite green assay was performed on HUVEC treated with varying doses of cilostazol or milrinone (**Figure 3.14 A and B**).

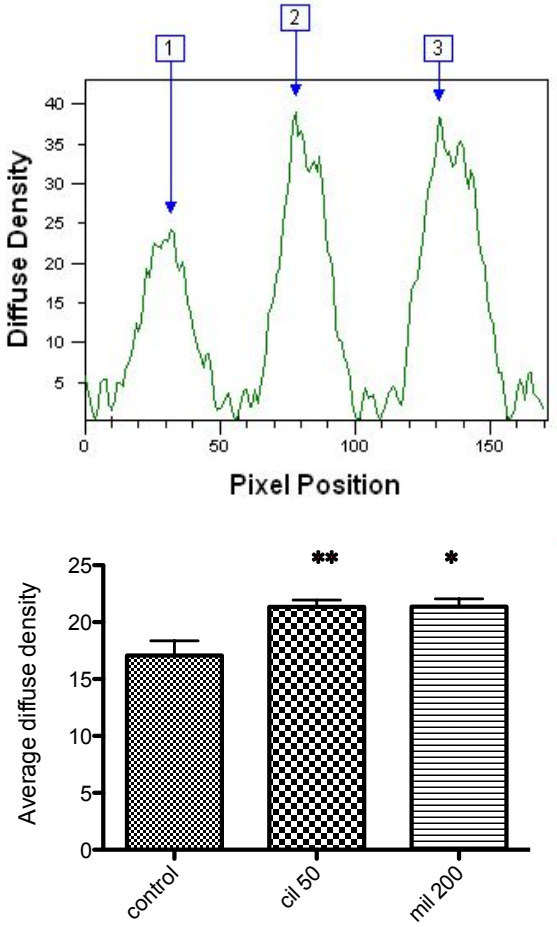

Figure 3.13. Functional assessment of CD39 activity following PDE3 using radio-thin-layer chromatography (TLC): Total cell lysates of HUVEC treated with either DMSO, cilostazol (50 μM), or milrinone (200 μM) were incubated with 14C-labeled ATP. Total ADP was measured and normalized to total protein and total radiation per lane (n=5, * = $p<0.05$, ** = $p<0.01$). Peak 1 indicates ADP measured in DMSO (control) treated samples, peak 2 indicates ADP measured in cilostazol treated samples, and peak 3 indicates ADP measured in milrinone treated samples.

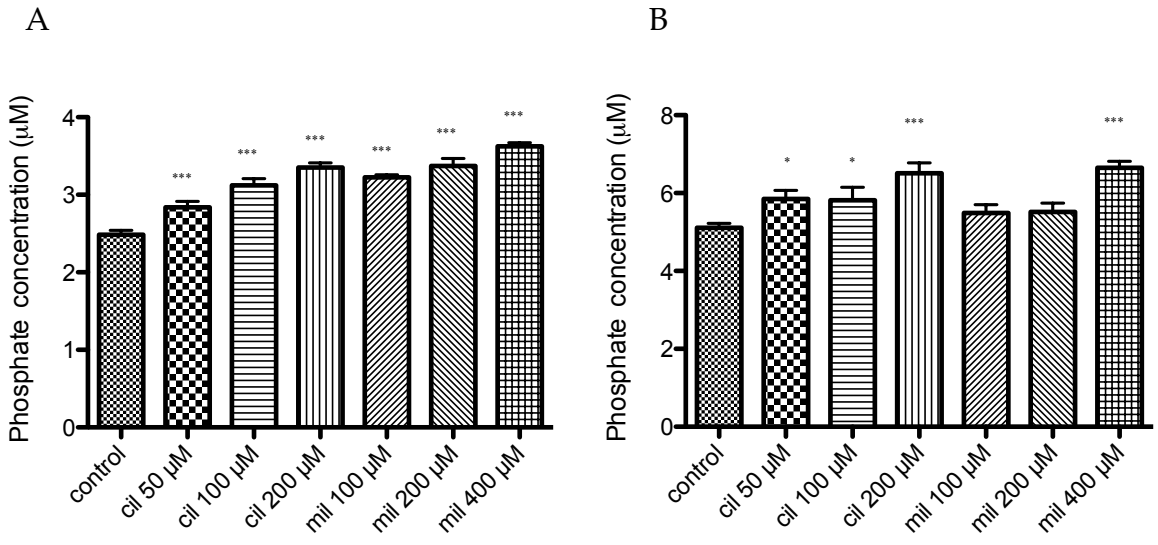

Figure 3.14. Measurement of inorganic phosphate generation following PDE3 inhibition using a malachite green assay: HUVEC were treated with either DMSO, along with

varying doses of either cilostazol (50-400 μM) or milrinone (100-400 μM). (a) inorganic phosphate levels after the addition of ADP, thus indicating relative ADPase activity. (b) inorganic phosphate levels after the addition of ATP, thus indicating relative levels of combined ATPase and ADPase activity. (n=6, *=p<0.05, **=p<0.01, ***=p<0.001)

Here, the presence of inorganic phosphates generated by the cleavage of ATP and ADP were measured, where higher concentrations of inorganic phosphate indicate greater apyrase activity. These measurements indicate that both ATP- and ADPase activity are elevated in cilostazol and milrinone treated samples, thus confirming the results of the TLC assay.

Discussion

CD39, a widely expressed plasmalemmal nucleotidase, occupies a unique niche in the vascular milieu, with a dichotomous role depending on physiologic or diseased conditions. Under normal conditions in the absence of stressors such as hypoxia/ischemia, high shear stress, and triggers for inflammation (cytokines/chemokines), CD39 helps to maintain a homeostatic environment (27-29), maintaining blood fluidity and inhibiting inflammation. In the presence of these injurious conditions, however, one of the most potent signals for platelet aggregation, ADP, as well as pro-inflammatory signals such as ATP, are released into the extracellular environment. When this occurs, the extracellular concentration of ADP and ATP increases markedly. Low levels of ATP act as communication between cells

that no injuries are present (30), and most receptors that bind ATP belonging to the class of P2X receptors are maximally activated at these low concentrations. However, the P2X7 receptor is only activated at the high levels of ATP (>100 μM)(31, 32) that signal danger, and therefore is the main ATP-driven signaling pathway of injury. The activation of this pathway leads to increased $\alpha_m\beta_2$ integrins and increased leukocyte recruitment. In short, the presence of high local concentrations of ATP serves as an acute sign of danger and triggers greater inflammation. CD39 acts to dissipate both ADP and ATP, limiting thrombosis, coagulation and inflammation (29). Though this role of CD39 has largely been determined, many questions surrounding the regulation of CD39 on both transcriptional and posttranslational levels remain unanswered.

Pleiotropy of PDE inhibition- Endothelial cells have been described to express several of the 11 phosphodiesterase family members, including PDE2, PDE4, PDE3, and PDE5 (33), and the latter three of these have been targeted for a diverse range of clinical uses. For example, roflumilast and cilomilast are PDE4 inhibitors developed for the treatment of chronic obstructive pulmonary disease, and other drugs targeting PDE4 inhibition have been researched as anti-depressants and have been shown to improve memory in a rodent model (34, 35). PDE5 inhibitors are best known for their role in facilitating vascular smooth muscle relaxation, and drugs such as sildenafil and tadalafil have been developed for the treatment of erectile dysfunction and for treatment of pulmonary arterial hypertension (34, 36). PDE3 inhibitors have also been a target of

interest, particularly useful as vasodilators in the treatment of heart failure, and two of these were specifically used herein as a tool to modulate intracellular cAMP levels. PDE3 is particularly interesting in relation to its potential effects on CD39, as it is important for regulating platelet aggregation by affecting intracellular cAMP levels. It is to this class that cilostazol and milrinone belong, the former developed as a vasodilator and platelet inhibitor and the latter as a regulator of cardiac contractility and vasodilator in the treatment of heart failure.

Effects of PDE3 inhibition- Cilostazol has been used in the treatment of intermittent claudication in the context of peripheral arterial disease (37). It is an antithrombotic that acts as an arterial vasodilator (38) and has been shown to prevent platelet aggregation stimulated by collagen, ADP, epinephrine, thrombin, arachidonic acid, and shear stress (37, 39). While the mechanism of action of cilostazol has yet to be fully elucidated, it is known that cilostazol acts as a specific inhibitor of phosphodiesterase III (PDE3). This inhibition of PDE3 leads to an increase in intracellular cAMP levels, which then potentiates other signaling pathways driven by cAMP, and finally results in vasodilation and suppression of platelet aggregation (40). It is different from other drugs of its class such as milrinone, in that cilostazol may also exert beneficial effects on the endothelium by reducing adenosine reuptake into endothelial cells, platelets, erythrocytes, and myocytes, thereby increasing extracellular adenosine signaling through A_1 and A_2 receptors (41, 42). Milrinone, in contrast to

cilostazol, has been used in the treatment of patients with heart failure (43). Though its half-life is considerably shorter than that of cilostazol, it has been shown to have a greater stimulatory effect on cAMP in ventricular myocytes compared to cilostazol, and to have a greater effect on contractility in hearts (23). Both drugs have been demonstrated to act specifically on PDE3 and increase intracellular cAMP, and are used herein to demonstrate that specific PDE3 inhibition, as opposed to drug-specific effects, is responsible for changes to CD39 expression.

Transcriptional regulation of human CD39- Very little is currently known about the transcriptional mechanisms responsible for the expression of CD39. However, we have recently established that CD39 mRNA and protein can be increased in murine RAW macrophages and murine peritoneal macrophages after exposing cells to 8-Br-cAMP (16). There are several cAMP response elements (44) in the murine CD39 promoter region, of which one is proximal to the transcriptional start site to regulate CD39 directly. The human CD39 promoter region, in contrast, has a handful of AP-1/cre-like sequences encoded distal to the start site, indicating that cAMP-driven effects in endothelial cells may indeed be different from the direct transcriptional pathway in murine macrophages. This is particularly evident here, where inhibition of PDE3 led to significant increases in protein expression and activity of endothelial CD39, but led to no differences in mRNA levels (**Figures 3.7, 3.8, 3.9, 3.10, 3.11, 3.13,** and **3.14**). This is in

contrast to RAW macrophages, which showed increases in both CD39 protein and mRNA (**Figures** 3.**1, 3.4,** and 3.**5**).

Differential regulation of CD39 in endothelial cells: Ubiquitination- The fact that CD39 can be detected in higher levels after an increase in intracellular cAMP despite relatively unaltered mRNA levels indicates that changes may be occurring on a posttranslational level. However, extremely little is known about the degradation and turnover of CD39. Here, we raise the possibility that CD39 may be ubiquitinated. Several lines of evidence led us to propose this as a possibility. Firstly, the literature suggests that PDE inhibition and the subsequent modulation of intracellular cAMP can inhibit ubiquitination (45). In this case, PDE4 inhibition led to the inhibition of ubiquitin-driven protein degradation in rat skeletal muscles. This activity seems to be dependent in part on an increase in intracellular cAMP, in that cAMP levels induced by a β_2-agonist led to the suppression of two ubiquitin ligases (46). Taken together with data presented here showing that cAMP treatment leads to significantly less ubiquitinated CD39, it may be indicative of an endothelial mechanism by which CD39 expression is modulated posttranslationally. A second indication that CD39 may be regulated by ubiquitination is that CD39 protein contains a RanBPM (or RanBP9) binding site on its N-terminus (47). RanBPM is a widely expressed protein, scaffolding protein that mediates interactions between the cytoplasmic domains of proteins and other signaling moieties, and its various

associated activities range from promoting apoptosis (48) to microtubule reorganization (49). Relevant to this study, others have shown that protein binding to RanBPM can inhibit ubiquitination (50, 51). These data suggest that CD39 association with RanBPM may play a role in how CD39 expression is regulated.

In conclusion, we have shown that while the inhibition of PDE3 results in an increase in CD39 expression in both macrophages and endothelial cells, the mechanisms governing this upregulation differs between the two. In macrophages, there is a strong basis for the direct involvement of cAMP in the transcriptional regulation of CD39. In contrast, endothelial cells are only affected at the protein level, and we have shown here that PDE3 inhibition results in differential ubiquitination, with elevation of CD39 protein levels. While further study into this mechanism is ongoing, the demonstration of CD39 modulation by PDE3 inhibition is unique. That this was achieved through the utilization of available therapeutics, cilostazol and milrinone, presents the potential of repurposing currently used PDE3 inhibitors for the targeted control of CD39 and extracellular nucleotide signaling.

REFERENCES

1. Wang, Q., Tang, X. N., and Yenari, M. A. (2007) The inflammatory response in stroke. *J Neuroimmunol* **184**, 53-68
2. Elkind, M. S. (2010) Inflammatory mechanisms of stroke. *Stroke* **41**, S3-8
3. Kaczmarek, E., Koziak, K., Sevigny, J., Siegel, J. B., Anrather, J., Beaudoin, A. R., Bach, F. H., and Robson, S. C. (1996) Identification and characterization of CD39/vascular ATP diphosphohydrolase. *J Biol Chem* **271**, 33116-33122
4. Koziak, K., Sevigny, J., Robson, S. C., Siegel, J. B., and Kaczmarek, E. (1999) Analysis of CD39/ATP diphosphohydrolase (ATPDase) expression in endothelial cells, platelets and leukocytes. *Thromb Haemost* **82**, 1538-1544
5. Marcus, A. J., Broekman, M. J., Drosopoulos, J. H., Islam, N., Alyonycheva, T. N., Safier, L. B., Hajjar, K. A., Posnett, D. N., Schoenborn, M. A., Schooley, K. A., Gayle, R. B., and Maliszewski, C. R. (1997) The endothelial cell ecto-ADPase responsible for inhibition of platelet function is CD39. *J Clin Invest* **99**, 1351-1360
6. Hyman, M. C., Petrovic-Djergovic, D., Visovatti, S. H., Liao, H., Yanamadala, S., Bouis, D., Su, E. J., Lawrence, D. A., Broekman, M. J., Marcus, A. J., and Pinsky, D. J. (2009) Self-regulation of inflammatory cell trafficking in mice by the leukocyte surface apyrase CD39. *J Clin Invest* **119**, 1136-1149
7. Liao, H., Hyman, M. C., Baek, A. E., Fukase, K., and Pinsky, D. J. (2010) cAMP/CREB-mediated transcriptional regulation of ectonucleoside triphosphate diphosphohydrolase 1 (CD39) expression. *The Journal of biological chemistry* **285**, 14791-14805
8. Gonzalez, G. A., and Montminy, M. R. (1989) Cyclic AMP stimulates somatostatin gene transcription by phosphorylation of CREB at serine 133. *Cell* **59**, 675-680
9. Montminy, M. R., Sevarino, K. A., Wagner, J. A., Mandel, G., and Goodman, R. H. (1986) Identification of a cyclic-AMP-responsive element within the rat somatostatin gene. *Proceedings of the National Academy of Sciences of the United States of America* **83**, 6682-6686
10. Mayr, B., and Montminy, M. (2001) Transcriptional regulation by the phosphorylation-dependent factor CREB. *Nature reviews. Molecular cell biology* **2**, 599-609
11. Yamamoto, K. K., Gonzalez, G. A., Biggs, W. H., 3rd, and Montminy, M. R. (1988) Phosphorylation-induced binding and transcriptional efficacy of nuclear factor CREB. *Nature* **334**, 494-498

12. Essler, M., Staddon, J. M., Weber, P. C., and Aepfelbacher, M. (2000) Cyclic AMP blocks bacterial lipopolysaccharide-induced myosin light chain phosphorylation in endothelial cells through inhibition of Rho/Rho kinase signaling. *J Immunol* **164**, 6543-6549
13. Stull, J. T. (1980) Phosphorylation of contractile proteins in relation to muscle function. *Adv Cyclic Nucleotide Res* **13**, 39-93
14. Adelstein, R. S., Conti, M. A., and Pato, M. D. (1980) Regulation of myosin light chain kinase by reversible phosphorylation and calcium-calmodulin. *Ann N Y Acad Sci* **356**, 142-150
15. Koga, S., Morris, S., Ogawa, S., Liao, H., Bilezikian, J. P., Chen, G., Thompson, W. J., Ashikaga, T., Brett, J., Stern, D. M., and et al. (1995) TNF modulates endothelial properties by decreasing cAMP. *Am J Physiol* **268**, C1104-1113
16. Liao, H., Hyman, M. C., Baek, A. E., Fukase, K., and Pinsky, D. J. (2010) cAMP/CREB-mediated transcriptional regulation of ectonucleoside triphosphate diphosphohydrolase 1 (CD39) expression. *J Biol Chem* **285**, 14791-14805
17. Zhang, W., Ke, H., and Colman, R. W. (2002) Identification of interaction sites of cyclic nucleotide phosphodiesterase type 3A with milrinone and cilostazol using molecular modeling and site-directed mutagenesis. *Mol Pharmacol* **62**, 514-520
18. Schror, K. (2002) The pharmacology of cilostazol. *Diabetes Obes Metab* **4 Suppl 2**, S14-19
19. Yano, M., Kohno, M., Ohkusa, T., Mochizuki, M., Yamada, J., Hisaoka, T., Ono, K., Tanigawa, T., Kobayashi, S., and Matsuzaki, M. (2000) Effect of milrinone on left ventricular relaxation and Ca(2+) uptake function of cardiac sarcoplasmic reticulum. *Am J Physiol Heart Circ Physiol* **279**, H1898-1905
20. Baek, A. E., Kanthi, Y., Sutton, N. R., Liao, H., and Pinsky, D. J. (2013) Regulation of ecto-apyrase CD39 (ENTPD1) expression by phosphodiesterase III (PDE3). *FASEB journal : official publication of the Federation of American Societies for Experimental Biology* **27**, 4419-4428
21. Jaffe, E. A., Nachman, R. L., Becker, C. G., and Minick, C. R. (1973) Culture of human endothelial cells derived from umbilical veins. Identification by morphologic and immunologic criteria. *J Clin Invest* **52**, 2745-2756
22. Fujiwara, Y., Banno, H., Shinkai, Y., Yamamoto, C., Kaji, T., and Satoh, M. (2011) Protective effect of pretreatment with cilostazol on cytotoxicity of cadmium and arsenite in cultured vascular endothelial cells. *J Toxicol Sci* **36**, 155-161

23. Cone, J., Wang, S., Tandon, N., Fong, M., Sun, B., Sakurai, K., Yoshitake, M., Kambayashi, J., and Liu, Y. (1999) Comparison of the effects of cilostazol and milrinone on intracellular cAMP levels and cellular function in platelets and cardiac cells. *J Cardiovasc Pharmacol* **34**, 497-504
24. Bramer, S. L., Forbes, W. P., and Mallikaarjun, S. (1999) Cilostazol pharmacokinetics after single and multiple oral doses in healthy males and patients with intermittent claudication resulting from peripheral arterial disease. *Clin Pharmacokinet* **37 Suppl 2**, 1-11
25. Gorodeski, E. Z., Chu, E. C., Reese, J. R., Shishehbor, M. H., Hsich, E., and Starling, R. C. (2009) Prognosis on chronic dobutamine or milrinone infusions for stage D heart failure. *Circ Heart Fail* **2**, 320-324
26. Zhong, X., Malhotra, R., Woodruff, R., and Guidotti, G. (2001) Mammalian plasma membrane ecto-nucleoside triphosphate diphosphohydrolase 1, CD39, is not active intracellularly. The N-glycosylation state of CD39 correlates with surface activity and localization. *J Biol Chem* **276**, 41518-41525
27. Eltzschig, H. K., Kohler, D., Eckle, T., Kong, T., Robson, S. C., and Colgan, S. P. (2009) Central role of Sp1-regulated CD39 in hypoxia/ischemia protection. *Blood* **113**, 224-232
28. Reutershan, J., Vollmer, I., Stark, S., Wagner, R., Ngamsri, K. C., and Eltzschig, H. K. (2009) Adenosine and inflammation: CD39 and CD73 are critical mediators in LPS-induced PMN trafficking into the lungs. *Faseb J* **23**, 473-482
29. Marcus, A. J., Broekman, M. J., Drosopoulos, J. H., Olson, K. E., Islam, N., Pinsky, D. J., and Levi, R. (2005) Role of CD39 (NTPDase-1) in thromboregulation, cerebroprotection, and cardioprotection. *Semin Thromb Hemost* **31**, 234-246
30. Trautmann, A. (2009) Extracellular ATP in the immune system: more than just a "danger signal". *Sci Signal* **2**, pe6
31. Wiley, J. S., Sluyter, R., Gu, B. J., Stokes, L., and Fuller, S. J. (2011) The human P2X7 receptor and its role in innate immunity. *Tissue Antigens* **78**, 321-332
32. Surprenant, A., Rassendren, F., Kawashima, E., North, R. A., and Buell, G. (1996) The cytolytic P2Z receptor for extracellular ATP identified as a P2X receptor (P2X7). *Science* **272**, 735-738
33. Netherton, S. J., and Maurice, D. H. (2005) Vascular endothelial cell cyclic nucleotide phosphodiesterases and regulated cell migration: implications in angiogenesis. *Mol Pharmacol* **67**, 263-272

34. Bender, A. T., and Beavo, J. A. (2006) Cyclic nucleotide phosphodiesterases: molecular regulation to clinical use. *Pharmacol Rev* **58**, 488-520
35. Bruno, O., Fedele, E., Prickaerts, J., Parker, L. A., Canepa, E., Brullo, C., Cavallero, A., Gardella, E., Balbi, A., Domenicotti, C., Bollen, E., Gijselaers, H. J., Vanmierlo, T., Erb, K., Limebeer, C. L., Argellati, F., Marinari, U. M., Pronzato, M. A., and Ricciarelli, R. (2011) GEBR-7b, a novel PDE4D selective inhibitor that improves memory in rodents at non-emetic doses. *Br J Pharmacol* **164**, 2054-2063
36. Rosen, R. C., and Kostis, J. B. (2003) Overview of phosphodiesterase 5 inhibition in erectile dysfunction. *Am J Cardiol* **92**, 9M-18M
37. Minami, N., Suzuki, Y., Yamamoto, M., Kihira, H., Imai, E., Wada, H., Kimura, Y., Ikeda, Y., Shiku, H., and Nishikawa, M. (1997) Inhibition of shear stress-induced platelet aggregation by cilostazol, a specific inhibitor of cGMP-inhibited phosphodiesterase, in vitro and ex vivo. *Life Sci* **61**, PL 383-389
38. Dindyal, S., and Kyriakides, C. (2009) A review of cilostazol, a phosphodiesterase inhibitor, and its role in preventing both coronary and peripheral arterial restenosis following endovascular therapy. *Recent Pat Cardiovasc Drug Discov* **4**, 6-14
39. Kimura, Y., Tani, T., Kanbe, T., and Watanabe, K. (1985) Effect of cilostazol on platelet aggregation and experimental thrombosis. *Arzneimittelforschung* **35**, 1144-1149
40. Dawson, D. L., Cutler, B. S., Meissner, M. H., and Strandness, D. E., Jr. (1998) Cilostazol has beneficial effects in treatment of intermittent claudication: results from a multicenter, randomized, prospective, double-blind trial. *Circulation* **98**, 678-686
41. Liu, Y., Fong, M., Cone, J., Wang, S., Yoshitake, M., and Kambayashi, J. (2000) Inhibition of adenosine uptake and augmentation of ischemia-induced increase of interstitial adenosine by cilostazol, an agent to treat intermittent claudication. *J Cardiovasc Pharmacol* **36**, 351-360
42. Liu, Y., Shakur, Y., Yoshitake, M., and Kambayashi Ji, J. (2001) Cilostazol (pletal): a dual inhibitor of cyclic nucleotide phosphodiesterase type 3 and adenosine uptake. *Cardiovasc Drug Rev* **19**, 369-386
43. Anderson, J. L., Baim, D. S., Fein, S. A., Goldstein, R. A., LeJemtel, T. H., and Likoff, M. J. (1987) Efficacy and safety of sustained (48 hour) intravenous infusions of milrinone in patients with severe congestive heart failure: a multicenter study. *J Am Coll Cardiol* **9**, 711-722
44. Ansermot, N., Albayrak, O., Schlapfer, J., Crettol, S., Croquette-Krokar, M., Bourquin, M., Deglon, J. J., Faouzi, M., Scherbaum, N., and Eap, C. B.

(2010) Substitution of (R,S)-methadone by (R)-methadone: Impact on QTc interval. *Arch Intern Med* **170**, 529-536

45. Lira, E. C., Goncalves, D. A., Parreiras, E. S. L. T., Zanon, N. M., Kettelhut, I. C., and Navegantes, L. C. (2011) Phosphodiesterase-4 inhibition reduces proteolysis and atrogenes expression in rat skeletal muscles. *Muscle Nerve* **44**, 371-381
46. Goncalves, D. A., Lira, E. C., Baviera, A. M., Cao, P., Zanon, N. M., Arany, Z., Bedard, N., Tanksale, P., Wing, S. S., Lecker, S. H., Kettelhut, I. C., and Navegantes, L. C. (2009) Mechanisms involved in 3',5'-cyclic adenosine monophosphate-mediated inhibition of the ubiquitin-proteasome system in skeletal muscle. *Endocrinology* **150**, 5395-5404
47. Wu, Y., Sun, X., Kaczmarek, E., Dwyer, K. M., Bianchi, E., Usheva, A., and Robson, S. C. (2006) RanBPM associates with CD39 and modulates ecto-nucleotidase activity. *Biochem J* **396**, 23-30
48. Atabakhsh, E., Bryce, D. M., Lefebvre, K. J., and Schild-Poulter, C. (2009) RanBPM has proapoptotic activities that regulate cell death pathways in response to DNA damage. *Mol Cancer Res* **7**, 1962-1972
49. Nakamura, M., Masuda, H., Horii, J., Kuma, K., Yokoyama, N., Ohba, T., Nishitani, H., Miyata, T., Tanaka, M., and Nishimoto, T. (1998) When overexpressed, a novel centrosomal protein, RanBPM, causes ectopic microtubule nucleation similar to gamma-tubulin. *J Cell Biol* **143**, 1041-1052
50. Kramer, S., Ozaki, T., Miyazaki, K., Kato, C., Hanamoto, T., and Nakagawara, A. (2005) Protein stability and function of p73 are modulated by a physical interaction with RanBPM in mammalian cultured cells. *Oncogene* **24**, 938-944
51. Wang, L., Fu, C., Cui, Y., Xie, Y., Yuan, Y., Wang, X., Chen, H., and Huang, B. R. (2012) The Ran-binding protein RanBPM can depress the NF-kappaB pathway by interacting with TRAF6. *Mol Cell Biochem* **359**, 83-94

Chapter IV: Protective Role of CD39 in Cerebral Ischemia

Abstract

Cerebral tissue damage after an ischemic event can be exacerbated by inflammation and thrombosis. Elevated levels of extracellular ATP and ADP are associated with cellular injury and promote inflammation and thrombosis. Ectonucleoside triphosphate diphosphohydrolase 1 (CD39), an enzyme expressed on the plasmalemma of leukocytes and endothelial cells, suppresses platelet activation and leukocyte infiltration by phosphohydrolyzing ATP and ADP. To investigate the effects of increased CD39 in an *in vivo* model of cerebral ischemia, we developed a transgenic mouse expressing human CD39 (hCD39). A floxed stop sequence was inserted prior to the hCD39 transcriptional start site, generating a mouse in which the expression of hCD39 can be controlled in a tissue-specific manner with specific Cre recombinase mice. Here, we generated mice that express hCD39 globally, by crossing these mice with those expressing EIIA Cre. Bone marrow analysis showed similar endogenous CD39 mRNA between transgenic (TG) and wild type (WT) mice while expression of the human transgene was >3,600-fold greater than the mouse gene ($p<0.0001$, $n=3$). Cerebral ischemia was induced using a photothrombotic model of middle cerebral artery (MCA) occlusion. After 48 hours, mice underwent brain MRI and infarct volumes were quantified. TG hCD39 mice had

37.8% smaller infarct volumes ($p<0.05$, n=5). TG mice showed lower neurologic deficit compared to WT (1.0 vs 1.5 based on an established 5-point scale $p<0.02$, n=8). Western blot analysis of non-ischemic hemispheres showed that TG mice had significantly more CD39 expression than WT mice (5.4-fold, n=3, $p<0.0001$). Leukocytes from ischemic and contralateral hemispheres were purified for flow cytometric analysis. While contralateral hemispheres had the same numbers of macrophages and neutrophils (CD45+/ F4/80+ and CD45+/Ly6g+ respectively), ischemic hemispheres from TG mice had 64% fewer infiltrating macrophages and 68% fewer neutrophils ($p<0.001$, n=8).

This is the first report of transgenic overexpression of CD39 in mice imparting a protective phenotype following stroke, with reduced leukocyte infiltration, smaller infarct volumes and decreased neurological deficit. CD39 overexpression appears to quench postischemic leukosequestration and reduce neurological injury after stroke.

Introduction

Ischemic events in the brain occur due to embolization of cholesterol-rich plaque or thrombus, which restricts blood flow. Cerebral ischemia can lead to neuronal death in those areas downstream of the occlusion, and a consequent deficit in cognitive function. Current tools used to mitigate tissue damage caused by acute thrombotic stroke involve the use of aspirin, or reperfusion by fibrinolytic treatment such as tissue plasminogen activator (rt-PA), but this must be administered within the first several hours of ischemia (1, 2). Intravenously administered rt-PA, in fact, remains one of the

very few therapies for acute ischemic stroke (3, 4). Inflammation further contributes to the detrimental effects of cerebral ischemia, with neutrophils, macrophages, and T cells composing the major component of infiltrating cells (5). Further innovations into more specific and localized treatments capable of targeting inflammation and thrombosis apart from hemostasis are necessary.

One molecular target that is being considered for antithrombotic and anti-inflammation therapeutic development include ecto-apyrases, which limit inflammation and thrombosis by enzymatically degrading extracellular nucleotides (6-8). Of these ecto-apyrases, CD39 (ENTPD1) is the dominant form expressed on the plasmalemma, and is responsible for dissipating the pro-inflammatory ATP and pro-thrombotic ADP to form AMP (8, 9). CD39-mediated degradation of pro-thrombotic and pro-inflammatory signals acts locally, and may be less likely to increase hemorrhagic risk (10).

Here, we have employed a well-established model of cerebral ischemia in which the middle cerebral artery (MCA) of mice was permanently occluded via a transcranial approach, in order to test whether augmentation of endogenous CD39 expression could be useful (11, 12). Furthermore, we have developed a floxed CD39 transgenic mouse in order to selectively overexpress CD39 in specific cells.

Methods

Generation of transgenic mice: C57Bl/6 mice were used to generate mice that selectively expressed a human CD39 transgene. A backbone construct (pcall-2, a gift from the Lobe laboratory) was modified (13, 14). A description of the final construct is as follows: a CAG promoter followed by two LoxP sequences flanking a 3 repetitions of a polyA sequence, followed by the starting sequence and full-length human CD39 cDNA (**Figure 4.1**). The sequence was purified and microinjected into fertilized eggs. Transgenic founders were identified via a specific PCR screen probing human CD39 DNA. Forward primer: 5′ ACA GGC GTG GTG CAT CAA GTA GAA 3′ and Reverse primer: 5' CCT GGC ACC CTG GAA GTC AAA G -3'.

Stable colonies were established and maintained before breeding to EIIA-Cre mice. EIIA-Cre mice have Cre expression driven by the EIIA promoter, and are often used when generating mice that express transgenes globally, including in the germline (15). Offspring of these breeding pairs generated mice expressing human CD39 globally. Mice carrying the floxed polyA sequence were subsequently bred to LysM-Cre mice (Jackson laboratories), and offspring overexpress human CD39 in myeloid lineage cells only.

Middle cerebral artery occlusion (MCAO) model – Mice were anesthetized using 2% isoflurane mized with oxygen, administered rose bengal dye (1 mg/25 g body weight dissolved in saline) retro-orbitally, and an incision made above the left eye, exposing

the temporalis muscle. A hole was drilled into the calvarium to visualize the MCA. The MCA was exposed to a 542-nm neon laser. MCA bloodflow was monitored using a laser Doppler flow probe (Transonic Systems Inc.), with occlusion was defined as 80% reduction in blood flow sustained for 10 minutes (16). The flow probe then remained for an additional 15 minutes before the probe was removed, the skin closed, and mice allowed to recover under a heat lamp.

Quantitative Reverse Transcription-PCR (qRT-PCR)- qRT-PCR was used to quantify RNA levels. Organs were harvested from transgenic or age-matched wild type C57Bl/6 mice and then immediately stored in measured volumes of RNAlater (Qiagen) at -80°C until ready for RNA isolation. Samples were cut to weight of 30 mg, and total RNA was isolated using RNAeasy kits (Qiagen). cDNA was made using cDNA synthesis kits (Applied Biosystems). Real time qPCR was carried out using the 7000 detection system (Applied Biosystems) with 2x universal mastermix and primers for human CD39 or mouse CD39 and mouse β-actin (Applied Biosystems). All data were normalized to β-actin.

Whole-Cell Protein Isolation- Organs were harvested from transgenic or age-matched wild type C57Bl/6 mice and immediately homogenized with a handheld tissue homogenizer in ice-cold RIPA buffer (25 mM Tris-HCL, 150 mM NaCl, 0.1% SDS, 0.1% Triton-X100, with all reagents from Sigma) containing protease inhibitor (Roche). Samples were incubated on ice for 20 minutes before centrifugation on a desktop

centrifuge for 10 minutes at 13,000 x g at 4°C. Resulting supernatants were transferred to new tubes. Concentrations were determined via a colorimetric protein assay (Bio-Rad). The samples were flash frozen in aliquots and stored at -80°C.

Western Blotting Assay- Total protein was quantified and added to 4x sample buffer (Invitrogen), boiled for 3 minutes at 100°C, separated by 10% SDS-PAGE, and electrophoretically-transferred onto PVDF membranes (Invitrogen). Membranes were probed with mouse monocolonal IgG_1 anti-CD39 antibodies (Abcam) and HRP-conjugated anti-mouse antibodies (Sigma), and then autoradiographed using the enhanced chemiluminescence (ECL) detection system (Amersham Biosciences). Blots were then washed and probed with mouse monoclonal β-actin IgG_1 conjugated to peroxidase (Sigma), and then autoradiographed using enhanced chemiluminescence.

Multiplex cytokine assay – Ischemia was induced in age-matched male wild type and transgenic mice for 6 hours, and then ipsilateral (ischemic) and contralateral cerebral hemispheres were harvested. Total protein was immediately collected by homogenizing tissue in ice-cold RIPA buffer without ionic detergent using a handheld homogenizer. Samples were snap frozen in liquid nitrogen until just prior to initiation of the assay. Samples were gently thawed on ice, and then centrifuged at 13,000 x g on a desktop centrifuge at 4°C for 10 minutes. Supernatants were collected into fresh microcentrifuge tubes. A 96-well filter plate provided in the mouse cytokine panel kit (Invitrogen) was prepared according to manufacturer instructions. Briefly, the filters

were incubated with wash buffer, and beads were sonicated and evenly distributed into each well. Duplicate standards were used, and total protein in samples was measured for normalization. After incubation with a biotinylated antibody and streptavidin, a Luminex 100 was used to read the plate.

MRI – After 48 hours of cerebral ischemia, prior to brain harvest, mice were anaesthetized with a mixture of 2% isoflurane and air, and placed in a 7.0 T Varian MR scanner (183-mm horizontal bore). Body temperature was maintained at 37°C with heated air. A double-tuned volume radio-frequency coil was used to scan the heads of the mice, and axial T_2-weighted images were acquired using a spin-echo sequence. Repetition time/effective echo time was 4000/40 ms, field size was 30 x 30 mm, matrix was 128 x 128, slice thickness was 0.5 mm, slice spacing was 0 mm, and 25 slices were taken for each brain. Infarct volumes were then calculated under blinded conditions.

Neurologic deficit Scoring: A 5-point scoring system was employed to assess mice 48 hours after MCAO(17). 1: normal function; 2: flexion of the torso and contralateral forelimb upon lifting of the animal by the tail; 3: circling to the contralateral side with normal posture at rest; 4: leaning to the contralateral side at rest; 5: no spontaneous motor activity.

Flow cytometry – After 48 hours of induced ischemia, brains were harvested. The cerebellum was excluded, and then hemispheres were separated into individual dishes. Brains were washed with sterile PBS on ice, and then minced with scissors. Samples

were then transferred into gentleMACS tubes (Miltenyi) and cells were dissociated using a gentleMACS dissociator (Miltenyi). Samples were then passed through a sterile 18 g syringe ten times in order to obtain a single-cell suspension. Red blood cells were lysed by incubating samples with ACK (Ammonium-Chloride-Potassium) lysis buffer (Invitrogen) for 6 minutes at room temperature in the dark. Samples were then washed and then mixed with a 30% Percoll solution, and centrifuged at 1,400 x g at 4°C for 10 minutes to separate myelin. Cells were then washed twice in FACS buffer (0.5% FBS, 0.1% sodium azide in PBS), and then 100,000 cells were distributed into each tube for antibody staining. Each experiment was performed with isotype controls. Cells were blocked for 30 minutes on ice with Fc-block (BD Biosciences), and then fluorescently labeled antibodies were added for 30 minutes on ice in the dark. Samples were washed twice in FACS buffer, and kept in the dark, on ice, until ready for analysis using a Becton Dickenson FACScalibur.

Immunostaining – Whole brains of mice were harvested after 6 or 48 hours (or as indicated) after MCA occlusion, and perfused with PBS, embedded in Tissue-Tek OCT (Sakura Finetek). They were then frozen at -80° C prior to sectioning. Coronal sections were cut to a thickness of 10 μM and mounted on glass slides. Sections were kept at -80° C until staining. Slides were allowed to warm briefly before fixation in ice-cold acetone for 10 minutes. Slides were then stained using the Vectastain Elite kit for mouse-derived antibodies, and then the signal amplified using a tyramide signal amplification kit

(Perkin-Elmer). CD39, P_2X_7 receptors, and TNFα were detected using primary monoclonal mouse (CD39 and TNFα) and rabbit (P_2X_7) antibodies (Abcam), and DAPI was used as a counter stain.

Isolation of bone marrow derived macrophages - Bone marrow macrophages were harvested from globally transgenic mice and wild type C57Bl/6 mice. Briefly, following humane euthanasia of mice, femurs were isolated, sterilized, and both ends of the bone severed. Femurs were flushed through with sterile media (DMEM-F12, 10% FBS, 10 mM Glutamine), and then spun down in at 190 x g for 10 minutes. Cells were suspended in cell culture medium and grown with GM-CSF overnight. All media and floating cells were transferred and incubated for 3 days. More GM-CSF was added to media, after which cells were incubated for 4 more days. All cells were then split into appropriate experimental wells and no further passaging was performed.

Malachite green assay to measure apyrase activity – Bone marrow macrophages were harvested from wild type and CD39 globally-transgenic mice and plated in 24-well plates (Corning). Cells were washed twice in PBS before the addition of ATP or ADP. Supernatants were collected and transferred to a flat-bottom 96-well plate. Standards were run alongside samples, and were prepared using serial dilutions of a solution of known concentration of phosphate into the same background buffer as the samples being measured. Finally, the working solution for the malachite green assay was added

(Bioassay Systems). Plates were incubated for 25 minutes before reading O.D. measurements at 620 nm.

Statistics- Statistical analysis was performed using analysis of variance to detect differences between groups. Groups were analyzed with a one-way ANOVA, and further *post hoc* analysis using the student Newman-Keuls method was applied (Prism®). Differences were considered significant if p was <0.05.

Results

Identification of transgenic mice - Conditional transgenic CD39 mice were generated in order to investigate the protective nature of CD39 in the event of cerebral ischemia. A backbone containing a floxed-stop sequence preceding the start codon (**Figure 4.1A**) was used to generate transgenic mice in a pure C57Bl/6 background.

A)

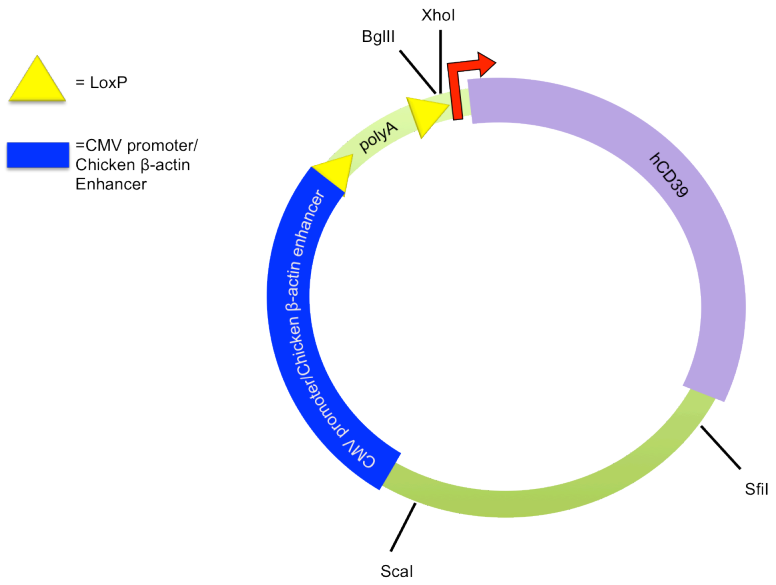

Figure 4.1: Transgenic mouse generation and confirmation of genotype and phenotype: A) A map of the plasmid used to generate CD39 transgenic mice. CD39 was inserted directly after the second loxp site.

B)

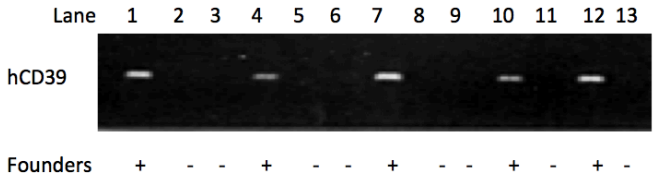

Figure 4.1B: Transgenic mice were identified via PCR using primers probing for human CD39. Of 17 potential mice, 5 were identified as transgenic founders.

C)

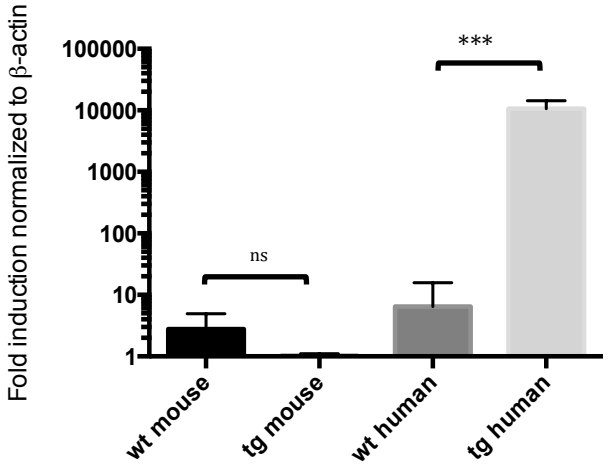

Figure 4.1C: Total RNA was isolated from brains of naïve wild type and transgenic mice and probed with human and mouse CD39 primers in a qPCR assay. Results were normalized to mouse β-actin.

D)

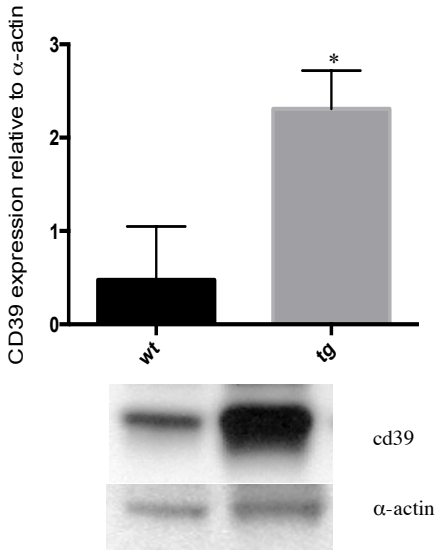

Figure 4.1D: Total protein was purified from hearts of naïve wild type and transgenic mice and probed with anti-CD39 antibodies via Western blot and normalized to α-actin expression.

E)

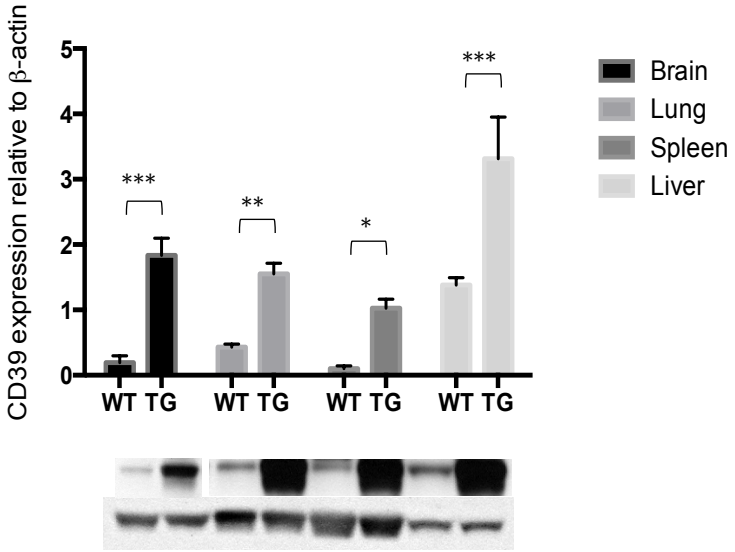

Figure 4.1E: Total protein was purified from brains, lungs, livers and spleens of naïve wild type and transgenic mice and probed with anti-CD39 antibodies via Western blot and normalized to β-actin expression.

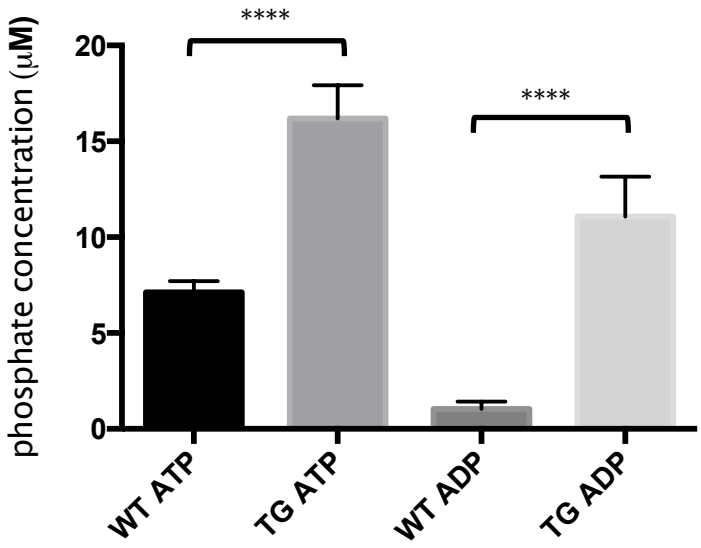

Figure 4.1F: Bone marrow was harvested from both wild type and transgenic mice, macrophages were grown, and phosphatase activity was measured. ATP or ADP was added as a substrate to live cells and free phosphate generation was quantified.

Five transgenic founders were identified using a PCR screen for the inserted transgene (**Figure 4.1B**). Mice were then bred to EIIA-cre mice with a C57bl/6 background, and transgenic offspring expressing human CD39 were identified using a second PCR screen. Brains were isolated from these mice in order to measure human CD39 mRNA expression in tissue. Transgenic mice expressed human CD39 mRNA, and endogenous levels of murine CD39 were no different from wild type C57BL/6 mice (**Figure 4.1C**). Western blots comparing tissue of wild type mice to transgenic mice shows that CD39 is ubiquitously over-expressed across a panel of different organ tissues. (**Figure 4.1D, 4.1E**). To confirm the functional significance of overexpressed CD39, a malachite green assay was performed (**Figure 4.1F**) on bone marrow derived macrophages of wild type and transgenic mice. This assay measures generation of inorganic phosphate from precursor substrates. These results demonstrate that phosphohydrolysis of ATP and ADP are significantly elevated in samples containing bone marrow derived

macrophages (BMDM) from transgenic mice compared to wild type mice. Complete blood counts were also taken (**Table 4.1**) from wild type and transgenic mice in order to determine whether any downstream differences could be accounted for by decreased platelet or leukocyte counts at baseline. These results show that across all parameters measured, there are no significant differences between the two groups.

	WT	TG	t-test
White blood cell (K/μL)	2.293 ± 1.54	2.95 ± 2.422	ns
Neutrophils (K/μL)	0.15 ± 0.118	0.397 ± 0.475	ns
Lymphocytes (K/μL)	2.083 ± 1.476	2.498 ± 1.942	ns
Monocyte (K/μL)	0.22 ± 0.385	0.0417 ± 0.031	ns
Eosinophil (K/μL)	0.005 ± 0.005	0.01 ± 0.009	ns
Basophil (K/μL)	0.002 ± 0.004	0.003 ± 0.005	ns
Red blood cell (M/μL)	7.23 ± 1.234	7.492 ± 1.192	ns
Hemoglobin (g/dL)	9.933 ± 1.988	10.067 ± 1.529	ns
Hematocrit (%)	36.05 ± 6.742	36.517 ± 5.871	ns
Mean corpuscular volume (fL)	49.7 ± 1.276	48.717 ± 0.708	ns
Mean corpuscular hemoglobin (pg)	13.65 ± 0.74	13.467 ± 0.446	ns
Mean corpuscular hemoglobin concentration (g/dL)	27.467 ± 1.122	27.633 ± 1.033	ns
Red cell distribution width (%)	15.45 ± 0.599	16.567 ± 1.194	ns
Platelets (K/μL)	246.667 ± 115.59	262.333 ± 149.396	ns

Table 1: Complete blood counts were measured for wild type and transgenic mice (n=6), and transgenic mice do not differ from wild type mice in any parameter.

CD39 mice are protected from effects of ischemia – Forty-eight hours after the induction of cerebral ischemia, brains were harvested and ischemic hemispheres were compared to contralateral hemispheres using flow cytometry. Cell counts for total leukocytes, macrophages and neutrophils, in the non-stroke (contralateral) hemisphere did not differ between WT and TG mice. Recruitment of macrophages was drastically suppressed in ischemic hemispheres of transgenic mice (**Figure 4.2A**). Similarly, recruitment of neutrophils was also suppressed in the ischemic hemispheres of transgenic mice (**Figure 4.2B**). There was significantly less inflammation in transgenic ischemic hemispheres compared to wild type ischemic hemispheres (**Figure 4.2C**).

Figure 4.2: Transgenic mice have less leukocyte infiltration into ischemic hemispheres. MCA of wild type and transgenic mice were occluded for 48 hours, and then left and right cerebral hemispheres were harvested for further analysis by flow cytometry. Cells were then stained with A) F4/80 (FITC) and CD45 (PE) to identify macrophages and B) Ly6g (FITC) and CD45 (PE) to identify neutrophils. C) Leukocytes were purified of myelin and cell debris and total leukocyte counts were obtained. D)

4.2A 4.2B 4.2C

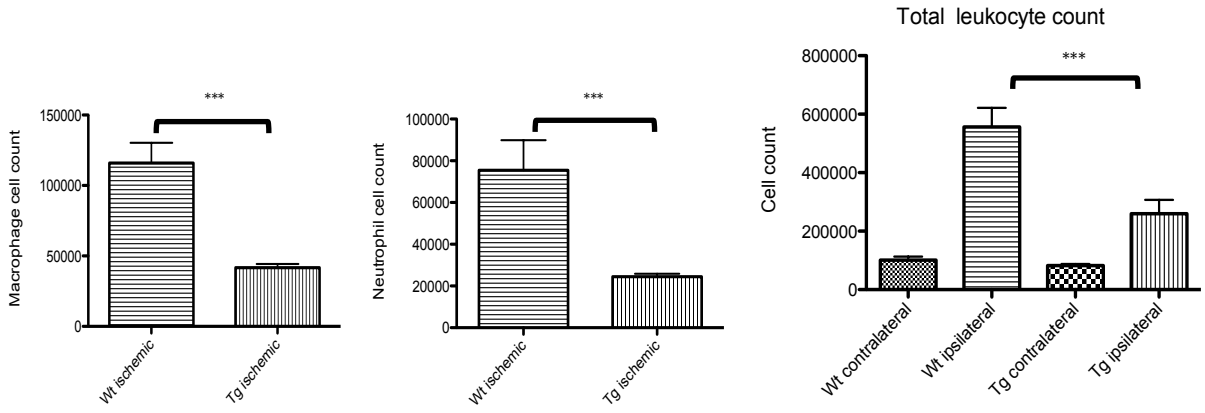

4.2D

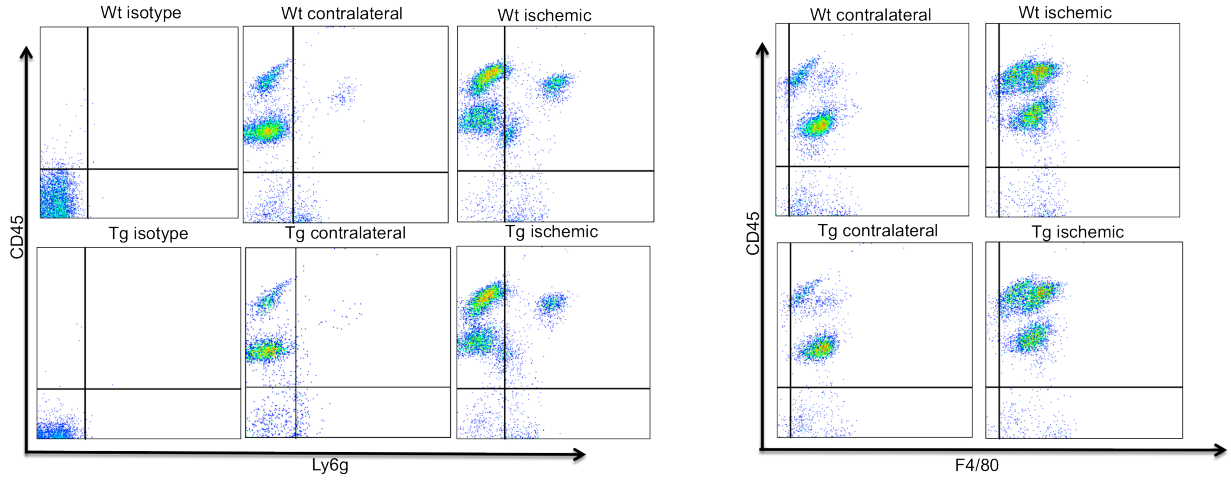

Figure 4.3: Transgenic mice have smaller infarct volumes. MCA of wild type and transgenic mice were occluded for 48 hours, and then mice were anesthetized in order to image brains via MRI. Scans of wild type (A) and transgenic (B) mouse brains are shown in coronal slices moving from anterior to posterior sections, where white areas indicate edematous tissue. C) Cerebral infarct volumes were calculated by integrating infarct area across all slices. D) Mice were scored for neurological deficit after 48 hours of MCAO. Higher scores indicate higher levels of neurological impairment.

4.3A

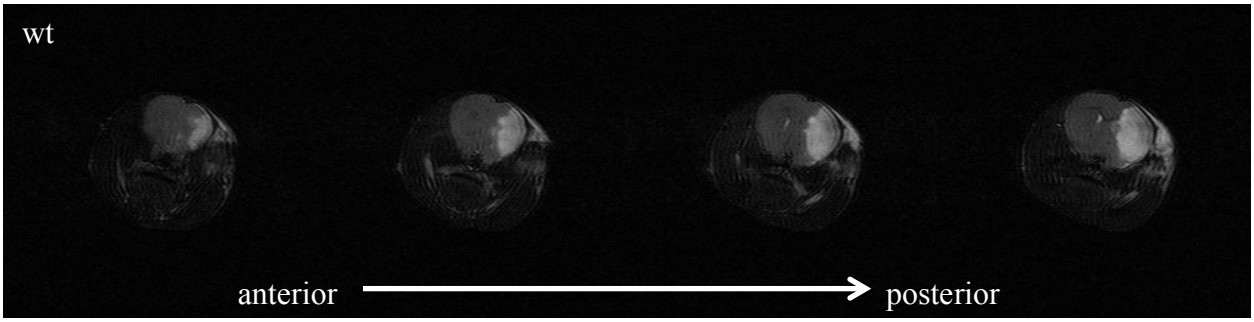

4.3B

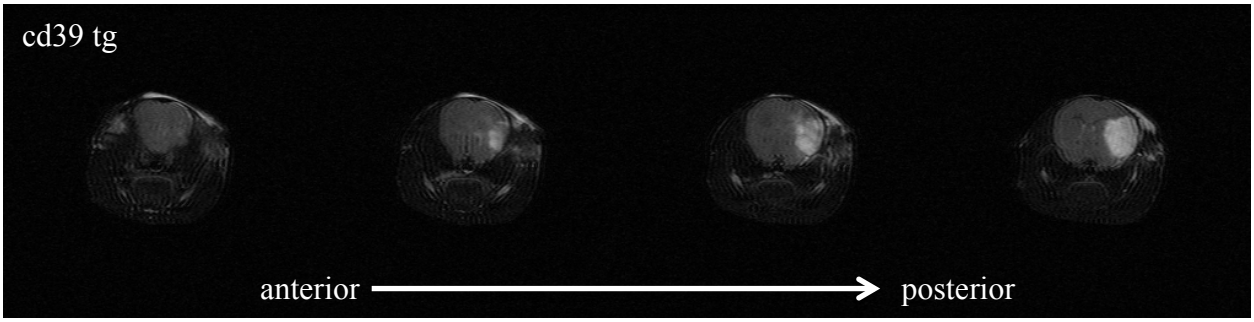

4.3C

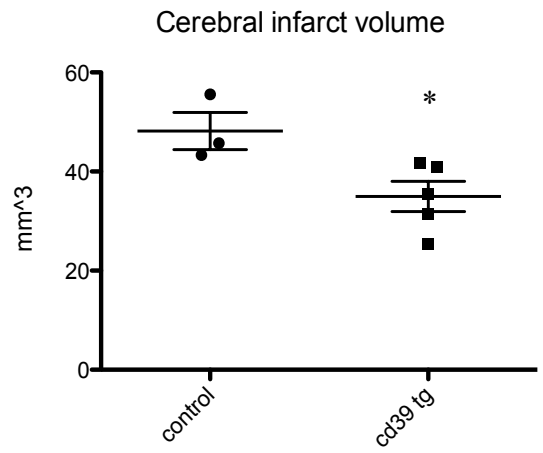

4.3D

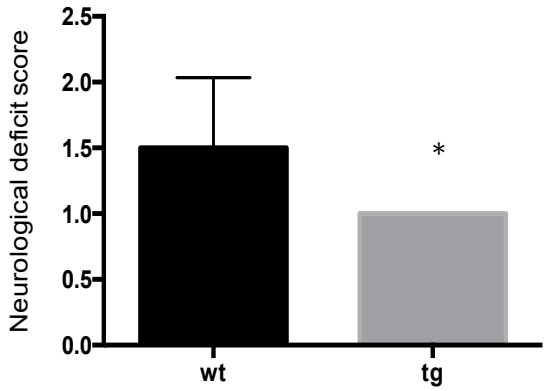

The suppression of inflammation in ischemic hemispheres of transgenic mice compared to wild type mice corresponded with smaller infarct volumes. MRIs were taken from mice 48 hours after induction of ischemia, and transgenic mice had 20% reduced infarct volumes compared to wild type mice. (**Figures 4.3A, B, C**). Mice were scored according to a 5-point neurological deficit scale after 48 hours of ischemia (**Figure 4.3D**).

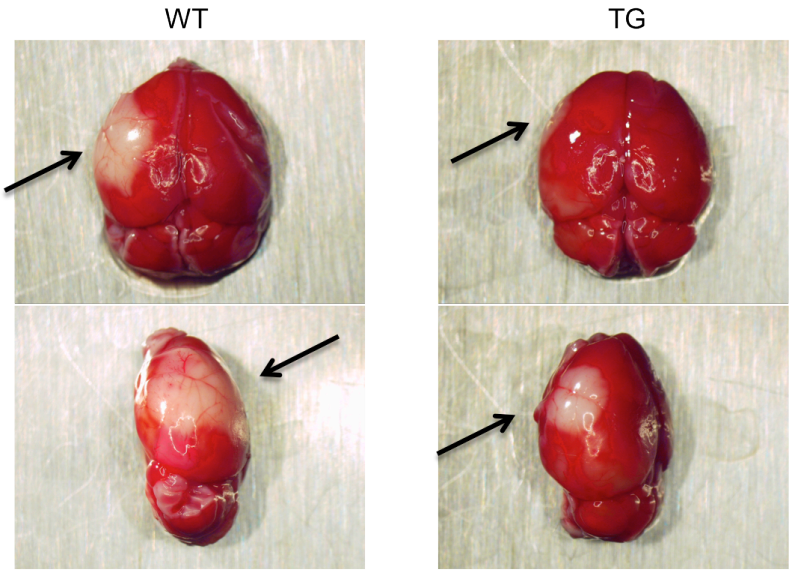

Figure 4.4: TTC staining of stroked brains. Wild type and CD39 transgenic mouse brains 24 hours after MCAO. Brains were harvested and then stained in TTC solution in order to visualize viable tissue, shown in red. Infarcted tissue appears white as indicated by arrows. Upper panels show dorsal views of WT and TG brains, and lower panels show left (ischemic) hemispheres.

Triphenyl tetrazolium chloride (TTC) staining was also performed to visualize corresponding tissue death following MCAO (**Figure 4.4**). TTC dissolved in PBS is nearly colorless until active mitochondria in living tissue reduce TTC to 1,3,5-triphenylformazan, which is red. Brains of wild type mice were observed to have much larger areas of inactive tissue in ischemic hemispheres relative to transgenic mice, which had much more contained inactive regions.

CD39 overexpression leads to differential cytokine expression following cerebral ischemia - Six hours after inducing cerebral ischemia, brains were harvested and contralateral and ipsilateral hemispheres were isolated separately, and homogenized in order to analyze

cytokine expression via a multiplex protein panel (**Figure 4.5**). Cytokine/chemokine expression levels in contralateral hemispheres of wild type and transgenic mice were not different from each other. However, ischemic hemispheres of wild type mice showed elevated levels of pro-inflammatory cytokines and chemokines. Classically designated anti-inflammatory cytokines showed mixed patterns of expression. Il-4 showed no significant differences between any of the hemispheres, whereas wild type ipsilateral hemispheres showed greater Il-5 expression compared to transgenic ipsilateral hemispheres. Il-6 was also more highly expressed in ischemic wild type cerebral hemispheres. One of the cytokines shown to be elevated in wild type ipsilateral (ischemic) hemispheres and conversely suppressed in transgenic mice, is TNF-α.

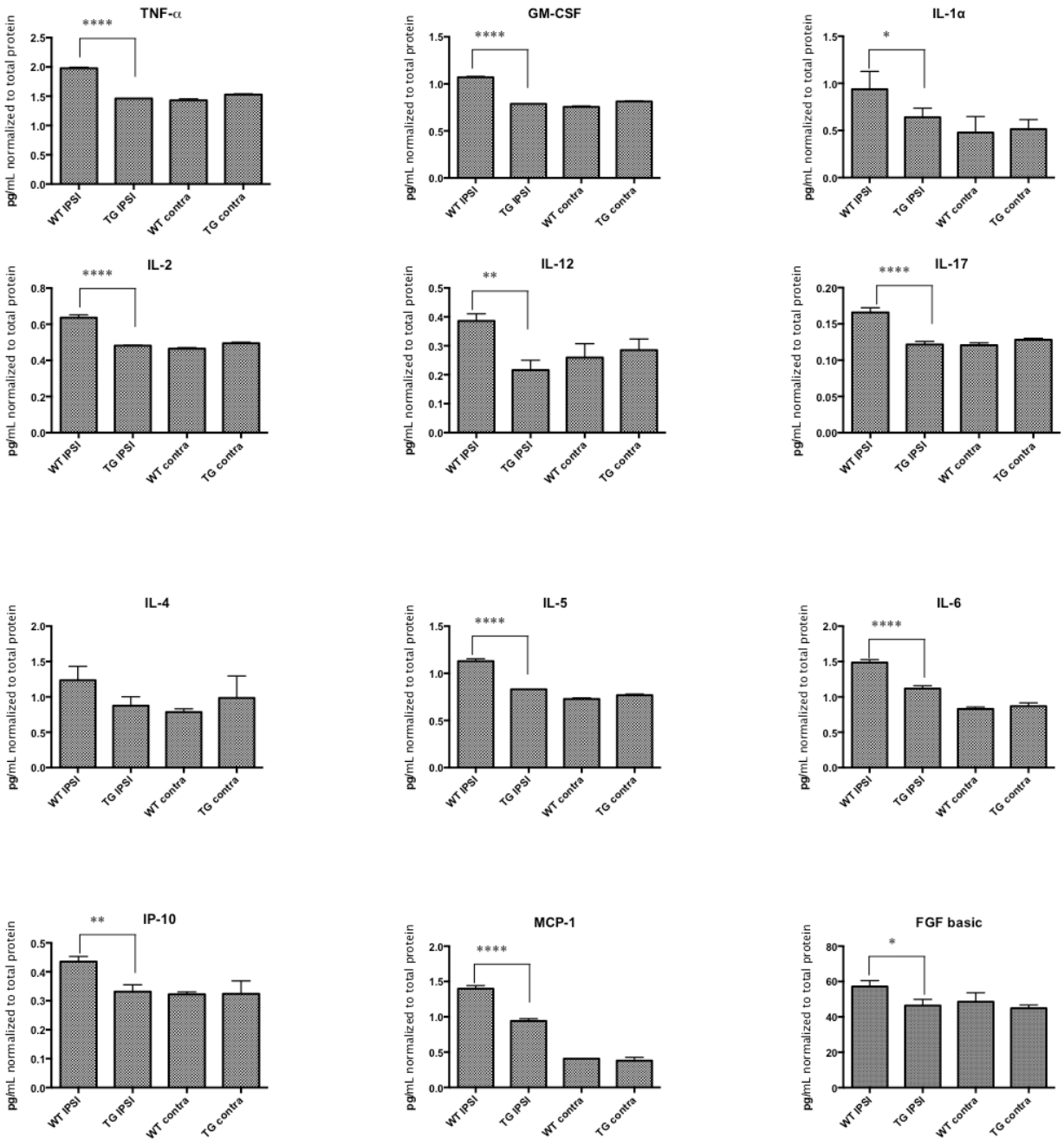

Figure 4.5: Measurement of cytokines from brains after stroke. MCA of wild type and transgenic mice were occluded for 6 hours, and then left and right cerebral hemispheres were harvested, and total protein purified. A panel of cytokine levels was measured using a multiplex bead assay. Cytokine levels in ischemic (ipsilateral) hemispheres were compared to contralateral hemispheres.

Figure 4.6: Immunofluorescent staining of coronal sections from stroked mice. MCA of wild type and transgenic mice were occluded for before freezing in OCT. Coronal sections of transgenic and wild type mouse brains were stained for A) TNF-α shown in green and CD39 shown in red after 6 hours of occlusion, B) P2X7 receptor shown in green and CD39 shown in red after 6 hours of occlusion, and C) P2X7 receptor shown in green and CD39 show in red after 48 hours of occlusion in LysM-Cre/CD39 transgenic mice. DAPI was used as a counter stain in all panels.

4.6A

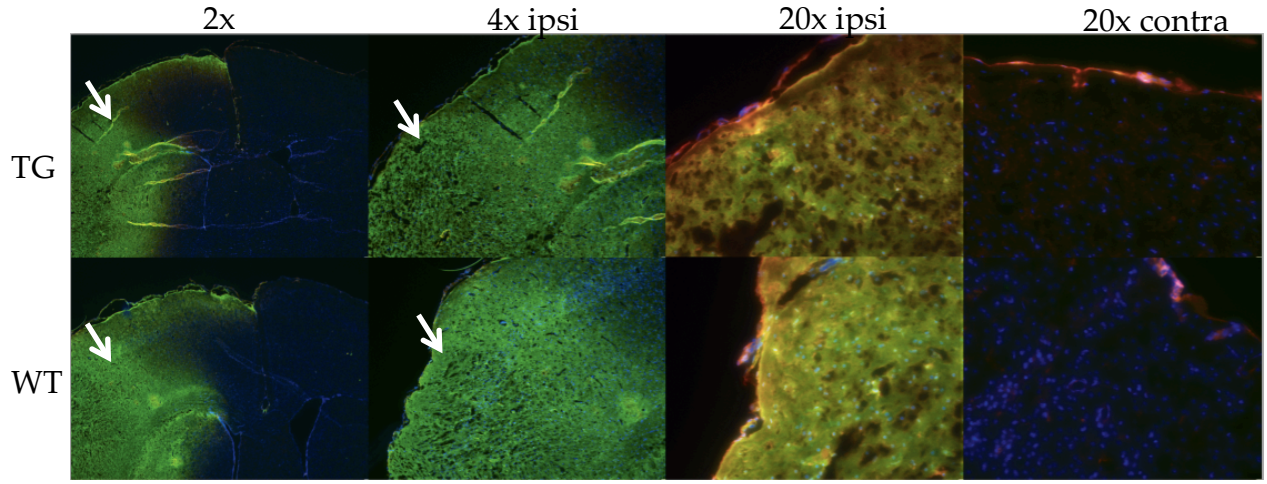

4.6B

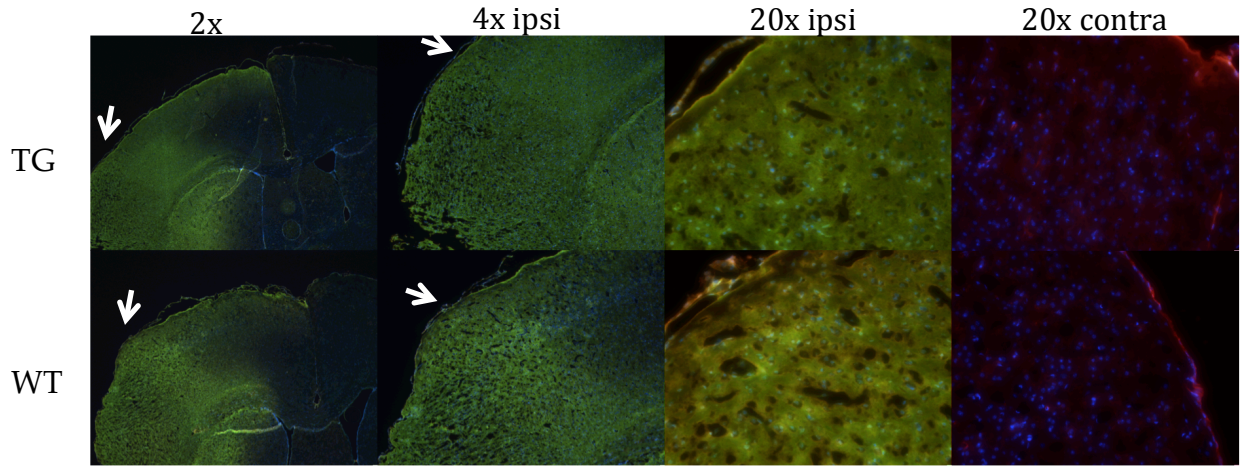

4.6C

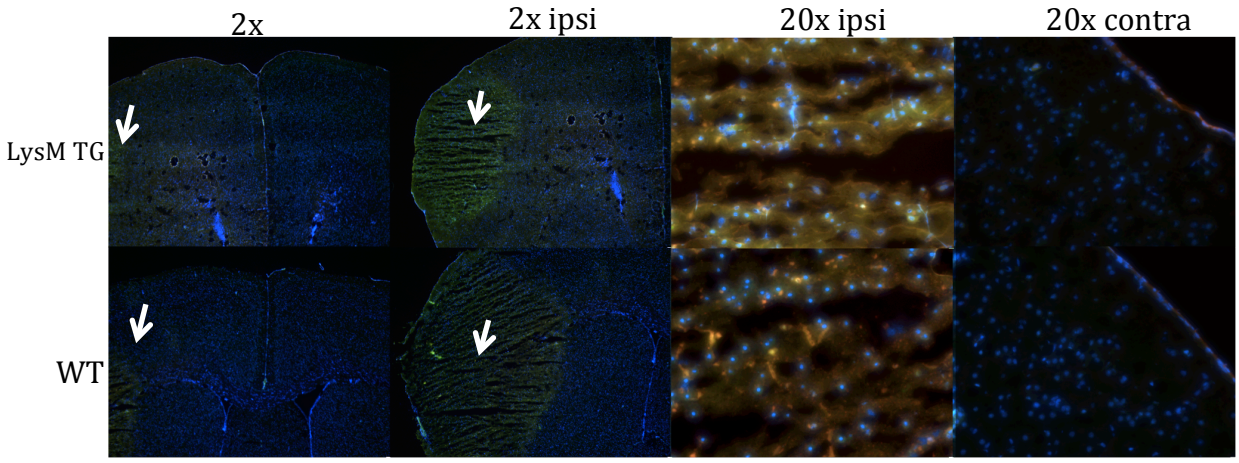

TNF-α expression across both ischemic and non-ischemic hemispheres in wild type and transgenic mice was visualized (**Figure 4.6A**). The upper row of panels shows a coronal section of a globally transgenic CD39 mouse in increasing magnification. The 2X image shows that TNF-α expression in the ischemic hemisphere of transgenic mice is limited relative to the wild type mouse. The contralateral image further shows that there is elevated CD39 present in the TG mouse, as expected. **Figure 4.6B** shows the distribution of P2X7 receptors after stroke. P2X7 receptor is widely expressed in macrophages and other circulating leukocytes (18), and as expected, it can be seen in ischemic hemispheres of both mice, whereas non-ischemic hemispheres appear unaffected. Again, transgenic mouse brains express higher levels of CD39 in contralateral hemispheres compared to wild type mice. **Figure 4.6C** shows coronal sections of tissue-specific, LysM-Cre/CD39 transgenic mice. These mice overexpress

CD39 in a tissue-specific manner in myeloid lineage cells only. After 48 hours of stroke, the 2x images show that the area affected by MCAO is much smaller in LysM-Cre transgenic mouse brains. Notably, there appears to be no large difference in CD39 expression between contralateral hemispheres.

The contribution of CD39 expressed on myeloid-lineage cells was tested by generating transgenic mice that express human CD39 in myeloid lineage cells only. These mice were generated by breeding mice carrying the unrecombined human CD39 gene to mice that express Cre driven by the LysM promoter. After 48 hours of cerebral ischemia, mice were imaged via MRI. These data show that LysM-Cre transgenic mice were also protected from tissue damage (**Figure 4.7**), as observed infarct volumes were lower compared to wild type mice.

A

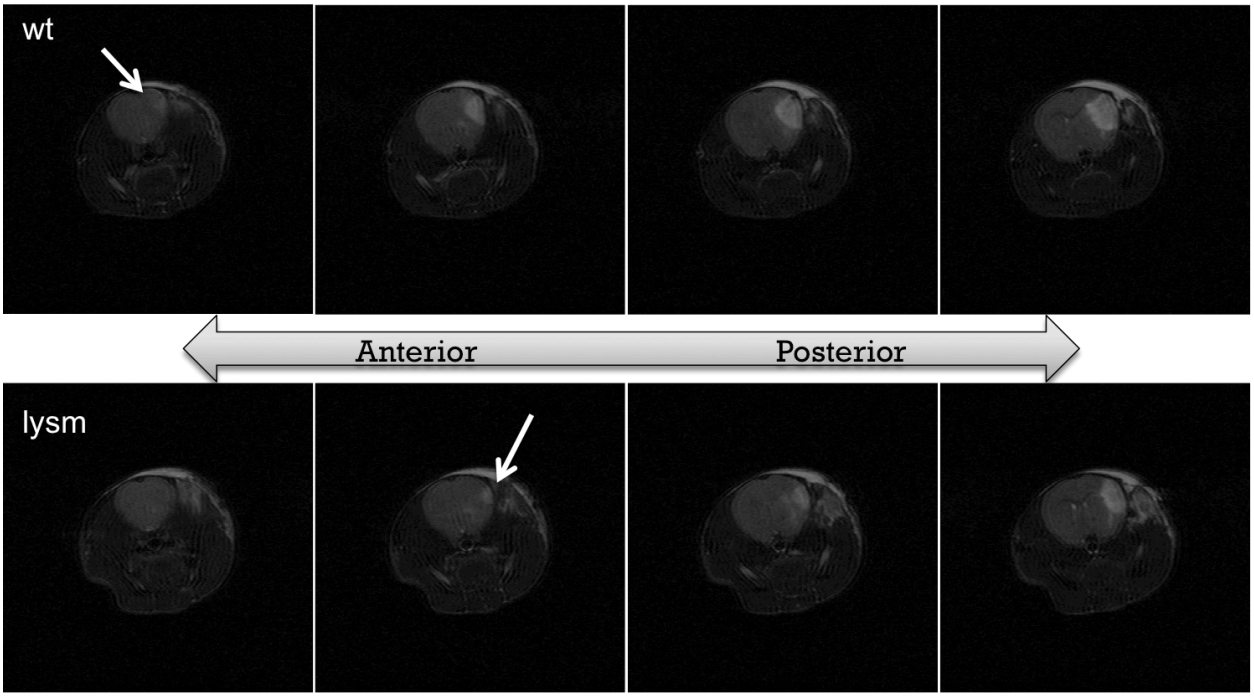

B

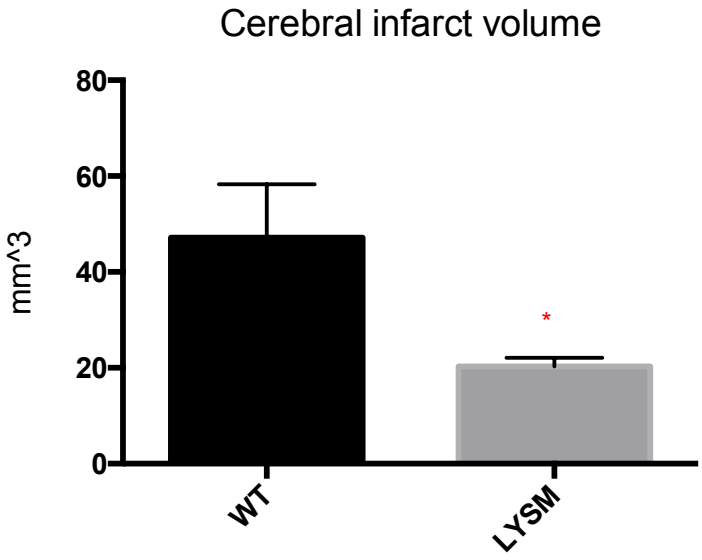

Figure 4.7: Lysm-Cre transgenic mice have smaller infarct volumes. MCA of wild type and LysM-Cre transgenic mice were occluded for 48 hours, and then mice were anesthetized in order to image brains via MRI. A) Scans of wild type and transgenic mouse brains are shown in coronal slices moving from anterior to posterior sections, where white areas indicate edematous tissue. B) Cerebral infarct volumes were calculated by integrating infarct area across all slices.

Discussion

Though some effective thrombolytic, fibrinolytic, and anti-platelet treatments exist which promote reperfusion in ischemic tissue, alternative approaches remain a priority target because current treatments are also associated with complications such as increased risk of intracerebral hemorrhage. A further limitation exists in the narrow time frame in which these existing stroke interventions have been shown to be most useful, in a range of 1 to 3 hours. As a result, only a relatively small portion of affected populations benefit from these interventions. The search for more selective methods of controlling hemostasis continues, wherein more anti-thrombotic and anti-inflammatory mechanisms can be employed in a specific and directed manner. Previous work readily establishes CD39 (ENTPDase1) as a strong mediator of thrombosis and inflammation. ATP and ADP, potent triggers of inflammation and thrombosis, respectively, can be present in high concentrations in localized areas of tissue damage. The apyrase activity of CD39 cleaves these signaling molecules to AMP, and the co-expressed partner enzyme of CD39, CD73, completes the cleavage of AMP to adenosine, which modulates inflammation and may protect against reperfusion injury (19-21).

Confirmation of the transgenic mouse design

In this study, we have developed a transgenic mouse that globally expresses elevated levels of CD39, and has the potential to be modified further to express greater levels of CD39 in specific tissue. To accomplish this, a vector containing a floxed stop

sequence between the promoter and the transcriptional start sequence of human CD39 was obtained, such that in the presence of the enzyme cre recombinase (22, 23), the stop sequence would be deleted and expression of human CD39 would be driven by a CAG promoter/enhancer sequence. This is the first description of such a mouse, which was developed to aid in future studies of CD39 which center on questions of the role of CD39 in specific tissues, and further characterization of CD39 function across different disease models. We have demonstrated herein that in our CD39 TG mice, human CD39 is detectable in DNA, RNA, and in protein samples. We are able to distinguish between the endogenous and transgene at the RNA level, and furthermore, we can see that this additional expression of CD39 elevates the total CD39 protein detected across a panel of different tissues.

Having confirmed the expected genotype and expected protein and RNA expression for the globally-transgenic mice, we have shown that CD39 overexpression is functional at baseline, as BMDMs from transgenic mice exhibited more apyrase activity compared to wild type. Our further studies have shown that this baseline difference in apyrase activity conferred a protective effect in transgenic mice against inflammation and tissue death after a cerebral ischemic insult. Most intriguingly, it can be seen that mice that only overexpress CD39 in their myeloid lineage cells are also protected in terms of infarct size. In the globally CD39 transgenic mice, while the total

percentage of infiltrating macrophages and neutrophils was not affected, total inflammation was significantly decreased in the first 48 hours after stroke, and this difference was shown to be confirmed by the MRIs showing a far smaller stroke volume as well as by neurological scoring which showed that transgenic mice suffered fewer neurological deficits than their wild type counterparts. These results were visually confirmed in direct TTC staining of live versus dead tissue, where wild type mice sustained more tissue death after MCAO relative to transgenic mice.

Concordant with the anatomic cerebral and functional protection in stroke conferred by transgenic overexpression of CD39, data from a cytokine/chemokine panel performed on tissue from mice post-ischemic stroke showed a less inflammatory post-stroke phenotype in CD39 TG mice. A general pattern of cytokine expression manifested, where across classically pro-inflammatory cytokines, levels in transgenic CD39 ischemic hemispheres were systematically lower than in the wild-type ischemic hemispheres. Contralateral non-ischemic hemispheres, on the other hand, which served as controls, did not appear to differ between the two genotypes. More importantly, the overexpression of CD39 appears to enable the ischemic hemisphere to generally maintain the same cytokine profile as observed on the non-ischemic contralateral side. In sum, these data support the generally anti-inflammatory state of transgenic mice even when challenged with a profound interruption of blood supply to a critical brain

region. The mice we have generated, according to a comparison of CBCs do not appear to be different from each other in any of the other parameters tested, thus supporting our hypothesis that CD39 overexpression is responsible for the protection from CNS inflammation and tissue death. The role of TNF-α across models of cerebral ischemia remains in discussion. While the elevated levels of TNF-α in acute stroke have been shown to impair survival, inhibition of TNF-α in the long term has been shown to impede repair (24, 25). Here, we have found that elevated TNF-α is associated with greater ischemic damage, and that the overexpression of CD39 mitigates the expression of TNF-α in the ischemic hemisphere.

This finding that elevated CD39 levels are protective in the setting of cerebral ischemia and supports the continued exploration of the mechanism of CD39-driven protection as well as methods of *in vivo* modulation of CD39 expression levels.

REFERENCES

1. Wardlaw, J. M., Murray, V., Berge, E., del Zoppo, G., Sandercock, P., Lindley, R. L., and Cohen, G. (2012) Recombinant tissue plasminogen activator for acute ischaemic stroke: an updated systematic review and meta-analysis. *Lancet* **379**, 2364-2372
2. Marler, J. R., and Goldstein, L. B. (2003) Medicine. Stroke--tPA and the clinic. *Science* **301**, 1677
3. Adams, H., Adams, R., Del Zoppo, G., and Goldstein, L. B. (2005) Guidelines for the early management of patients with ischemic stroke: 2005 guidelines update a scientific statement from the Stroke Council of the American Heart Association/American Stroke Association. *Stroke* **36**, 916-923

4. Jauch, E. C., Saver, J. L., Adams, H. P., Jr., Bruno, A., Connors, J. J., Demaerschalk, B. M., Khatri, P., McMullan, P. W., Jr., Qureshi, A. I., Rosenfield, K., Scott, P. A., Summers, D. R., Wang, D. Z., Wintermark, M., and Yonas, H. (2013) Guidelines for the early management of patients with acute ischemic stroke: a guideline for healthcare professionals from the American Heart Association/American Stroke Association. *Stroke* **44**, 870-947
5. Jin, R., Yang, G., and Li, G. (2010) Inflammatory mechanisms in ischemic stroke: role of inflammatory cells. *J Leukoc Biol* **87**, 779-789
6. Fung, C. Y., Marcus, A. J., Broekman, M. J., and Mahaut-Smith, M. P. (2009) P2X(1) receptor inhibition and soluble CD39 administration as novel approaches to widen the cardiovascular therapeutic window. *Trends Cardiovasc Med* **19**, 1-5
7. Qawi, I., and Robson, S. C. (2000) New developments in anti-platelet therapies: potential use of CD39/vascular ATP diphosphohydrolase in thrombotic disorders. *Curr Drug Targets* **1**, 285-296
8. Marcus, A. J., Broekman, M. J., Drosopoulos, J. H., Pinsky, D. J., Islam, N., and Maliszewsk, C. R. (2001) Inhibition of platelet recruitment by endothelial cell CD39/ecto-ADPase: significance for occlusive vascular diseases. *Ital Heart J* **2**, 824-830
9. Kaczmarek, E., Koziak, K., Sevigny, J., Siegel, J. B., Anrather, J., Beaudoin, A. R., Bach, F. H., and Robson, S. C. (1996) Identification and characterization of CD39/vascular ATP diphosphohydrolase. *J Biol Chem* **271**, 33116-33122
10. Dwyer, K. M., Robson, S. C., Nandurkar, H. H., Campbell, D. J., Gock, H., Murray-Segal, L. J., Fisicaro, N., Mysore, T. B., Kaczmarek, E., Cowan, P. J., and d'Apice, A. J. (2004) Thromboregulatory manifestations in human CD39 transgenic mice and the implications for thrombotic disease and transplantation. *J Clin Invest* **113**, 1440-1446
11. Bederson, J. B., Pitts, L. H., Tsuji, M., Nishimura, M. C., Davis, R. L., and Bartkowski, H. (1986) Rat middle cerebral artery occlusion: evaluation of the model and development of a neurologic examination. *Stroke* **17**, 472-476
12. Chiang, T., Messing, R. O., and Chou, W. H. (2011) Mouse model of middle cerebral artery occlusion. *J Vis Exp*
13. Li, T., Hung, M. S., Wang, Y., Mao, J. H., Tan, J. L., Jahan, K., Roos, H., Xu, Z., Jablons, D. M., and You, L. (2011) Transgenic mice for cre-inducible overexpression of the Cul4A gene. *Genesis* **49**, 134-141
14. Sunmonu, N. A., Chen, L., and Li, J. Y. (2009) Misexpression of Gbx2 throughout the mesencephalon by a conditional gain-of-function transgene leads to deletion of the midbrain and cerebellum in mice. *Genesis* **47**, 667-673
15. Murthy, S. C., Bhat, G. P., and Thimmappaya, B. (1985) Adenovirus EIIA early promoter: transcriptional control elements and induction by the viral pre-early

EIA gene, which appears to be sequence independent. *Proc Natl Acad Sci U S A* **82**, 2230-2234

16. Su, E. J., Fredriksson, L., Geyer, M., Folestad, E., Cale, J., Andrae, J., Gao, Y., Pietras, K., Mann, K., Yepes, M., Strickland, D. K., Betsholtz, C., Eriksson, U., and Lawrence, D. A. (2008) Activation of PDGF-CC by tissue plasminogen activator impairs blood-brain barrier integrity during ischemic stroke. *Nat Med* **14**, 731-737
17. Hata, R., Mies, G., Wiessner, C., Fritze, K., Hesselbarth, D., Brinker, G., and Hossmann, K. A. (1998) A reproducible model of middle cerebral artery occlusion in mice: hemodynamic, biochemical, and magnetic resonance imaging. *J Cereb Blood Flow Metab* **18**, 367-375
18. Khakh, B. S., and North, R. A. (2006) P2X receptors as cell-surface ATP sensors in health and disease. *Nature* **442**, 527-532
19. Hasko, G., Linden, J., Cronstein, B., and Pacher, P. (2008) Adenosine receptors: therapeutic aspects for inflammatory and immune diseases. *Nat Rev Drug Discov* **7**, 759-770
20. Kim, J., Kim, M., Song, J. H., and Lee, H. T. (2008) Endogenous A1 adenosine receptors protect against hepatic ischemia reperfusion injury in mice. *Liver Transpl* **14**, 845-854
21. Hyman, M. C., Petrovic-Djergovic, D., Visovatti, S. H., Liao, H., Yanamadala, S., Bouis, D., Su, E. J., Lawrence, D. A., Broekman, M. J., Marcus, A. J., and Pinsky, D. J. (2009) Self-regulation of inflammatory cell trafficking in mice by the leukocyte surface apyrase CD39. *J Clin Invest* **119**, 1136-1149
22. Ansermot, N., Albayrak, O., Schlapfer, J., Crettol, S., Croquette-Krokar, M., Bourquin, M., Deglon, J. J., Faouzi, M., Scherbaum, N., and Eap, C. B. (2010) Substitution of (R,S)-methadone by (R)-methadone: Impact on QTc interval. *Arch Intern Med* **170**, 529-536
23. Ding, H., Wu, X., and Nagy, A. (2002) Mice with Cre recombinase activatable PDGF-C expression. *Genesis* **32**, 181-183
24. Heldmann, U., Thored, P., Claasen, J. H., Arvidsson, A., Kokaia, Z., and Lindvall, O. (2005) TNF-alpha antibody infusion impairs survival of stroke-generated neuroblasts in adult rat brain. *Exp Neurol* **196**, 204-208
25. Wang, X., Feuerstein, G. Z., Xu, L., Wang, H., Schumacher, W. A., Ogletree, M. L., Taub, R., Duan, J. J., Decicco, C. P., and Liu, R. Q. (2004) Inhibition of tumor necrosis factor-alpha-converting enzyme by a selective antagonist protects brain from focal ischemic injury in rats. *Mol Pharmacol* **65**, 890-896

Chapter V: Conclusions and Future Directions

The projects described in this work are unified by their overarching aims of better understanding the regulation of CD39 on different levels, from posttranslational modification, to transcriptional regulation, to *in vivo* actions in a murine model of cerebral ischemia.

Posttranslational modification of CD39

The first project had the aim of examining differences in the intracellular protein trafficking of CD39 in response to the pharmaceutical actions of cholesterol-synthesis blockade. In this effort, we observed that CD39, a protein characterized by multiple glycosylation sites, which are integral to its native trafficking and correct folding, is post-translationally modified in the presence of statins. Furthermore, the presence of statins downregulated caveolin-1 protein, which is necessary for the formation of caveolae, and disrupted the classical caveolar microdomain in which CD39 is known to reside. Additionally, the cellular localization of CD39 was altered in the presence of statins, with expression patterns becoming more diffuse rather than punctate. The total expression of functional CD39 was also elevated. This suggests an important role for cholesterol biosynthesis in the topographic localization of CD39.

Taken together, these data suggest that intracellular CD39 trafficking, in the presence of statins, is no longer directed through caveolae. The global *in vivo* downstream effect of disrupting the canonical trafficking pathway on endogenous CD39 function is unknown. Statins have been shown to be effective as primary preventative drugs for cardiovascular disease (1, 2). Because they are highly effective in lowering plasma cholesterol, they are in wide use. The role of CD39 as an enzyme that maintains homeostasis of the vascular milieu, inhibits platelet aggregation and limits inflammation is supported, and work from this lab suggests that CD39 is atheroprotective independent of statins (Kanthi et al., manuscript in review). In future work towards the development of CD39 as a potential therapeutic, it will be important to know how CD39 expression and function can be altered, not solely in response to statins, but in response to a dynamic *in vivo* environment. With this goal in mind, a research plan has been outlined that focuses on the posttranslational regulation of CD39.

Research Plan for Future Investigation of CD39 Posttranslational Modification

Aim 1: To determine whether the increase of CD39 activity observed after statin treatment is mediated by changes in topographic CD39 localization, by altered CD39 post-translational modifications, or both mechanisms in concert. *It is hypothesized that*

statin-mediated disruption of caveolae will result in non-caveolar CD39 membrane localization and an increase in CD39 activity that is driven by post-translational modifications of CD39.

Aim 2: To determine whether statin-driven changes in CD39 expression, localization, and/or activity contribute to the anti-inflammatory and anti-thrombotic effects of CD39 *in vivo*. *It is hypothesized that statins drive changes in CD39 topographic localization and posttranslational modification, and these affect platelet aggregation in mice.*

Aim 1

To determine whether the increase of CD39 activity observed after statin treatment is mediated by changes in topographic CD39 localization, by altered CD39 post-translational modifications, or both mechanisms in concert.

To test whether the effects of statins on CD39 are due to lowered cholesterol levels

Earlier experiments described in Chapter II (Figures 2.1-2.6) show that statins elevate CD39 mRNA, protein, expression pattern, and activity. This experiment will address the question of whether it is the cholesterol-lowering function of statins or a secondary action of statins that affects CD39 expression. HUVECs will be treated with statin, mevalonate, or both. Mevalonate is formed by the action of HMG-CoA reductase in the cholesterol synthesis pathway. All statins inhibit this step. The addition of mevalonate will restore cholesterol synthesis, and therefore determine whether changes in CD39

levels are attributable to reduced levels of cholesterol as a consequence of inhibition of HMG-CoA reductase. Whole-cell and membrane-protein levels of CD39 and CAV1 will be measured by Western blot. It is expected that if statin effects on CD39 are independent of lower cholesterol, then the addition of mevalonate will have no effect on CD39 protein levels.

To test whether cholesterol is involved in the localization and function of CD39

CD39 activity after siCav treatment, with or without mevalonate or statin, will be observed. In other treatment conditions, cholesterol will be reconstituted in membranes depleted of cholesterol, and controls will include mevalonate, as well as cholestenone treatments. Cholestenone is an oxidation product of cholesterol (3). Although it is similar in structure and can be delivered to cholesterol-depleted membranes, the addition of cholestenone does not restore cholesterol-specific processes. Its use here will determine whether cholesterol reconstitution by itself can affect CD39 activity. Caveolar morphology, occupancy, and CD39 presence and activity will all be measured. With respect to CD39 protein measurements, the possibility of increased CD39 shedding with altered cholesterol levels will be considered. CD39 in the culture media will be measured by ELISA (5). It is expected that the caveolar localization of CD39 depends on cholesterol, and that the restoration of the mevalonate pathway following statin treatment with mevalonate will restore caveolae to the plasma membrane and

that CD39 will localize to caveolar structures. The function of CD39, however, may depend on cholesterol to the extent that it is required for active CD39, but not to the extent that it requires a caveolar environment.

To determine wheather CD39 activity is inhibited by caveolae

Here, we will determine whether CD39 activity is inhibited in caveolae. Statins may increase CD39 protein levels as a consequence of disrupting caveolae. For example, endothelial nitric oxide synthase (eNOS), is subject to allosteric inhibition by caveolin-1 (4). The potential contribution of this pathway to statin-mediated stimulation of CD39 activity should be assessed. To determine the role of caveolae, HUVECs will be treated with methyl-β-cyclodextrin, a reagent used to disrupt caveolae. CD39 activity will be measured in the presence or absence of statin treatment to determine whether the presence vs absence of caveolae affects CD39 activity.

To determine whether statin-induced increases in CD39 expression results in increased CD39 enzymatic activity

HUVECs will be transfected with either a control or Cav1 siRNA, and then treated with either a statin or DMSO. Thin-layer chromatography will be used to measure CD39 activity. A second set of HUVECs will also be tested for their ability to reduce ADP-dependent platelet aggregation. Purified membranes will be incubated

with platelets, and platelet aggregation will be measured. Higher CD39 activity will result in less aggregation of platelets. I expect that statin treatment will result in significantly more CD39 activity and less platelet aggregation relative to control samples.

To determine whether statins affect the ability of CD39 to localize to caveolae

In order to quantitatively assess changes in the relationship between caveolae and CD39 after statin treatment, caveolae will be isolated from HUVECs that have been treated with either DMSO or statin, and CD39 protein levels will be measured. Caveolae will be purified according an established method that isolates caveolae based on the buoyant density of caveolae (5), in order to avoid detergent-based purification of caveolae. A detergent-based protocol may inadvertently solubilize some proteins from caveolae, and fail to yield a full complement of caveolar proteins. Briefly, cells will be harvested by scraping, homogenized in a buffer containing 0.25 M sucrose, 1 mM EDTA, and 20 mM Tricine, pH 7.8, and then centrifuged. The resulting postnuclear supernatant fraction will then be overlaid onto a 30% Percoll solution and centrifuged at 84,000 x g for 30 minutes. A visible band containing the plasma membrane fraction will be collected, and sonicated. The sonicate will be placed into 23% OptiPrep (Sigma-Aldrich). A 20 to 10% linear gradient of OptiPrep poured on top of the sample, and the sample will be centrifuged at 52,000 x g for 90 minutes. The top 5 mL of the gradient

will be collected, mixed with 4 mL of a buffer containing 50% OptiPrep, and overlaid with 2 mL of a 5% OptiPrep buffer. The sample will be centrifuged once more and a band appearing within the 5% overlay containing caveolar membranes will be collected.

To measure whether there are differences in CD39 posttranslational modifications after statin treatment

The CD39 posttranslational glycosylation and phosphorylation states will be assessed via mass spectrometry after statin treatment. Glycosylation states are relevant to CD39, as glycosylation is required for CD39 activity, and may have an effect on its relative level of activity (6, 7).

Mass spectrometry will also be used to test which glycosylation sites are affected by statin treatment. As an alternative approach to test glycosylation sites affected by statin treatment, lentiviruses expressing glycosylation site mutants of HA-tagged CD39 will be designed and used to transduce COS7 cells. These cells will be treated with either DMSO or fluvastatin, and assessed for CD39 activity by TLC as described above. A second set of similarly treated cells will be surface-biotinylated. CD39 will be precipitated using streptavidin-agarose beads. Precipitated proteins will be separated via Western Blot, and probed for HA, to assess relative levels of CD39 expression on the surface and enable calculation of relative ATPase activity of different CD39s. From

these data, it will be possible to determine which glycosylation sites are necessary for the enzymatic activity increase observed after statin treatment.

Phosphorylation events will also be investigated for effects on CD39 activity and localization. CD39 can be phosphorylated on two tyrosine residues, Y49 and Y65. These residues are located in the extracellular domain, and the roles of these residues have not been identified. Lentiviruses expressing HA-tagged CD39 or phosphorylation site mutants will be used to transduce COS7 cells. Cells will be treated with either DMSO or fluvastatin over a time course. HA-CD39 will be visualized using immunofluorescence via confocal microscopy, to determine whether CD39 accumulation and localization patterns are affected by phosphorylation site mutations. The activity of CD39 for these mutants will also be assayed via TLC as described above.

Potential limitations and alternative methods: The isolation of caveolae without disturbing or artificially affecting levels of CD39 in the caveolae may prove to be difficult. Alternative protocols for caveolar isolation are available for testing (8, 9). For example, while many methods call for a final step of antibody-coated bead separation, some methods call for either an addition of detergent, sonication, or both. More involved methods also include the initial step of silica coating of the plasma menbrane in order to promote more efficient separation of plasma membrane regions from caveolae, which will not be coated due to their invaginated structure. These various methods will be

optimized until the results from protein analysis after the isolations yield consistent results.

Aim 2

To determine whether statin-driven changes in CD39 expression, localization, and/or activity contribute to the anti-inflammatory and anti-thrombotic effects of CD39 *in vivo*.

Planned Experimental Mice

1. Control: WT (C57Bl/6) male and female mice
2. Cav1 mutant mouse: Cav1
3. Globally overexpressed CD39 mouse: $CD39^{OE}$

To test the hypothesis, there will be one condition with caveolae present in endothelial cells, and one condition without caveolae in endothelial cells. Therefore normal WT mice will be compared to Cav1 mutant mice, which, due to a targeted mutation over exons 1 and 2 of *CAV1,* produce no detectable protein products, and have been shown to lack endothelial caveolae. Mice overexpressing CD39 will be used to show effects of CD39 overexpression that are separate from statin treatment.

Fluvastatin will be administered by gavage at a dose of 80 mg/kg/d for two weeks to 1 month, and agarose gel will serve as the control. DMSO was used as the control in the cell culture model of aim 1, but its confounding anti-inflammatory effects make it unsuitable as a control *in vivo*.

To determine whether CD39 and CAV1 changes after statin treatment are cholesterol-dependent

To determine whether any changes in CD39 activity, CD39 localization, CAV1 expression and caveola formation are cholesterol-dependent, mice will be injected intraperitoneally with mevalonate to restore the cholesterol synthesis pathway. If the results from this group show a reversal of statin effects on CD39 and CAV1, then these effects are likely dependent on cholesterol.

Analysis of statin effects on caveolae and CD39 localization and distribution

All three types of mice will also be treated with fluvastatin (80 mg/kg/d for 1 month) and analyzed as described above in order to ascertain whether statins can elicit responses in accord with results from Aim 1. After 1 month of fluvastatin administration, aortas will be harvested. CAV1, and CD39 protein expression patterns will be assessed by Western blot and immunofluorescent staining of aortic tissue sections. It is expected that statins will decrease CAV1 protein in the endothelium of all

mice except the CAV1 knockout mouse, and CD39 protein will be upregulated on the luminal surface of endothelial cells.

To determine whether statin treatment changes endothelial caveolae formation

In order to confirm the *in vitro* results that show impaired caveolar structure formation in HUVECs, caveolin-1 levels will be evaluated in mouse aortas after fluvastatin or agarose treatment. These aortas will be harvested for caveolin-1 mRNA, protein, IHC, and electron microscopy. It is expected that WT and $CD39^{OE}$ mice will have diminished caveolae/caveolin-1 protein after fluvastatin treatment, whereas Cav1 mice will not exhibit any changes in terms of caveolae/caveolin-1 expression. Caveolin-1 mRNA levels are not expected to change. In the event that statin treatment does not result in any significant decrease in caveola formation, then the possibility that caveolae may be affected by statins through other parallel pathways will be considered. For example, in non-endothelial cells, some have reported an increase in Cav1 after statin treatment (10). Investigating the reason for these differential responses to statin treatment based on cell type may lead to either an explanation for a lack of statin effect on caveolae *in vivo*, or information on other mechanisms of caveolar regulation. Differential responses to statin treatment may be on either a transcriptional or post-translational basis, and either result will be informative in addressing the nature of the CD39/caveola relationship.

To determine whether changes in CD39 activity are due to changes in geographic localization and post-translational modifications of CD39

Since glycosylation has been shown to determine CD39 activity, this N-linked modification will be explored first. Mice will be treated with fluvastatin or agarose, and then their aortas harvested for IHC and an electron microscopy-based measurement of CD39 activity and Cav1 expression. Mass spectrometry will also be performed on protein samples purified from aortas of similarly treated mice, in order to analyze glycosylation and phosphorylation of CD39.

It is expected that in mice of all groups will show an increase in CD39 activity and glycosylation levels after treatment with fluvastatin, regardless of whether caveolae are present. It is also expected that $CD39^{OE}$ and WT mice will show an increase in CD39 activity and CD39 localization outside of caveolae after fluvastatin treatment, concurrent with a significant reduction in caveola formation. Cav1 mice are expected to show an increase in CD39 activity after statin treatment, but should show no changes in relation to caveolae, which are absent for mice in this group.

Potential limitations and alternative methods:

Tissue-specific overexpressing mice generated through Cre-lox systems may have some limitations. They should be well characterized before use by measuring the

expression and activity of CD39, alongside CAV1. Their thrombogenic, inflammatory, and atherogenic phenotypes should be assessed to establish the most accurate baseline for each group as is possible.

Transcriptional Regulation of CD39 through cAMP and PDEIII inhibition

The second project was designed to understand CD39 protein upregulation in cells, and *in silico* analysis suggested that cAMP may be an important regulator of CD39. One CRE-like sequence was found proximal to the start site of CD39 transcription in the CD39 promoter, and treatment of RAW macrophages and mouse peritoneal macrophages with 8-Bromo-cAMP elevated CD39 RNA, protein, and activity. Truncations of the putative promoter binding site resulted in a loss of cAMP-induced reporter gene expression. Further analysis of the binding site through ChIP experiments determined that after treatment with cAMP, the CRE-like sequence is bound by CREB/ATF2.

Our findings were published in 2010 (11), and focus was shifted to modulation of CD39 via the inhibition of PDEIII. This study was published in 2013 (12) and ultimately made the following three conclusions. The first was that CD39 modulation is possible using a currently approved and safely utilized class of drugs, PDE3 inhibitors. While evidence for the protective effects of CD39 against thrombosis and excessive

inflammation is strong, future work dealing with CD39 towards the ultimate goal of delivery into humans (or amplification of endogenous CD39) requires safe methods for regulating CD39 *in vivo*. This study demonstrated that PDE3 inhibitors may eventually be repurposed towards this goal.

The second conclusion of this project was that CD39 expression in response to cAMP modulation is controlled differently in macrophages and endothelial cells. This work furthers understanding in dealing with CD39 in a systemic setting, and provides further insight into different pathways of CD39 regulation. Whereas in macrophages, the pathway of CD39 upregulation by cAMP is transcriptional, endothelial CD39 upregulation by cAMP appears to be driven at the level of post-translational regulation. This observation led to the third conclusion that CD39 turnover involves ubiquitination, which provides the first insight into the degradation pathway regulating CD39.

Future Directions for cAMP Regulation of CD39

To date, there is very little published information regarding protein turnover of CD39. While we have shown that the turnover mechanism of CD39 includes ubiquitination, CD39 ubiquitination sites remain unknown. *In silico* analysis of the full-length CD39 protein sequence through the UCSD protein ubiquitination site prediction

algorithm (UbPred) returns three putative sites of ubiquitination at lysine residues 5, 71, and 398. Residues 5 and 71 are predicted at medium confidence and residue 398 at low confidence. These sites have yet to be analyzed, and could be mutated to test whether mutating these sites decreases ubiquitination of CD39 and increases CD39 protein stability. If so, there may be implications for future CD39-derived therapies. For example, prolonged protein stability as a result of mutated ubiquitination sites is a known concept, particularly in the context of tumor cells (13). In a therapeutic approach, techniques that deliberately inhibit ubiquitination have been suggested for developing more stable protein-based anti-tumor drugs (14). Similar approaches may be relevant in the discussion of CD39-based therapies as well.

Effect of CD39 Overexpression *In Vivo* in Cerebral Ischemia

The third and final project was designed to observe the effects of globally elevated CD39 in a murine model, and specifically in the setting of cerebral ischemia. A novel transgenic mouse was created using a Cre-Lox transgenic construct to be able to observe the effects of overexpression when such overexpression is limited to specific tissues. To this end, two mouse strains were generated from the founder strain of mice carrying the transgene. One mouse strain overexpressed human CD39 in all tissues and one mouse strain overexpressed human CD39 in myeloid lineage cells only.

When cerebral ischemia was induced in each mouse model, both strains of transgenic mice exhibited significantly smaller stroke volumes compared to wild type mice as measured by MRI. Both were also more protected from adverse stroke outcomes compared to wild type mice according to neurological deficit scoring. Mice expressing human CD39 globally also had less infiltration of leukocytes into the ischemic hemisphere. In a panel of cytokines measured in brains of wild type and globally transgenic mice, TNF-α levels were of considerable interest as it has been shown in many stroke models as a critical cytokine in the development and outcome of stroke.

Future Directions for Understanding *In Vivo* action of CD39

Future work on this project may include an increased range of time points of ischemia, in order to investigate the effect of CD39 upregulation on both early and late stroke. It will also be important to determine whether CD39 upregulation has any effect on blood flow and clot dissipation in the context of cerebral ischemia, or whether the observed decrease in injury in transgenic mice can be attributed solely to decreased inflammation overall. Furthermore, the strain of mice expressing human CD39 specifically in myeloid lineage cells will be tested further.

The field of CD39 research is still growing. While significant findings about CD39 have emerged since its discovery, there is still very little known about its most basic qualities. For example, until 2012, there was no crystal structure available of CD39, and now further research can be performed on manipulation of CD39 to increase its efficiency.

CD39 has been established as a potentially promising therapeutic target in ameliorating the harmful effects of thrombosis and to an increasing extent, inflammation. The work described herein has contributed meaningfully to this body of knowledge in the scope of CD39 regulation, but in this growing field, there remains much to be discovered.

REFERENCES

1. Ebrahim, S., Taylor, F. C., and Brindle, P. (2014) Statins for the primary prevention of cardiovascular disease. *Bmj* **348**, g280
2. Ray, K. K., Seshasai, S. R., Erqou, S., Sever, P., Jukema, J. W., Ford, I., and Sattar, N. (2010) Statins and all-cause mortality in high-risk primary prevention: a meta-analysis of 11 randomized controlled trials involving 65,229 participants. *Archives of internal medicine* **170**, 1024-1031
3. Papanikolaou, A., Papafotika, A., Murphy, C., Papamarcaki, T., Tsolas, O., Drab, M., Kurzchalia, T. V., Kasper, M., and Christoforidis, S. (2005) Cholesterol-dependent lipid assemblies regulate the activity of the ecto-nucleotidase CD39. *The Journal of biological chemistry* **280**, 26406-26414
4. Ju, H., Zou, R., Venema, V. J., and Venema, R. C. (1997) Direct interaction of endothelial nitric-oxide synthase and caveolin-1 inhibits synthase activity. *The Journal of biological chemistry* **272**, 18522-18525

5. Smart, E. J., Ying, Y. S., Mineo, C., and Anderson, R. G. (1995) A detergent-free method for purifying caveolae membrane from tissue culture cells. *Proceedings of the National Academy of Sciences of the United States of America* **92**, 10104-10108
6. Zhong, X., Malhotra, R., Woodruff, R., and Guidotti, G. (2001) Mammalian plasma membrane ecto-nucleoside triphosphate diphosphohydrolase 1, CD39, is not active intracellularly. The N-glycosylation state of CD39 correlates with surface activity and localization. *The Journal of biological chemistry* **276**, 41518-41525
7. Zhong, X., Kriz, R., Kumar, R., and Guidotti, G. (2005) Distinctive roles of endoplasmic reticulum and golgi glycosylation in functional surface expression of mammalian E-NTPDase1, CD39. *Biochimica et biophysica acta* **1723**, 143-150
8. Oh, P., and Schnitzer, J. E. (1999) Immunoisolation of caveolae with high affinity antibody binding to the oligomeric caveolin cage. Toward understanding the basis of purification. *The Journal of biological chemistry* **274**, 23144-23154
9. Pilch, P. F., Souto, R. P., Liu, L., Jedrychowski, M. P., Berg, E. A., Costello, C. E., and Gygi, S. P. (2007) Cellular spelunking: exploring adipocyte caveolae. *Journal of lipid research* **48**, 2103-2111
10. Patel, H. H., Zhang, S., Murray, F., Suda, R. Y., Head, B. P., Yokoyama, U., Swaney, J. S., Niesman, I. R., Schermuly, R. T., Pullamsetti, S. S., Thistlethwaite, P. A., Miyanohara, A., Farquhar, M. G., Yuan, J. X., and Insel, P. A. (2007) Increased smooth muscle cell expression of caveolin-1 and caveolae contribute to the pathophysiology of idiopathic pulmonary arterial hypertension. *FASEB journal : official publication of the Federation of American Societies for Experimental Biology* **21**, 2970-2979
11. Liao, H., Hyman, M. C., Baek, A. E., Fukase, K., and Pinsky, D. J. (2010) cAMP/CREB-mediated transcriptional regulation of ectonucleoside triphosphate diphosphohydrolase 1 (CD39) expression. *The Journal of biological chemistry* **285**, 14791-14805
12. Baek, A. E., Kanthi, Y., Sutton, N. R., Liao, H., and Pinsky, D. J. (2013) Regulation of ecto-apyrase CD39 (ENTPD1) expression by phosphodiesterase III (PDE3). *FASEB journal : official publication of the Federation of American Societies for Experimental Biology* **27**, 4419-4428
13. Lukashchuk, N., and Vousden, K. H. (2007) Ubiquitination and degradation of mutant p53. *Molecular and cellular biology* **27**, 8284-8295
14. Bachran, C., Gupta, P. K., Bachran, S., Leysath, C. E., Hoover, B., Fattah, R. J., and Leppla, S. H. (2014) Reductive methylation and mutation of an anthrax toxin fusion protein modulates its stability and cytotoxicity. *Scientific reports* **4**, 4754